ISSN 2095-8137 CN 53-1229/Q
Volume 39 Issue 5
18 September 2018

ZR

Zoological Research

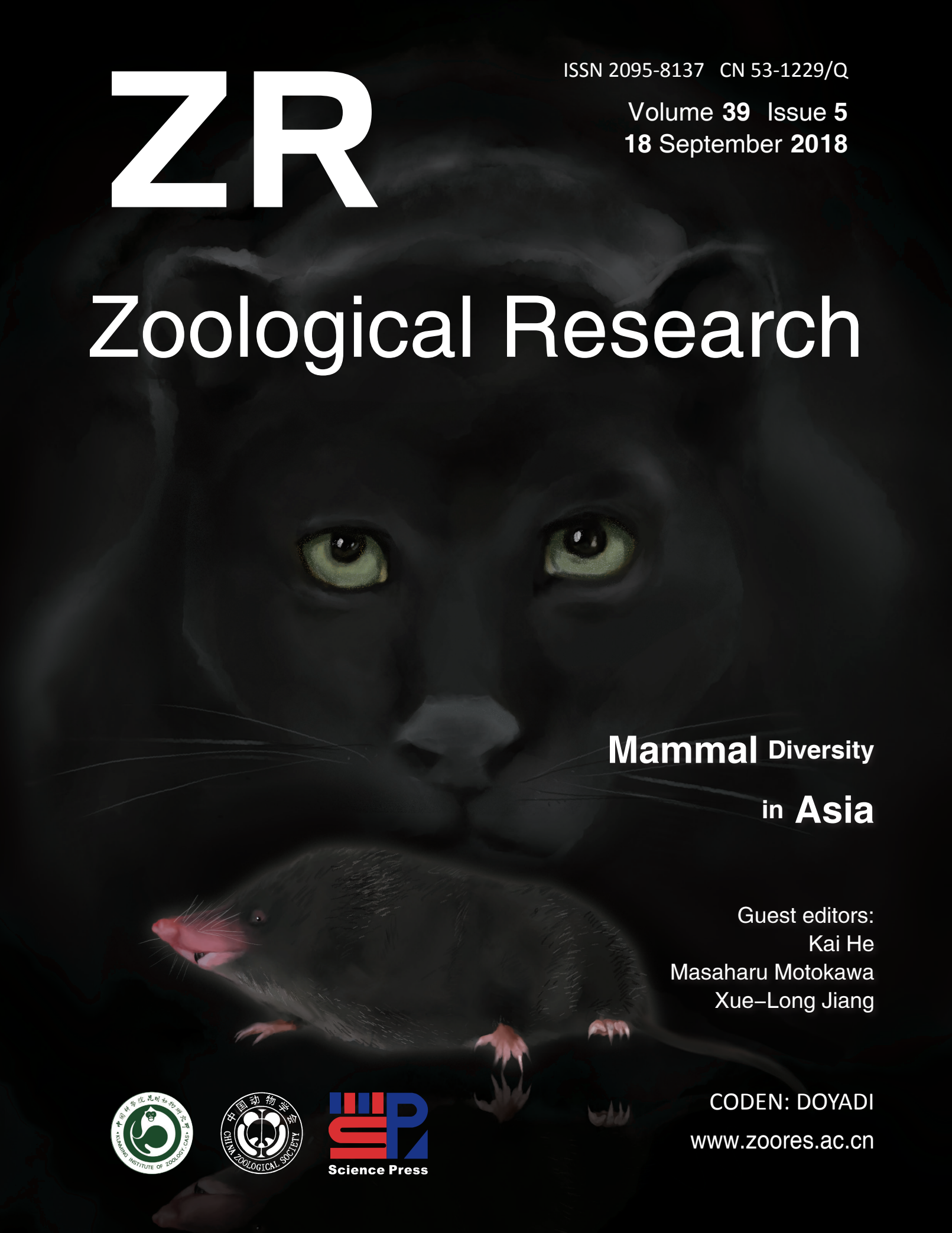

Mammal Diversity in Asia

Guest editors:
Kai He
Masaharu Motokawa
Xue–Long Jiang

CODEN: DOYADI
www.zoores.ac.cn

Science Press

ZOOLOGICAL RESEARCH

Volume 39, Issue 5 18 September 2018

CONTENTS

Special Issue for Mammal Diversity in Asia

Review

Articles

Guest editors: Kai He, Masaharu Motokawa, Xue-Long Jiang

Cover image: The new panther shrew and its etymological origin, the black panther. Illustration by Xue Mi

ZOOLOGICAL RESEARCH

Species delimitation based on diagnosis and monophyly, and its importance for advancing mammalian taxonomy

Eliécer E. Gutiérrez[1,2,*], Guilherme S. T. Garbino[3]

[1] *Pós-Graduação em Biodiversidade Animal, Departamento de Ecologia e Evolução, Centro de Ciências Naturais e Exatas, Universidade Federal de Santa Maria, Santa Maria, RS* 97105-900*, Brazil*

[2] *Division of Mammals, National Museum of Natural History, Smithsonian Institution, Washington DC* 20013-7012*, USA*

[3] *Pós-graduação, Departamento de Zoologia, Instituto de Ciências Biológicas, Universidade Federal de Minas Gerais, Belo Horizonte, Minas Gerais* 31270-901*, Brazil*

ABSTRACT

A recently proposed taxonomic classification of extant ungulates sparked a series of publications that criticize the Phylogenetic Species Concept (PSC) claiming it to be a particularly poor species concept. These opinions reiteratively stated that (1) the two fundamental elements of the "PSC", i.e., monophyly and diagnosability, do not offer objective criteria as to where the line between species should be drawn; and (2) that extirpation of populations can lead to artificial diagnosability and spurious recognitions of species. This sudden eruption of criticism against the PSC is misleading. Problems attributed to the PSC are common to most approaches and concepts that modern systematists employ to establish species boundaries. The controversial taxonomic propositions that sparked criticism against the PSC are indeed highly problematic, not because of the species concept upon which they are based, but because no evidence (whatsoever) has become public to support a substantial portion of the proposed classification. We herein discuss these topics using examples from mammals. Numerous areas of biological research rest upon taxonomic accuracy (including conservation biology and biomedical research); hence, it is necessary to clarify what are (and what are not) the real sources of taxonomic inaccuracy.

Keywords: Alpha taxonomy; Phylogenetic Species Concept; Species concepts; Taxonomic inertia; Taxonomic inflation

INTRODUCTION

A recently proposed taxonomic classification for extant ungulates (Groves & Grubb, 2011) sparked a series of publications criticizing the species concept upon which the classification was based, i.e., Phylogenetic Species Concept (PSC) (Heller et al., 2013; Zachos et al., 2013; Zachos, 2013, 2015; Zachos & Lovari, 2013), albeit previous published opinions had already presented some of the same arguments against the PSC (e.g., Frankham et al., 2012; Garnett & Christidis, 2007; Isaac et al., 2004; Tattersall, 2007). Two main claims about the PSC have been reiteratively used to highlight it as a particularly poor species concept: (1) the two fundamental elements of the PSC, i.e., monophyly and diagnosability, do not offer objective criteria as to where the line between species should be drawn; and (2) the extirpation of populations can lead to artificial diagnosability and spurious recognitions of species. Moreover, these criticisms portray the use of the PSC as detrimental to conservation efforts. We argue that the problems attributed to the PSC are common to most methodological approaches to species limits and to the most commonly used species concepts that have been the basis for the taxonomic classifications of mammals currently in use. Furthermore, we present evidence that the PSC based on diagnosability and monophyly as operational criteria has helped to substantially advance mammalian systematics. In addition, we show that the recent criticism against Groves & Grubb's (2011) ungulate taxonomy is mistakenly focused on an "alleged poverty" of the PSC (see a brief comment relevant to this general topic by Tsang et al., 2016, p. 529), whereas the real cause of taxonomic inflation in that proposed classification

Received: 14 December 2017; Accepted: 12 February 2018; Online: 08 March 2018

*Corresponding author, E-mail: ee.gutierrez.bio@gmail.com

DOI: 10.24272/j.issn.2095-8137.2018.037

lays on numerous empirical problems.

PHYLOGENETIC SPECIES CONCEPT (PSC)

Before we discuss these matters, we must clarify that the name "Phylogenetic Species Concept" has been associated to various concepts (e.g., McKitrick & Zink, 1988; Nixon & Wheeler, 1990), two of which are central in the above-mentioned debate. These concepts can be better regarded as sets of criteria for species delimitation rather than "concepts", as proposed by de Queiroz (2007); however, herein we refer to these sets of criteria as "concepts" only to facilitate communication by using the same terminology employed by authors of previous articles. These concepts are as follows (see summaries by Groves et al., 2017; Zachos, 2016a):

> Phylogenetic species concept, diagnosis-based version (dPSC): "*The smallest diagnosable cluster of individual organisms within which there is a parental pattern of ancestry and descent*" (Cracraft, 1983, p.170). Subsequently formulated as "*... the smallest aggregation of populations (sexual) or lineages (asexual) diagnosable by a unique combination of character states in comparable individuals (semaphoronts)*" (Nixon & Wheeler, 1990). A more recent version states that species are "*... the smallest population or aggregation of populations which has fixed heritable differences from other such populations or aggregations*" (Groves & Grubb, 2011; see also Groves, 2017).
>
> Phylogenetic species concept, monophyly-based version (mPSC) "*... a geographically constrained group of individuals with some unique apomorphous character, is the unit of evolutionary significance*" (Rosen, 1978, p. 176).

A third concept that must be incorporated in the discussion is as follows (see Groves et al., 2017):

> Phylogenetic species concept, diagnosis-and-monophyly-based version (dmPSC), defined as "*... the smallest diagnosable cluster of individual organisms forming a monophyletic group within which there is a parental pattern of ancestry and descent*" (Mayden, 1997, p. 407; McKitrick & Zink, 1988).

DO THESE VERSIONS OF THE PSC OFFER OBJECTIVE CRITERIA AS TO WHERE THE LINE BETWEEN SPECIES SHOULD BE DRAWN?

The short answer is "no", but "no" would also be the answer if the question were asked with regard to any other species concept, including the Biological Species Concept (BSC) when applied to allopatric populations (see Groves, 2012 and references therein). However, the three phylogenetic species concepts described above differ importantly regarding the degree of objectivity with which they can be applied.

With regard to the dPSC (sensu Cracraft, 1983; see also Eldredge & Cracraft, 1980; Nixon & Wheeler, 1990; Wheeler & Meier, 2000 and references therein), we agree with previous criticisms (Heller et al., 2013, 2014; Zachos & Lovari, 2013, Zachos, 2016a) in that this concept is prone to promote spurious recognition of mere geographic (including subspecies) or even individual variants of a single species as if such variants were each a valid species. This is due to the high degree of subjectivity and arbitrariness implicit in the task of judging what characteristics are to be deemed adequate to diagnose species and distinguishing such characteristics from those that would simply lead to diagnoses of populations, or groups thereof, within a single species (but see Wiens & Servedio, 2000). Species are not phenotypically and genotypically homogeneous across geography, therefore it is always the case that various populations within a single species can be diagnosed. These diagnoses by themselves must not be a justification to regard such populations as different species. This limitation of the dPSC is exacerbated when sample sizes are small, as is often the case for medium and large mammals. In these cases, a researcher may erroneously infer the existence of phenotypic discontinuity and the presence of characteristics enabling the diagnosis of a sample—the latter based on a set of specimens that at the time were perceived as worthy of species-level recognition. However, as more samples are obtained, individuals with intermediate phenotypes with respect to the putative new species and other geographic samples may be found. This would render the putative new species, which was previously thought to be diagnosable, conspecific with an already recognized species (e.g., Peres et al., 1996). Examples of these plausible problems are abundant in the proposed classification of ungulates by Groves & Grubb (2011) (see below), but are by no means exclusive to it (e.g., Díaz et al., 1999, 2002; Fonseca & Pinto, 2004; Solari, 2004; van Roosmalen et al., 2000, 2007); numerous examples exist in early contributions to mammalian taxonomy (e.g., Miller, 1912; Pocock, 1941; Robinson & Lyon, 1901), and even the last decade has seen claims advocating for the recognition of a species made on the basis of phenotypic diagnoses of as few as one or two specimens—e.g., Meijaard et al., 2017 p. 513; see also Mantilla-Meluk (2013) for a monkey subspecies named on the basis of morphometric data and pelage coloration from only four specimens. Unfortunately, in some cases descriptions of species have been carried out not only with unacceptably small sample sizes but also merely based on images (illustrations, photos, or both) and lacking preserved type specimens (see Pine & Gutiérrez, 2018 for a review of cases and problems associated to this phenomenon). Although no data exist to support the notion that the collection of a single individual (for it to properly serve as a preserved holotype) significantly increases the probability of an already endangered species to become extinct, some researchers may prefer not to carry out such collection (e.g., Donegan, 2008; but see Dubois & Nemésio, 2007; Dubois, 2009), or it may be unfeasible due to impediments in obtaining collection permits. In such cases, a wide survey of museum specimens might

lead to the discovery and subsequent use of specimens in taxonomic descriptions. Undertaking comprehensive surveys of museum specimens may be disregarded by describers of new species, but the possible data yielded, which may be coupled with photos of living animals, might ameliorate the detrimental effects of extremely small sample sizes and help in unveiling geographic and non-geographic (ontogenetic, sexual) variation (e.g., Garbino et al., 2016).

The second concept, the mPSC, under which species must be both monophyletic and geographically restricted, seems indefensible. Within a species there can be large numbers of monophyletic groups that are geographically restricted only due to recent changes in their environment. An example of this is the populations of brocket deer of the Cordillera de Mérida, Venezuela, which for decades were recognized as a valid species, *Mazama bricenii*. This recognition was based on no data whatsoever and on the assumption of a plausible differentiation due to its supposed geographic isolation. However, a recent study that employed ecological niche modeling found that, if these populations were truly isolated in modern time, such isolation commenced not long ago (Gutiérrez et al., 2015). The study also found that while the focal population formed a monophyletic haplogroup, it was embedded within a larger (yet shallow) clade whose terminal branches corresponded to *Mazama rufina*. Results from that study showed that what was once known as *Mazama bricenii* actually corresponds to *Mazama rufina* (Gutiérrez et al., 2015), and illustrate how the application of the mPSC would have led to mistakenly recognize *M. bricenii* as if it were a valid species. Such taxonomic recognition would be a mPSC-based artifact caused by (1) the fact that sequences obtained from specimens from the Cordillera de Mérida (where the populations to which the name *M. bricenii* would apply occur) were recovered in a monophyletic haplogroup; and (2) because those populations might be geographically isolated in modern time.

The third concept, dmPSC, for which species must be both monophyletic and diagnosable, has been useful for improving mammalian taxonomy. As previously noted, many monophyletic groups are found within a single species, and that monophyly per se does not constitute a criterion to determine where the line between species should be drawn. However, it is also true that assessing whether a candidate species is monophyletic or not provides a fundamental basis for its potential recognition as a valid species. Recognizing a polyphyletic taxon as if it were a valid species would be absurd. On the other hand, in some situations (e.g., species originating from peripheral isolation) a candidate species might meet the criteria (i.e., monophyly and diagnosability) for validity under the dmPSC, but its recognition renders the species in which the candidate had thus far been included as paraphyletic. No consensus has been reached as to whether taxonomists should accept paraphyletic species as valid, or, alternatively, if taxonomists should recognize as valid only those that are monophyletic (see Carter et al., 2015; Crisp & Chandler, 1996; Dias et al., 2005; Ebach et al., 2006; Freudenstein, 1998; Funk & Omland, 2003; Hörandl, 2006, 2007; Nelson et al., 2003; Nixon & Wheeler, 1990; de Queiroz & Donoghue, 1988; Zachos, 2014b; Zander, 2007; see also Funk & Omland, 2003). Discussing these views requires a much more extensive text and would distract from the aim of this perspective piece—i.e., clarifying that despite the recent criticisms made against PSCs, at least one of these concepts has served to positively advance mammalian systematics. By requiring monophyly, the application of the dmPSC secures that a phylogenetic inference is conducted to describe or revalidate a species, thus decreasing the chances that polyphyletic groups of populations would be named as a species. These phylogenetic estimates also provide frameworks for evaluating alternatives in cases in which the description or recognition of a clade as a species would render an already recognized species as paraphyletic. In such cases, researchers might simply not describe or formally recognize that clade at all—which might be acceptable, as not every clade in a phylogenetic tree represents a taxon worth naming—or describe it at the subspecies level—with paraphyly persisting at a lower taxonomic rank—or describe it and accept paraphyletic species as valid, in which case the researcher could not invoke any species concept that requires monophyly (including the dmPSC) upon which to base the description. Whichever of these alternatives the researcher prefers, and attempts to justify, due to philosophical, pragmatic, or both considerations, the fact that the dmPSC requires a phylogenetic estimate is an advantage over other concepts that do not, including the dPSC and the BSC.

The requirement that a candidate species must also be diagnosable in order to be recognized under the dmPSC is indispensable. A species must have a series of genetically fixed characteristics that are common to its members and that serve to distinguish it from other such species. However, as already discussed (see above), diagnosability alone is, in general, an inadequate approach to establish species limits.

Acknowledging the existence of the dmPSC is important because it does represent one of the most explicit methods to infer species limits—contra authors that ignored the existence of this concept in their arguments against or in favor of the "PSC" (e.g., Gippoliti et al., 2018; Groves, 2012, 2017; Heller et al., 2013; Zachos & Lovari, 2013; Zachos et al., 2013; Zachos, 2013, 2014a, 2015, 2016a). Some operational steps in delimiting species will always be arbitrary. In this sense, the advantage of the dmPSC over other concepts is that its operational criteria for recognition of species can be objectively tested. In other words, monophyly and diagnosability are, in general, more easily testable for allopatric populations than reproductive barriers (BSC), and more objectively demonstrated than the central criteria upon which other concepts define species, such as “ecological roles” in the Ecological Species Concept (Van Valen, 1976). When applied based on sufficient geographic and taxonomic sampling, and, ideally (but not strictly necessary; see below), employing phylogenetic inferences using data from independent sources (e.g., DNA sequence data obtained from independently inherited genes), the dmPSC has improved the taxonomic classifications of various groups of mammals,

some of which remained problematic for decades. Among studies that exemplify how the dmPSC has helped to advance mammalian systematics, even if some of them used this species concept without explicitly or correctly invoking it, are those on didelphid marsupials (e.g., Díaz-Nieto & Voss, 2016; Giarla et al., 2010; Gutiérrez et al., 2010; Martínez-Lanfranco et al., 2014; Pavan et al., 2017; Voss et al., 2018), rodents (e.g., Hawkins et al., 2016; do Prado & Percequillo, 2017; Rogers & González, 2010; Voss et al., 2013), bats (e.g., Baird et al., 2008; Molinari et al., 2017; Moras et al., 2016; Velazco et al., 2010), and medium and large mammals (e.g., Bornholdt et al., 2013; Gutiérrez et al., 2015; Helgen et al., 2009, 2013; Janečka et al., 2008; Koepfli et al., 2008; Miranda et al., 2017; do Nascimento & Feijó, 2017 (and references therein for phylogenetic evidence)). These studies have not only unraveled the true-species nature of previously unrecognized species, but in many cases have shown that taxa considered as valid species for decades are not valid species at all.

The application of any PSC can promote rampant taxonomic inflation when applied without sufficient rigor. In our opinion, this inflation is caused less by philosophical aspects and properties of the PSCs and more by empirical shortcomings. In several studies, geographic and individual variation do not appear to be satisfactorily addressed, and names are applied to what could be intraspecific variants (see examples in Tattersall, 2007). On other occasions, monophyletic groups recovered from molecular phylogenies based on sequence data from a single locus promptly receive new or revalidated names (e.g., Boubli et al., 2012; Thinh et al., 2010). Nevertheless, it is important to note that when the established, traditional taxonomic classification of a focal group is the result of dogmatic acceptance of expert opinions (often past-century authorities), without support from data (see Gutiérrez & Helgen, 2013), then even the use of limited evidence—e.g., analyses of sequence data from a single locus (despite the well-known shortcomings of this approach; see Dávalos & Russell, 2014; Knowles & Carstens, 2007; Maddison, 1997), ideally coupled with qualitative and/or quantitative analyses of morphological data—can well justify taxonomic changes if based on adequate sampling (e.g., Gutiérrez et al., 2010, 2015, 2017; Voss et al., 2013; contra Zachos, 2009, 2016b).

The proposed ungulate taxonomic classification that sparked the recent series of criticism against the PSC is particularly problematic, but not because it was based on the dPSC. Most controversial aspects of this proposed classification are not at all associated to any species concept, as it might seem if one reads the recent debate between Frank Zachos and Colin Groves and their co-authors with regard to the "PSC", but rather to more practical aspects of such a monograph, to name just a few (see also Heller et al., 2013; Holbrook, 2013; Zachos, 2014a, p. 1): (1) Groves & Grubb (2011) did not assess geographic variation at all for most of the species they recognized; (2) unfortunately, for some species recognized by these authors, the sample size employed was not indicated nor any published study cited to support the taxonomic proposals, whereas for many other alleged species the sample sizes were extremely low—e.g., *Alcelaphus tora*, *Dorcatragus megalotis*, *Eudorcas nasalis*, *Eudorcas tilonura*, *Gazella acaciae*, *Gazella karamii*, *Gazella shikarii*, *Lama mensalis*, *Madoqua hararensis*, *Mazama fuscata*, *Mazama jucunda*, *Mazama trinitatis*, and *Redunca cottoni*; (3) no published phylogenetic information seems to be the basis of most of their taxonomic propositions; (4) in general, no detailed discussions were presented on whether recognizing a taxon as a valid species was more appropriate and justifiable than regarding it as a subspecies, and it seems that the objective of the authors was to merely recognize as valid species as many taxa as possible, without critical evaluation of alternatives (e.g., recognizing subspecies when appropriate); (5) a list of the specimens examined was not provided, and hence it is difficult for the scientific community to evaluate the authors' assertions on specimen morphologies based on the same material with certainty; (6) no data were made available that would enable reproduction and testability of the analyses that were the basis of the taxonomic propositions; (7) although the authors cite published studies for some of the taxonomic changes they proposed, for others they did not and nowhere in their monograph can be found results from any quantitative analyses. We cannot understand why Groves & Grubb (2011) failed to publish the results of their quantitative analyses given current possibilities to do so (see below). Unfortunately, this problem is not unique to the proposed ungulate taxonomic classification of Groves & Grubb. An important volume on mammals of South America (Patton et al., 2015) contained the first modern taxonomic treatments of various rodent groups (e.g., family Sciuridae, genera *Aepeomys*, *Oecomys*, *Rhipidomys*, *Thomasomys*), but results from analytical procedures assessing geographic and non-geographic variation of those groups have not been published (in the book or elsewhere), and in some cases it seems unlikely they will ever be published. Luckily, several unpublished Ph.D. dissertations that served as the basis for the book sections treating those taxa have been privately shared among colleagues. Clearly, making these Ph.D. dissertations (and other unpublished material) digitally available to the scientific community free of charge from a repository on the Internet (e.g., Dryad, Figshare, Internet Archive, ResearchGate, Zenodo), if their authors grant authorization, should be considered by the editors of this book, and similar actions should be considered by authors and editors of future monographs introducing taxonomic classifications.

CAN EXTIRPATION OF POPULATIONS LEAD TO ARTIFICIAL DIAGNOSABILITY AND SPURIOUS RECOGNITIONS OF SPECIES UNDER THE dmPSC?

The short answer is "it can", but again the same answer would apply if the question were asked about other species concepts, including the BSC. In their criticism of the "PSC", Zachos & Lovari (2013) claimed that the fact that extirpation of populations can lead to artifactual diagnosability and monophyly is one of the weaknesses of the PSC that makes this concept a particularly poor one. They stated that "*There is yet another line of argumentation that clearly shows the shortcomings of both diagnosability and monophyly as yardsticks for species delimitation and that we believe is another coup de grâce for the PSC. Diagnosability (just like reciprocal monophyly) can and*

often does occur as a consequence of extinction of intermediate forms...". Unfortunately, Zachos & Lovari (2013) did not realize that extirpation of intermediate populations is one of the natural causes of speciation. These events lead to speciation, affecting gene flow and ecological adaptation of extreme phenotypes in populations that previously were genetically connected by the existence of intermediate populations. In fact, it could be said that living taxa that can be validly recognized on the planet exist as separate biological entities and as taxonomically diagnosable units only because of the extinction of intermediate forms. If all intermediate forms that have lived since the beginning of life on Earth were still with us, then all living organisms, from prokaryotes to eukaryotes and from plants to animals, would exist as a single morphological and reproductive continuum: no distinguishable taxa would exist! Logically, in cases in which extirpations have taken place fairly recently (e.g., due to human-related causes) no speciation may have yet occurred. In such cases, the extirpation of populations can potentially lead to artifactual recognitions of species under the PSCs, but this issue is far from being associated only to the PSCs; rather, it is a problem that can potentially affect most, if not all, species concepts currently in use. For example, this issue can lead to artifactual recognition of species under the BSC. Let us imagine a species, species A, with wide distribution and showing geographic variation by way of a cline in several qualitative cranial traits believed to be taxonomically important, i.e., used by most authors to distinguish species within the corresponding genus. We will illustrate these traits as color and shape in polygons that represent populations of species A (Figure 1, panel 1). If recent extirpations of intermediate populations take place and only those populations occurring at the opposite extremes of species A's range remain as extant, then these populations will become allopatric and it would be highly likely that they would be considered as members of different species under the BSC (Figure 1, panel 2). The BSC would fail to regard these populations as conspecific, even employing the approach presented by Tobias et al. (2010; see also Brooks & Helgen, 2010), which uses the degree of differentiation known to exist between different but sympatric species (i.e., species A and B in Figure 1) as a standard to assess the taxonomic relevance of differentiation between allopatric populations (i.e., populations of species A in North and South America in Figure 1)—in order words, this approach uses the former degree of differentiation as a threshold at which (or above) allopatric populations could be treated as different species under the BSC.

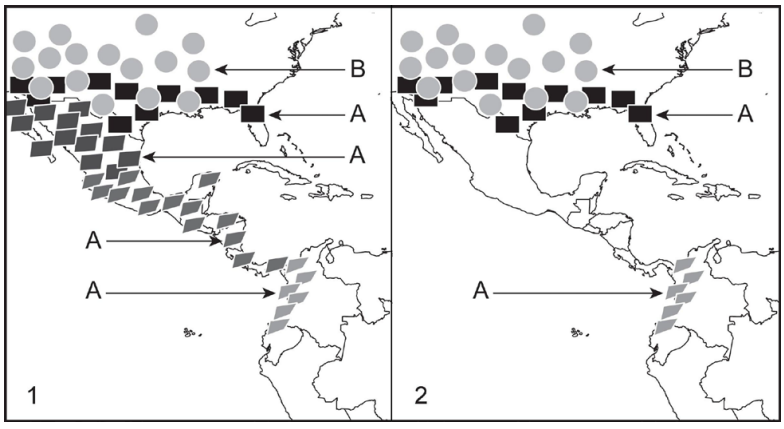

Figure 1 Illustration of how population extirpations can promote artifactual recognition of populations of a single species as if they were different species under the Biological Species Concept (and many other concepts)

Species A, which is represented by quadrilaterals (rectangle and rectangle-like polygons), possesses a wide distribution and geographic variation by way of a cline in several qualitative cranial traits considered taxonomically important; herein these traits are illustrated as color and shape of the polygons (panel 1). Species B, which is represented by circles, is restricted to North America, where it occurs in sympatry with some North American populations of species A (panel 1). If extirpation of populations of species A takes place and only those populations occurring at the opposite extremes of species A's range remain as extant, then these populations will become allopatric (panel 2). In that scenario, it would be highly likely that the remaining extant populations would be considered as members of a different species under the BSC (panel 2). The BSC would fail to regard these populations as conspecific, even employing the approach presented by Tobias et al. (2010; see also Brooks & Helgen, 2010), which uses the degree of differentiation known to exist between different but sympatric species (i.e., species A and B) as a standard to assess the taxonomic relevance of differentiation between allopatric populations (i.e., populations of species A in North and South America).

CONCLUSIONS

Major differences exist among the different concepts labeled as the "Phylogenetic Species Concept", and the one that uses both diagnosis and monophyly (dmPSC) to delimit species has been, and will continue to be, important for positively advancing mammalian taxonomy. Our preceding discussion should rectify misunderstandings that could arise

from claims made in recently published opinions debating alleged pros and cons of the "PSC". Although we partially agree with some of the arguments presented by participants of that debate, the proposed taxonomic classification of ungulates (Groves & Grubb, 2011) that motivated this debate is highly deficient, in our view, not so much because of the species concept it employed (i.e., dPSC), but rather due to serious empirical problems. Among them is the absence of statistical assessments of geographic and non-geographic variation in diagnostic traits. Although in many instances the number of specimens available in museums should have permitted statistically satisfactory assessments of geographic and non-geographic variation, results from those analyses were not presented by Groves & Grubb (2011) in their monograph. In other instances, extremely low sample sizes precluded proper statistical analyses.

To refrain from producing taxonomic hypotheses because of limited material (e.g., few available museum specimens) would hamper progress in medium and large mammal taxonomy. As previously mentioned, collecting new samples of such mammals can be logistically impracticable, and some researchers may simply prefer not to collect them due to conservation concerns (but see clarification above). Thus, even when the available material consists of only a few specimens, taxonomic studies should still be carried out, but the taxonomist should bear in mind the statistical limitations of a small sample, such as inadequate estimations of population ranges and lower confidence levels. Collating information from multiple data sources, such as nucleotide sequences, discrete and continuous morphological data, and behavior—an approach nowadays called “integrative taxonomy” (e.g., Dayrat, 2005)—has long been considered useful as it theoretically increases the probability of correctly identifying and delimiting taxonomic entities (Simpson, 1961; Tinbergen, 1959).

Numerous areas of biological research rest upon taxonomic accuracy (including conservation biology and biomedical research); hence, it is necessary to clarify what are (and what are not) the real sources of taxonomic inaccuracy.

COMPETING INTERESTS

The authors declare that they have no competing interests.

AUTHORS' CONTRIBUTIONS

The writing of a first draft of the manuscript was led by E.E.G. Both authors substantially contributed to all aspects of this publication.

ACKNOWLEDGEMENTS

We thank the editor and two anonymous reviewers for their comments, which helped improve an earlier version of the now-published manuscript. We are thankful to our colleagues Kai He, Xue-Long Jiang, and Masaharu Motokawa for their invitation to contribute to this special issue on mammal biodiversity of Asia.

REFERENCES

Baird AB, Hillis DM, Patton JC, Bickham JW. 2008. Evolutionary history of the genus *Rhogeessa* (Chiroptera: Vespertilionidae) as revealed by mitochondrial DNA sequences. *Journal of Mammalogy,* **89**(3): 744–754.

Bornholdt R, Helgen K, Koepfli KP, Oliveira L, Lucherini M, Eizirik E. 2013. Taxonomic revision of the genus *Galictis* (Carnivora: Mustelidae): species delimitation, morphological diagnosis, and refined mapping of geographical distribution. *Zoological Journal of the Linnean Society,* **167**(3): 449–472.

Boubli JP, Rylands AB, Farias IP, Alfaro ME, Alfaro JL. 2012. *Cebus* phylogenetic relationships: a preliminary reassessment of the diversity of the untufted capuchin monkeys. *American Journal of Primatology,* **74**(4): 381–393.

Brooks TM, Helgen KM. 2010. Biodiversity: a standard for species. *Nature,* **467**(7315): 540–541.

Carter JG, Altaba CR, Anderson LC, Campbell DC, Fang ZJ, Harries PJ, Skelton PW. 2015. The Paracladistic Approach to Phylogenetic Taxonomy. Lawrence, Kansas, USA: Paleontological Institute, 1–9.

Cracraft J. 1983. Species concepts and speciation analysis. *In:* Johnston RF. Current Ornithology. Boston, MA: Springer, 159–187.

Crisp MD, Chandler GT. 1996. Paraphyletic species. *Telopea,* **6**(4): 813–844.

Dávalos LM, Russell AL. 2014. Sex-biased dispersal produces high error rates in mitochondrial distance-based and tree-based species delimitation. *Journal of Mammalogy,* **95**(4): 781–791.

Dayrat B. 2005. Towards integrative taxonomy. *Biological Journal of the Linnean Society,* **85**(3): 407–415.

Dias P, Assis LCS, Udulutsch RG. 2005. Monophyly vs. paraphyly in plant systematics. *Taxon,* **54**(4): 1039–1040.

Díaz MM, Barquez RM, Braun JK, Mares MA. 1999. A new species of *Akodon* (Muridae: Sigmodontinae) from northwestern Argentina. *Journal of Mammalogy,* **80**(3): 786–798.

Díaz MM, Flores DA, Barquez RM. 2002. A new species of gracile mouse opossum, genus *Gracilinanus* (Didelphimorphia: Didelphidae), from Argentina. *Journal of Mammalogy,* **83**(3): 824–833.

Díaz-Nieto JF, Voss RS. 2016. A revision of the didelphid marsupial genus *Marmosops*, Part 1. Species of the subgenus *Sciophanes*. *Bulletin of the American Museum of Natural History,* **402**: 1–70.

de Queiroz K. 2007. Species concepts and species delimitation. *Systematic Biology,* **56**(6): 879–886.

de Queiroz K, Donoghue MJ. 1988. Phylogenetic systematics and the species problem. *Cladistics,* **4**(4): 317–338.

do Nascimento FO, Feijó A. 2017. Taxonomic revision of the tigrina *Leopardus tigrinus* (Schreber, 1775) species group (Carnivora, Felidae). *Papéis Avulsos de Zoologia (São Paulo),* **57**(19): 231–264.

do Prado JR, Percequillo AR. 2017. Systematic studies of the genus *Aegialomys* Weksler et al., 2006 (Rodentia: Cricetidae: Sigmodontinae): geographic variation, species delimitation, and biogeography. *Journal of Mammalian Evolution,* doi: 10.1007/s10914-016-9360-y.

Donegan TM. 2008. New species and subspecies descriptions do not and should not always require a dead type specimen. *Zootaxa,* **1761**: 37–48.

Dubois A, Nemésio A. 2007. Does nomenclatural availability of nomina of new species or subspecies require the deposition of vouchers in collections? *Zootaxa,* **1409**: 1–22.

Dubois A. 2009. Endangered species and endangered knowledge. *Zootaxa,* **2201**: 26–29.

Ebach MC, Williams DM, Morrone JJ. 2006. Paraphyly is bad taxonomy. *Taxon,* **55**(4): 831–832.

Eldredge N, Cracraft J. 1980. Phylogenetic Patterns and the Evolutionary Process: Method and Theory in Comparative Biology. New York: Columbia University Press.

Fonseca RM, Pinto CM. 2004. A new *Lophostoma* (Chiroptera: Phyllostomidae: Phyllostominae) from the Amazonia of Ecuador. Occasional Papers of the Museum of Texas Tech University, Texas: Texas Tech University, **242**: 1–11.

Frankham R, Ballou JD, Dudash MR, Eldridge MDB, Fenster CB, Lacy RC, Mendelson JR, Porton IJ, Ralls K, Ryder OA. 2012. Implications of different species concepts for conserving biodiversity. *Biological Conservation,* **153**: 25–31.

Freudenstein JV. 1998. Paraphyly, ancestors, and classification: a response to Sosef and Brummitt. *Taxon,* **47**(1): 95–104.

Funk DJ, Omland KE. 2003. Species-level paraphyly and polyphyly: frequency, causes, and consequences, with insights from animal mitochondrial DNA. *Annual Review of Ecology, Evolution, and Systematics,* **34**: 397–423.

Garbino GST, Rezende GC, Valladares-Padua C. 2016. Pelage variation and distribution of the black lion tamarin, *Leontopithecus chrysopygus*. *Folia Primatologica*, **87**(4): 244–261.

Garnett ST, Christidis L. 2007. Implications of changing species definitions for conservation purposes. *Bird Conservation International,* **17**(3): 87–195.

Giarla TC, Voss RS, Jansa SA. 2010. Species limits and phylogenetic relationships in the didelphid marsupial genus *Thylamys* based on mitochondrial DNA sequences and morphology. *Bulletin of the American Museum of Natural History,* **346**: 1–67.

Gippoliti S, Cotterill FPD, Zinner D, Groves CP. 2018. Impacts of taxonomic inertia for the conservation of African ungulate diversity: an overview. *Biological Reviews,* **93**(1): 115–130.

Groves C. 2012. Species concept in primates. *American Journal of Primatology,* **74**(8): 687–691.

Groves C. 2017. Phylogenetic species concept. *In:* Fuentes A. The International Encyclopedia of Primatology. Hoboken, NJ: John Wiley & Sons, Inc., 1–2.

Groves CP, Grubb P. 2011. Ungulate Taxonomy. Baltimore: Johns Hopkins University Press.

Groves CP, Cotterill FPD, Gippoliti S, Robovský J, Roos C, Taylor PJ, Zinner D. 2017. Species definitions and conservation: a review and case studies from African mammals. *Conservation Genetics,* **18**(6): 1247–1256.

Gutiérrez EE, Jansa SA, Voss RS. 2010. Molecular systematics of mouse opossums (Didelphidae: *Marmosa*): assessing species limits using mitochondrial DNA sequences, with comments on phylogenetic relationships and biogeography. *American Museum Novitates,* **3692**: 1–22.

Gutiérrez EE, Helgen KM. 2013. Outdated taxonomy blocks conservation. *Nature,* **495**(7441): 314.

Gutiérrez EE, Helgen KM, McDonough MM, Bauer F, Hawkins MTR, Escobedo-Morales LA, Patterson BD, Maldonado JE. 2017. A gene-tree test of the traditional taxonomy of American deer: the importance of voucher specimens, geographic data, and dense sampling. *ZooKeys,* **697**: 87–131.

Gutiérrez EE, Maldonado JE, Radosavljevic A, Molinari J, Patterson BD, Martínez-C JM, Rutter AR, Hawkins MTR, Garcia FJ, Helgen KM. 2015. The taxonomic status of *Mazama bricenii* and the significance of the Táchira depression for mammalian endemism in the cordillera de Mérida, Venezuela. *PLoS One,* **10**(6): e0129113.

Hawkins MTR, Helgen KM, Maldonado JE, Rockwood LL, Tsuchiya MTN, Leonard JA. 2016. Phylogeny, biogeography and systematic revision of plain long-nosed squirrels (genus *Dremomys*, Nannosciurinae). *Molecular Phylogenetics and Evolution,* **94**: 752–764.

Helgen KM, Kays R, Helgen LE, Tsuchiya-Jerep MTN, Pinto CM, Koepfli KP, Eizirik E, Maldonado JE. 2009. Taxonomic boundaries and geographic distributions revealed by an integrative systematic overview of the mountain coatis, *Nasuella* (Carnivora: Procyonidae). *Small Carnivore Conservation,* **41**: 65–74.

Helgen KM, Pinto CM, Kays R, Helgen LE, Tsuchiya MTN, Quinn A, Wilson DE, Maldonado JE. 2013. Taxonomic revision of the olingos (*Bassaricyon*), with description of a new species, the Olinguito. *ZooKeys,* **324**: 1–83.

Heller R, Frandsen P, Lorenzen ED, Siegismund HR. 2013. Are there really twice as many bovid species as we thought? *Systematic Biology,* **62**(3): 490–493.

Heller R, Frandsen P, Lorenzen ED, Siegismund HR. 2014. Is diagnosability an indicator of speciation? Response to "Why one century of phenetics is enough". *Systematic Biology,* **63**(5): 833–837.

Holbrook LT. 2013. Taxonomy interrupted. *Journal of Mammalian Evolution,* **20**(2): 153–154.

Hörandl E. 2006. Paraphyletic versus monophyletic taxa-evolutionary versus cladistic classifications. *Taxon,* **55**(3): 564–570.

Hörandl E. 2007. Neglecting evolution is bad taxonomy. *Taxon,* **56**(1): 1–5.

Isaac NJB, Mallet J, Mace GM. 2004. Taxonomic inflation: its influence on macroecology and conservation. *Trends in Ecology & Evolution,* **19**(9): 464–469.

Janečka JE, Helgen KM, Lim NTL, Baba M, Izawa M, Boeadi, Murphy WJ. 2008. Evidence for multiple species of Sunda colugo. *Current Biology,* **18**(21): R1001–R1002.

Knowles LL, Carstens BC. 2007. Delimiting species without monophyletic gene trees. *Systematic Biology,* **56**(6): 887–895.

Koepfli KP, Kanchanasaka B, Sasaki H, Jacques H, Louie KDY, Hoai T, Dang NX, Geffen E, Gutleb A, Han SY, Heggberget TM, LaFontaine L, Lee H, Melisch R, Ruiz-Olmo J. 2008. Establishing the foundation for an applied molecular taxonomy of otters in Southeast Asia. *Conservation Genetics,* **9**(6): 1589–1604.

Maddison WP. 1997. Gene trees in species trees. *Systematic Biology,* **46**(3): 523–536.

Mantilla-Meluk H. 2013. Subspecific variation: an alternative biogeographic hypothesis explaining variation in coat color and cranial morphology in *Lagothrix lugens* (Primates: Atelidae). *Primate Conservation,* **26**: 33–48.

Martínez-Lanfranco JA, Flores D, Jayat JP, d'Elía G. 2014. A new species of lutrine opossum, genus *Lutreolina* Thomas (Didelphidae), from the South American Yungas. *Journal of Mammalogy,* **95**(2): 225–240.

Mayden RL. 1997. A hierarchy of species concepts: the denouement in the saga of the species problem. *In:* Claridge MF, Dawah HA, Wilson MR. Species: The Units of Biodiversity. London: Chapman & Hall, 381–423.

McKitrick MC, Zink RM. 1988. Species concepts in ornithology. *The Condor,* **90**(1): 1–14.

Meijaard E, Chua MAH, Duckworth JW. 2017. Is the northern chevrotain, *Tragulus williamsoni* Kloss, 1916, a synonym or one of the least-documented mammal species in Asia? *Raffles Bulletin of Zoology,* **65**: 506–514.

Miller GS. 1912. A small collection of bats from Panama. *Proceedings of the United States National Museum,* **42**(1882): 21–26.

Miranda FR, Casali DM, Perini FA, Machado FA, Santos FR. 2017. Taxonomic review of the genus *Cyclopes* Gray, 1821 (Xenarthra, Pilosa), with the revalidation and description of new species. *Zoological Journal of the Linnean Society,* doi: 10.1093/zoolinnean/zlx079/4716749.

Molinari J, Bustos XE, Burneo SF, Camacho MA, Moreno SA, Fermín G. 2017. A new polytypic species of yellow-shouldered bats, genus *Sturnira* (Mammalia: Chiroptera: Phyllostomidae), from the Andean and coastal mountain systems of Venezuela and Colombia. *Zootaxa,* **4243**(1): 75–96.

Moras LM, Tavares VC, Pepato AR, Santos FR, Gregorin R. 2016. Reassessment of the evolutionary relationships within the dog-faced bats, genus *Cynomops* (Chiroptera: Molossidae). *Zoologica Scripta,* **45**(5): 465–480.

Nelson G, Murphy DJ, Ladiges PY. 2003. Brummitt on paraphyly: a response. *Taxon,* **52**(2): 295–298.

Nixon KC, Wheeler QD. 1990. An amplification of the phylogenetic species concept. *Cladistics,* **6**(3): 211–223.

Patton JL, Pardiñas UFJ, D'Elía G. 2015. Mammals of South America, volume 2: Rodents. Chicago, London: University of Chicago Press.

Pavan SE, Mendes-Oliveira AC, Voss RS. 2017. A new species of *Monodelphis* (Didelphimorphia: Didelphidae) from the Brazilian amazon. *American Museum Novitates,* **3872**: 1–20.

Peres CA, Patton JL, Da Silva MNF. 1996. Riverine barriers and gene flow in Amazonian saddle-back tamarins. *Folia Primatologica,* **67**(3): 113–124.

Pine RH, Gutiérrez EE. 2018. What is an 'extant' type specimen? Problems arising from naming mammalian species-group taxa without preserved types. *Mammal Review.* DOI: 10.1111/mam.12108

Pocock RI. 1941. The races of the ocelot and the margay. *Field Museum of Natural History, Zoological Series*, **27**: 319–369.

Robinson W, Lyon Jr MW. 1901. An annotated list of mammals collected in the vicinity of La Guaira, Venezuela. *Proceedings of the United States National Museum,* **24**(1246): 135–162.

Rogers DS, González MW. 2010. Phylogenetic relationships among spiny pocket mice (*Heteromys*) inferred from mitochondrial and nuclear sequence data. *Journal of Mammalogy,* **91**(4): 914–930.

Rosen DE. 1978. Vicariant patterns and historical explanation in biogeography. *Systematic Biology,* **27**(2): 159–188.

Simpson GG. 1961. Principles of Animal Taxonomy. New York: Columbia University Press.

Solari S. 2004. A new species of *Monodelphis* (Didelphimorphia: Didelphidae) from southeastern Peru. *Mammalian Biology-Zeitschrift für Säugetierkunde,* **69**(3): 145–152.

Tattersall I. 2007. Madagascar's lemurs: cryptic diversity or taxonomic inflation? *Evolutionary Anthropology: Issues, News, and Reviews,* **16**(1): 12–23.

Tinbergen N. 1959. Behaviour, systematics, and natural selection. *IBIS,* **101**(3–4): 318–330.

Tobias JA, Seddon N, Spottiswoode CN, Pilgrim JD, Fishpool LDC, Collar NJ. 2010. Quantitative criteria for species delimitation. *IBIS,* **152**(4): 724–746.

Tsang SM, Cirranello AL, Bates PJJ, Simmons NB. 2016. The roles of taxonomy and systematics in bat conservation. *In:* Voigt CC, Kingston T. Bats in the Anthropocene: Conservation of Bats in a Changing World. Cham: Springer.

Thinh VN, Mootnick AR, Thanh VN, Nadler T, Roos C. 2010. A new species of crested gibbon, from the central Annamite mountain range. *Vietnamese Journal of Primatology,* **4**: 1–12.

van Roosmalen MGM, Frenz L, van Hooft P, De Iongh HH, Leirs H. 2007. A new species of living peccary (Mammalia: Tayassuidae) from the Brazilian Amazon. *Bonner Zoologische Beiträge,* **55**(2): 105–112.

van Roosmalen MGM, van Roosmalen T, Mittermeier RA, Rylands AB. 2000. Two new species of marmoset, genus *Callithrix* erxleben, 1777 (Callitrichidae, Primates), from the Tapajós/Madeira interfluvium, South Central Amazonia, Brazil. *Neotropical Primates,* **8**: 2–18.

Van Valen L. 1976. Ecological species, multispecies, and oaks. *Taxon,* **25**(2–3): 233–239.

Velazco PM, Gardner AL, Patterson BD. 2010. Systematics of the *Platyrrhinus helleri* species complex (Chiroptera: Phyllostomidae), with descriptions of two new species. *Zoological Journal of the Linnean Society,* **159**(3): 785–812.

Voss RS, Hubbard C, Jansa SA. 2013. Phylogenetic relationships of New World porcupines (Rodentia, Erethizontidae): implications for taxonomy, morphological evolution, and biogeography. *American Museum Novitates,* **3769**: 1–36.

Voss RS, Díaz-Nieto JF, Jansa SA. 2018. A revision of *Philander* (Marsupialia: Didelphidae), Part 1: *P. quica*, *P. canus*, and a new species from Amazonia. *American Museum Novitates,* **3891**: 1–70.

Wheeler QD, Meier R. 2000. Species Concepts and Phylogenetic Theory: A Debate. New York: Columbia University Press.

Wiens JJ, Servedio MR. 2000. Species delimitation in systematics: inferring diagnostic differences between species. *Proceedings of the Royal Society B: Biological Sciences,* **267**(1444): 631–636.

Zachos FE. 2009. Gene trees and species trees–mutual influences and interdependences of population genetics and systematics. *Journal of Zoological Systematics and Evolutionary Research,* **47**(3): 209–218.

Zachos FE, Apollonio M, Bärmann EV, Festa-Bianchet M, Göhlich U, Habel JC, Haring E, Kruckenhauser L, Lovari S, McDevitt AD, Pertoldi C, Rössner GE, Sánchez-Villagra MR, Scandura M, Suchentrunk F. 2013. Species inflation and taxonomic artefacts—a critical comment on recent trends in mammalian classification. *Mammalian Biology-Zeitschrift für Säugetierkunde,* **78**(1): 1–6.

Zachos FE. 2013. Species splitting puts conservation at risk. *Nature,* **494**(7435): 35.

Zachos FE, Lovari S. 2013. Taxonomic inflation and the poverty of the Phylogenetic Species Concept-a reply to Gippoliti and Groves. *Hystrix,* **24**(2): 142–144.

Zachos FE. 2014a. Commentary on taxonomic inflation, species delimitation and classification in Ruminantia. *Zitteliana B,* **32**: 213–216.

Zachos FE. 2014b. Paraphyly—again!? A plea against the dissociation of taxonomy and phylogenetics. *Zootaxa,* **3764**(5): 594–596.

Zachos FE. 2015. Taxonomic inflation, the phylogenetic species concept and lineages in the tree of life–a cautionary comment on species splitting. *Journal of Zoological Systematics and Evolutionary Research,* **53**(2): 180–184.

Zachos FE. 2016a. Species Concepts in Biology: Historical Development, Theoretical Foundations and Practical Relevance. Cham: Springer.

Zachos FE. 2016b. Tree thinking and species delimitation: guidelines for taxonomy and phylogenetic terminology. *Mammalian Biology-Zeitschrift für Säugetierkunde,* **81**(2): 185–188.

Zander RH. 2007. Paraphyly and the species concept, a reply to Ebach & al. *Taxon,* **56**(3), 642–644.

How many species of *Apodemus* and *Rattus* occur in China? A survey based on mitochondrial cyt *b* and morphological analyses

Shao-Ying Liu[1,*], Kai He[2], Shun-De Chen[2,3], Wei Jin[1], Robert W. Murphy[4], Ming-Kun Tang[1], Rui Liao[1], Feng-Jun Li[3]

[1] *Sichuan Academy of Forestry, Chengdu Sichuan* 610081*, China*
[2] *Kunming Institute of Zoology, Chinese Academy of Sciences, Kunming Yunnan* 650223*, China*
[3] *College of Life Sciences, Sichuan Normal University, Chengdu Sichuan* 610066*, China*
[4] *Centre for Biodiversity and Conservation Biology, Royal Ontario Museum, Toronto* M5S 2C6*, Canada*

ABSTRACT

Apodemus (mice) and *Rattus* (rats) are the top rodent reservoirs for zoonoses in China, yet little is known about their diversity. We reexamined the alpha diversity of these two genera based on a new collection of specimens from China and their cyt *b* sequences in GenBank. We also tested whether species could be identified using external and craniodental measurements exclusively. Measurements from 147 specimens of *Apodemus* and 233 specimens of *Rattus* were used for morphological comparisons. We analysed 74 cyt *b* sequences of *Apodemus* and 100 cyt *b* sequences of *Rattus* to facilitate phylogenetic estimations. Results demonstrated that nine species of *Apodemus* and seven species of *Rattus*, plus a new subspecies of *Rattus nitidus*, are distributed in China. Principal component analysis using external and craniodental measurements revealed that measurements alone could not separate the recognized species. The occurrence of *Rattus pyctoris* in China remains uncertain.

Keywords: Alpha diversity; *Apodemus*; DNA-barcoding; *Rattus*; Taxonomy; Phylogenies; New subspecies

INTRODUCTION

Small volant and nonvolant mammals are important components of ecological communities and play vital roles in ecological systems. They are among the most common agents for infections and, thus, have strongly affected human history. For example, black rats (*Rattus rattus*) are considered likely agents for the spread of Oriental rat fleas, which drove the Black Death plague throughout Europe and the Mediterranean during the 14th century and killed 30%–60% of the European population (Barnett, 2001; Duplantier et al., 2003). More recent examples of small mammal zoonoses include severe acute respiratory syndrome (SARS) caused by a coronavirus and Ebola hemorrhagic fever caused by *Ebolavirus*, with hosts including, but not limited to, bats and civets (Klein & Calisher, 2007; Menachery et al., 2015). Rodent-borne diseases such as plague and hantavirus have made considerable contributions to human illnesses and are responsible for more deaths than all wars combined (Klein & Calisher, 2007). New pathogens, especially hantaviruses, have been isolated from rodents in China and adjacent countries annually (Huang et al., 2017). Because different species have specific immune systems and different levels of tolerance to zoonotic infections, identification of rodent reservoirs of zoonotic pathogens is a high priority (Meerburg et al., 2009).

Rats and mice often top the zoonoses reservoir list of the Chinese Center for Disease Control and Prevention (China CDC) because of the large number of species, substantial population sizes, and high potential for carrying zoonotic pathogens (Wu et al., 2017). Unfortunately, we still do not know how many species of rats and mice occur in

Received: 20 March 2018; Accepted: 07 May 2018; Online: 19 June 2018

Foundation items: This research was funded by the National Natural Science Foundation of China (31470110; 31301869; 31670388), Key Research Program of the Chinese Academy of Sciences (KJZD-EW-L07), Yunnan Applied Basic Research Projects (2014FB176), and China Postdoctoral Science Foundation (2015M570801)

[*]Corresponding author, E-mail: shaoyliu@163.com

DOI: 10.24272/j.issn.2095-8137.2018.053

China, or which species carry what pathogens, even for the most common genera such as *Apodemus* and *Rattus*. The reasons for this are complicated. Both *Apodemus* and *Rattus* have complex evolutionary and taxonomic histories, with classifications continuously being updated. Switching between valid species and synonyms causes considerable confusion, especially for non-specialist researchers. Furthermore, many species occur only in remote mountains or near national borders with high species diversity, such as Yunnan, Xizang (Tibet), and Xinjiang. Indeed, the rats and mice of southern Xizang and western Xinjiang remain to be studied carefully. Finally, many rodents are difficult to identify to species level due to the number of morphologically similar species (Galan et al., 2012).

The latest version of Mammal Species of the World (Musser & Carleton, 2005) recognized 20 species of *Apodemus* and 162 synonyms. Several scenarios for the classification of *Apodemus* have been proposed (Filippucci, 1992; Martin et al., 2000; Musser et al., 1995; Serizawa et al., 2000; Zimmermann, 1962), but none are strongly supported, and phylogenies remain poorly resolved despite molecular efforts (Liu et al., 2004; Serizawa et al., 2000; Suzuki et al., 2003). Furthermore, the number of species in China remains unknown, with previous estimations varying from six (Corbet, 1978; Xia, 1984), seven (Liu et al., 2002; Liu et al., 2004), eight (Smith et al., 2008), and nine species (Nowak, 1999; Wang, 2003). Many authors have suggested that *A. sylvaticus* occurs in Xinjiang, China (Corbet, 1978; Xia, 1984; Wang, 2003), whereas others have argued that the species is *A. uralensis* (Smith et al., 2008). The former species occurs in Western Europe (Bousbouras, 1999; Macholán et al., 2001; Mezhzherin & Zykov, 1991; Michaux et al., 1996), and its incorrect identification in China likely relates to outdated taxonomy.

Rattus, another problematic genus, has had 25 subgenera and more than 550 species and subspecies named (Simpson, 1945). Currently, 66 species are recognized but uncertainty persists. Previous supermatrix analysis did not obtain a monophyletic *Rattus*, indicating that systematics is far from resolved (Steppan & Schenk, 2017). Arguments also persist for the most common species, including black rats whose species boundary remains unfixed (Aplin et al., 2011). The number of species of *Rattus* in China is also uncertain and varies from four (Corbet, 1978), seven (Smith et al., 2008), and nine (Wang, 2003).

Similar to other rodents, species in these two genera are difficult to identify or distinguish morphologically due to their similar appearance, overlapping measurements, and key factors involving the single cusp on their teeth. Diagnosis often requires clean skulls, which are not always available or correctly prepared. DNA barcoding is a promising approach but requires a solid reference database (Moritz & Cicero, 2004). Unfortunately, GenBank data are problematic because many rodent sequences are uploaded by non-specialists such as epidemiological researchers. This reduces the reliability of environmental assessment reports and hampers our understanding of host and disease associations.

Herein, we revisited the alpha diversity of *Apodemus* and *Rattus* in China based on a collection of more than 400 specimens and the integration of cyt *b* sequences. We evaluated the species of both genera in China and assessed if they could be identified easily using traditional morphometric approaches.

MATERIALS AND METHODS

Morphological diagnoses and analyses

We examined 147 specimens of *Apodemus* and 233 specimens of *Rattus* collected from multiple localities across China. External and skull measurements followed Liu et al. (2012). External measurements of fresh specimens in the field were taken to the nearest 0.5 mm using a steel tape. These included head-body length (HBL), hind-foot length (HFL), ear length (EL) and tail length (TL) (museum specimens from original records). We measured eight skull variables using a digital caliper graduated to the nearest 0.01 mm from 147 intact skulls of *Apodemus* and 233 intact skulls of *Rattus*, including greatest length of skull (SGL), nasal bone length (NBL), zygomatic breadth (ZB), skull basal length (SBL), upper toothrow length (UTRL), upper molar row length (UMRL), auditory bulla length (ABL), and mandible length (ML). Examined specimens (Supplementary Table S1) were deposited in the Kunming Institute of Zoology (KIZ), Sichuan Academy of Forestry (SAF), Beijing Institute of Zoology (BIZ), Guangdong Key Laboratory of Animal Conservation and Resource Utilization, and Fujian Center for Disease Control Prevention.

Specimens were roughly identified based on external and craniodental morphology, following Kaneko (2010) and Smith et al. (2008). External and craniodental measurements largely overlapped between species (see Results) and were inadequate for identification. However, several diagnostic characters on the upper molars were constructive in classification, including the number of lingual angles of the first and second upper molar, presence/absence of cusp t3 on the first upper molar, and numbers of internal lobes on the third upper molars. We also cross-checked results based on morphological diagnoses with molecular sequences (when available) to refine identification. All specimens were identified by the same researcher (SYL) for consistency. We finally assigned our specimens to nine species of *Apodemus*, seven species of *Rattus*, and a new subspecies of *Rattus nitidus*, respectively.

We analyzed morphometric variation using principal component analyses (PCAs) on log10-transformed variables using two datasets for each species. The first dataset included both external and craniomandibular variables, whereas the second dataset included craniomandibular variables only. Inclusion of the external data tested whether these measurements could increase the accuracy of identification. Statistical analysis was performed using SPSS v16.0 (SPSS Inc., USA). When two or more recognized species were not well separated in the principal component (PC) plots, analysis of variance (ANOVA) was applied to analyze among group differences.

Molecular analysis

We sequenced mitochondrial cyt *b* for 74 and 100 specimens of *Apodemus* and *Rattus*, respectively. Localities of molecular samples used from China are mapped in Figure 1. All sequenced specimens were deposited in the SAF. Total genomic DNA was extracted using the standard phenol-chloroform method (Sambrook & Russell, 2001). We used the universal primers of mammalian cyt *b* L14724/H15915 for amplification (Irwin et al., 1991). Polymerase chain reaction (PCR) was conducted in a 25-μL reaction volume, including 2.5 μL of 10×EX Taq buffer (Mg^{2+} Free), 2 μL of 2.5 mmol/L dNTP, 1.5 μL of 25 mmol/L $MgCl_2$, 1 μL of 10 μmol/L primers, and 1 unit of EX Taq polymerase (TaKaRa Biotech, Dalian, China). The product was purified using an EZNA™ Gel Extraction Kit (Omega, USA), and was sequenced using the same primers for amplification on an ABI 3730XL sequencer. Sequences were assembled and edited using SeqMan and EditSeq (DNASTAR, Lasergene v7.1) before subsequent analyses.

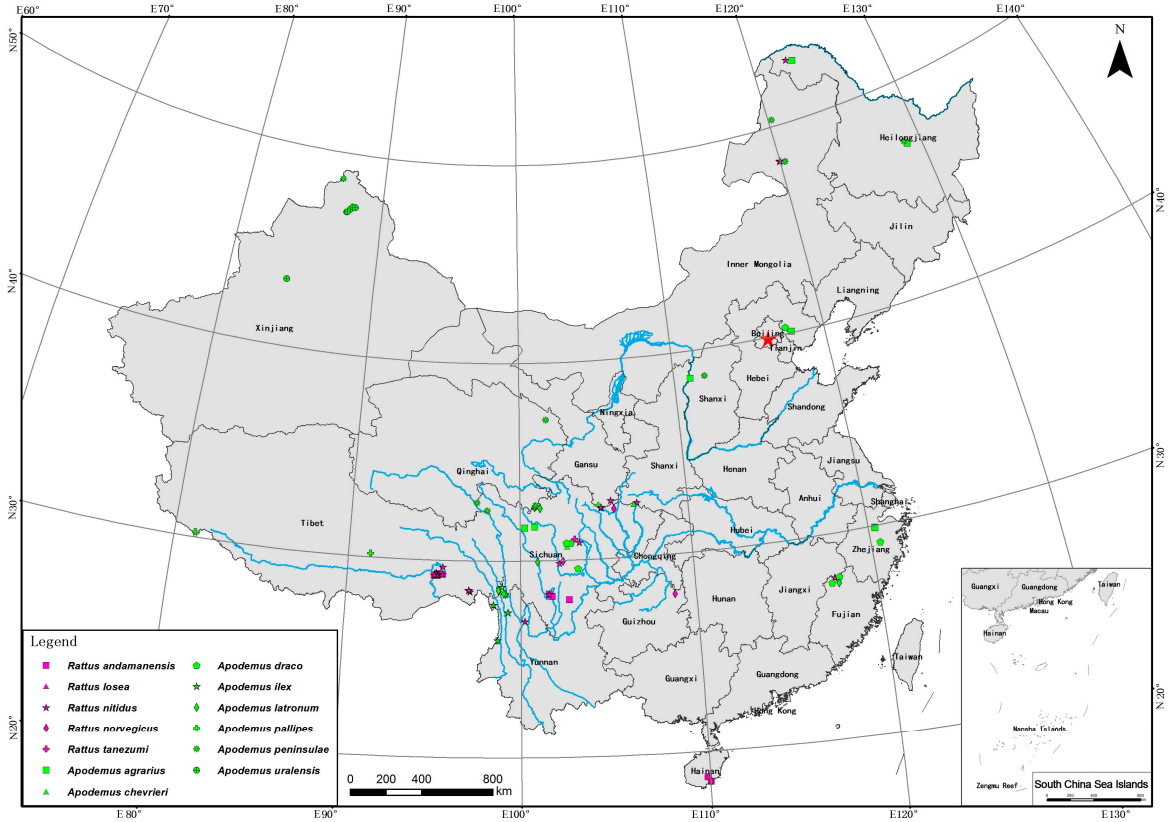

Figure 1 Localities of molecular samples from China in this study

To avoid misidentification, we first conducted a "naïve identification" for the obtained sequences using the "identify organism" workflow in Geneious v11 (Biomatters, New Zealand). The software blasted each sequence against the GenBank nucleotide collection (nr/nt) database. When pairwise identity between the query (our sequence) and subject (in GenBank) sequences was higher 98%, Geneious considered them as the same species. We cross-checked the results of both morphological and molecular identifications, and when the identification was inconsistent, we revisited the skin and skull specimens before applying an identity.

To provide a better picture of species diversity in China, we downloaded cyt *b* sequences of *Apodemus* (*n*=477) and *Rattus* (*n*=273) in China from GenBank, discarding sequences shorter than 800 bp. We also included cyt *b* data representing another 12 species of *Apodemus* and 14 species of *Rattus* from outside of China. An additional five sequences of *R. pyctoris* from Nepal were included. For better estimation of phylogenetic relationships, we downloaded the mitochondrial genomes (mitogenomes) of seven species of *Apodemus* and 14 species of *Rattus* (Supplementary Table S2). One mitogenome under the name of "*Apodemus chejuensis*" may not have been a valid species. Cyt *b* of *Tokudaia* spp. (*n*=3) and a mitogenome of *Bandicota indica* were selected as outgroup representatives for *Apodemus* and *Rattus*, respectively, following Steppan & Schenk (2017). In total, the datasets for *Apodemus* and *Rattus* included 572 (with seven mitogenomes) and 397 sequences (15 mitogenomes), respectively. We aligned the sequences for

each genus using MAFFT v7.3 implemented in Geneious v11. We removed all tRNAs, D-loop, and *ND6* sequences from the alignments, and only used rRNAs and 13 protein-coding genes for phylogenetic analyses. Sequence genetic distances were calculated for cyt *b* using MEGA v.5 (Tamura et al., 2011) under the Kimura 2-parameter model (Kimura, 1980).

Phylogenetic analyses

We employed RAxML v8.2.10, a maximum likelihood-based approach, for phylogenetic analyses. We partitioned the alignments by genes, except for cyt *b*, which we partitioned into the 1st+2nd and 3rd codon positions. Analyses were performed on the CIPRES Science Gateway. We used GTR+G as the evolutionary model for each partition because RAxML does not accept models other than GTR or GTR+G. We ran each analysis using the rapid bootstrapping algorithm and let RAxML halt bootstrapping automatically. We also repeated analyses using alternative strategies, such as different partitioning schemes (e.g., partitioned by gene and codon positions for all coding genes) and evolutionary models (e.g., using GTR model instead of GTR+G), none of which strongly altered phylogenetic relationships (i.e., different relationships supported by bootstrap values (BS) $\geq$75)).

RESULTS

Morphological analysis

Morphological analysis of *Apodemus*

Morphological measurement statistics of the eight *Apodemus* species, excluding *A. semotus*, are given in Table 1. In the first PCA, using all 12 measurements (n=139), the first and second principal components accounted for 57.6% (eigenvalue=6.9; Table 2, a) and 11.7% (eigenvalue=1.4) of total variation, respectively, with all other principal components having eigenvalues smaller than 1. PC1 was positively correlated with all craniodental variables (loadings>0.63), and PC2 was positively correlated with external measurements (loadings>0.55). The PC1 and PC2 plot (Figure 2A) did not clearly separate the species. *Apodemus latronum* plotted on the positive regions of PC1 and PC2, indicating a large body, long tail, long hindfeet, and long ears. In accordance with its small skull and small external measurements, *A. uralensis* occurred along the negative regions of PC1 and PC2. The sister- or closely related species *A. agrarius* and *A. chevrieri* as well as *A. pallipes* and *A. uralensis* were well separated, but both pairs overlapped with *A. peninsulae*, *A. draco*, and *A. ilex*, which, in turn, largely overlapped. For the second PCA, using eight craniodental measurements (n=141), the first principal component accounted for 69.5% of variation (eigenvalue=5.6; Table 2, b). The other principal components accounted for less than 9.4% (eigenvalue$\leq$0.75) of total variation, indicating they were not stable (Shankardass, 2000). Seven variables were positively correlated with PC1 (loading>0.56), except for UMRL (loading=0.076), which was positively correlated with PC2 (loading=0.93). The PC1 and PC2 plot (Figure 2B) was similar to the previous plot. None of these species were clearly separated from all others. *Apodemus chevrieri* and *A. latronum* plotted on the positive regions of PC1, indicating a relatively large skull, and *A. uralensis* occurred along the negative region of PC1 in accordance with its small skull.

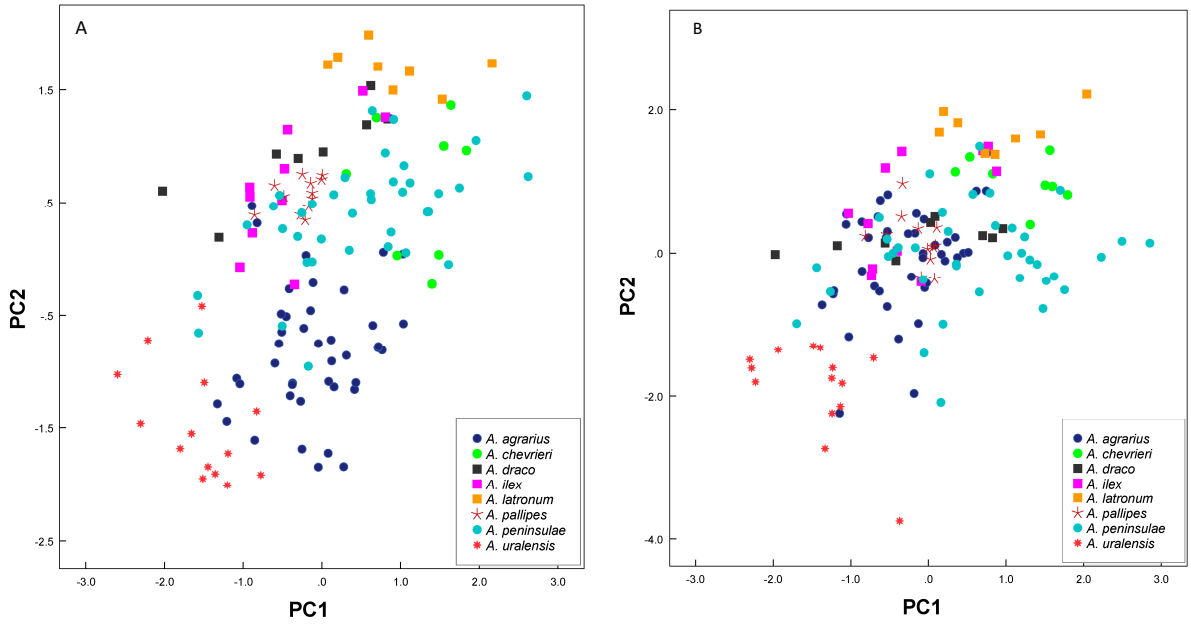

Figure 2 Principal component analysis of the first three principal components among the eight species of *Apodemus* based on both external and craniomandibular variables (A) and craniomandibular variables only (B)

Table 1 Measurement statistics of *Apodemus*

	SGL					NBL					ZB					SBL				
	n	**Mean**	***SD***	**Minimum**	**Maximum**	**Mean**	***SD***	**Minimum**	**Maximum**	**Mean**	***SD***	**Minimum**	**Maximum**	**Mean**	***SD***	**Minimum**	**Maximum**
A. latronum	15	28.03	2.54	20.23	30.86	11.12	0.60	9.70	12.17	13.41	0.67	12.38	14.96	25.21	1.58	22.37	27.52
A. peninsulae	38	27.76	1.60	24.31	31.75	10.64	1.02	8.09	12.42	13.49	0.96	12.01	15.35	25.58	1.87	22.50	29.81
A. chevrieri	8	29.02	0.83	27.83	29.99	10.65	0.74	9.16	11.63	13.63	0.34	13.06	14.02	26.29	1.24	24.47	27.57
A. agrarius	41	26.57	0.97	24.55	28.51	9.55	0.53	8.50	10.67	12.56	0.52	11.23	13.34	24.65	1.20	20.82	26.73
A. ilex	10	26.63	1.25	25.31	28.88	10.10	0.79	9.13	11.44	12.61	0.37	12.09	13.31	23.42	1.19	22.17	25.45
A. draco	9	26.80	1.63	23.83	29.19	10.56	1.06	8.65	11.80	12.59	0.52	11.83	13.27	23.64	1.59	20.97	25.41
A. pallipes	12	26.84	0.58	25.76	27.98	10.37	0.37	9.45	10.95	12.73	0.26	12.26	13.13	23.63	0.56	22.37	24.30
A. uralensis	14	24.37	0.89	22.49	25.45	8.72	0.48	7.96	9.74	12.38	0.52	11.68	13.20	22.66	0.96	20.49	23.82
	UTRL					**UOSL**				**TBL**				**ML**			
	n	**Mean**	***SD***	**Minimum**	**Maximum**	**Mean**	***SD***	**Minimum**	**Maximum**	**Mean**	***SD***	**Minimum**	**Maximum**	**Mean**	***SD***	**Minimum**	**Maximum**
A. latronum	15	14.41	0.76	12.94	15.60	5.00	0.23	4.47	5.39	5.52	0.35	4.90	6.38	10.48	3.58	6.16	14.41
A. peninsulae	38	13.71	0.94	11.52	15.82	4.27	0.29	3.41	5.10	5.34	0.40	4.53	6.17	13.25	1.11	11.02	15.79
A. chevrieri	8	14.55	0.64	13.57	15.52	4.59	0.23	4.24	4.91	5.90	0.25	5.52	6.19	14.61	0.67	13.70	15.74
A. agrarius	41	12.97	0.73	10.99	14.64	4.18	0.27	3.45	4.84	5.22	0.31	4.55	5.69	12.61	0.70	10.28	14.06
A. ilex	10	12.74	0.66	11.98	13.95	4.42	0.37	3.97	4.97	5.33	0.25	4.90	5.73	13.21	0.83	11.97	14.97
A. draco	9	13.10	0.72	11.98	14.03	4.24	0.06	4.15	4.35	5.23	0.35	4.50	5.62	13.03	1.09	11.36	14.32
A. pallipes	12	13.25	0.32	12.73	13.83	4.34	0.16	4.14	4.67	4.83	0.13	4.62	5.12	13.51	0.40	12.98	14.10
A. uralensis	14	11.23	0.47	10.51	12.00	3.60	0.25	2.89	3.82	4.68	0.29	4.30	5.23	11.57	0.50	10.50	12.28
	HBL					**TL**				**HFL**				**EL**			
	n	**Mean**	***SD***	**Minimum**	**Maximum**	**Mean**	***SD***	**Minimum**	**Maximum**	**Mean**	***SD***	**Minimum**	**Maximum**	**Mean**	***SD***	**Minimum**	**Maximum**
A. latronum	15	100.90	9.84	88.00	115.00	104.27	8.41	90.00	122.00	24.17	0.98	22.50	26.00	20.20	0.80	19.00	22.00
A. peninsulae	38	100.32	11.96	73.00	137.00	94.26	10.96	72.00	121.00	22.95	1.59	18.00	25.00	16.08	1.58	14.00	21.00
A. chevrieri	8	102.50	8.78	90.00	113.00	94.12	9.40	82.00	105.00	23.63	1.69	21.00	26.00	16.12	1.89	13.00	18.00
A. agrarius	41	100.17	8.28	85.00	120.00	82.54	11.55	50.00	101.00	19.55	1.86	14.00	24.00	13.39	1.05	12.00	16.00
A. ilex	10	86.30	5.83	80.00	98.00	92.80	11.24	72.00	107.00	21.90	1.10	20.00	24.00	17.50	1.43	15.00	19.00
A. draco	9	92.11	9.85	75.00	103.00	105.11	12.08	84.00	119.00	48.89	77.30	21.00	255.00	17.33	0.71	16.00	18.00
A. pallipes	12	93.75	3.93	87.00	99.00	95.67	4.14	90.00	104.00	21.58	0.67	21.00	23.00	16.58	0.52	16.00	17.00
A. uralensis	14	83.86	7.31	67.00	94.00	74.36	4.99	65.00	83.00	19.82	1.14	18.00	22.00	12.11	2.65	9.00	17.00

Abbreviations are explained in the Materials and Methods section. All measurements are in mm.

One-way analysis of variance (ANOVA) revealed that the seven species differed significantly (P<0.05) in all external and cranial characters tested, except for NBL (P=0.497), TL (P=0.064), and HFL (P=0.094). Results showed significant differences as follows: UTRL, MRL, ABL, and ML between *A. peninsulae* and *A. chevrieri*; ZB, SBL, UTRL, HBL, and EL between *A. peninsulae* and *A. ilex*; SGL, ZB, SBL, HBL, TL, HFL, and EL between *A. peninsulae* and *A. draco*; ZB, SBL, and ABL between *A. peninsulae* and *A. pallipes*; SGL, ZB, SBL, UTRL, ABL, ML, HBL, and EL between *A. chevrieri* and *A. ilex*; SGL, ZB, SBL, MRL, UTRL, ABL, ML, HBL, TL, and HFL between *A. chevrieri* and *A. draco*; SGL, ZB, SBL, UTRL, MRL, ABL, and ML between *A. chevrieri* and *A. pallipes*; TL and HFL between *A. ilex* and *A. draco*; and ABL, TL, and HFL between *A. draco* and *A. pallipes*. Thus, morphological analysis indicated that the eight species of *Apodemus* could be separated by the 12 morphological characters, validating the taxonomic status of these species in China.

Table 2 Factor loadings and percentage of variance explained for principal component analysis

	Apodemus				*Rattus*			
	a		b		c		d	
Variables	**PC1**	**PC2**	**PC1**	**PC2**	**PC1**	**PC2**	**PC1**	**PC2**
SGL	0.82	0.07	0.83	0.08	0.96	–0.05	0.97	–0.03
NBL	0.64	0.39	0.84	0.08	0.89	–0.06	0.90	–0.03
ZB	0.83	0.00	0.99	–0.24	0.92	–0.08	0.92	–0.08
SBL	1.01	–0.17	0.95	–0.09	0.97	–0.08	0.97	0.01
UTRL	0.80	0.23	0.72	0.37	0.95	–0.16	0.97	–0.19
UMRL	0.29	0.55	0.08	0.93	0.71	0.15	0.71	–0.35
ABL	0.77	0.00	0.56	0.34	0.68	0.14	0.70	0.65
ML	0.64	0.24	0.71	0.17	0.92	–0.14	0.93	0.02
HBL	0.69	–0.09	N/A	N/A	0.79	–0.25	N/A	N/A
TL	0.13	0.74	N/A	N/A	0.67	0.52	N/A	N/A
HZL	–0.04	0.82	N/A	N/A	0.74	–0.24	N/A	N/A
EL	–0.09	0.94	N/A	N/A	0.40	0.84	N/A	N/A
Eigenvalues	6.9	1.4	5.60	0.75	7.99	1.21	6.32	0.57
Total variance explained (%)	57.6	11.7	69.50	9.40	66.54	10.08	79.05	7.08

For abbreviations see Materials and Methods. N/A: Not available.

Morphological analysis of *Rattus*

Morphological measurement statistics of the seven species of *Rattus* and a putatively new subspecies of *R. nitidus* (from southern Xizang) are given in Table 3. In the first PCA, which used all 12 measurements (n=233), the first and second principal components accounted for 66.54% (eigenvalue=7.99) and 10.08% (eigenvalue=1.21) of total variation, respectively (Table 2, c), with all other principal components having eigenvalues smaller than 1. Most species largely overlapped (Figure 3A). In the second PCA, which used eight craniodental measurements (n=233), the first and second principal components accounted for 79.05% (eigenvalue=6.32) and 7.08% (eigenvalue=0.57) of total variation, respectively (Table 2, d). The PC1 and PC2 plot (Figure 3B) revealed largely overlapping species.

One-way ANOVA demonstrated significant differences (P<0.05) between the seven species in all external and cranial characters tested. Results showed significant differences as follows: SGL, NBL, ZB, SBL, UTRL, UMRL, ML, BL, HBL, HFL, and EL between *R. nitidus* and *R. losea*; NBL, UTRL, and HFL between *R. nitidus* and *R. tanezumi*; HBL and HFL between *R. nitidus* and *R. andamanensis*; BL, HBL, and EL between *R. nitidus* and *R. norvegicus*; SGL, NBL, ZB, SBL, UTRL, UMRL, ML, BL, HFL, and EL between *R. nitidus* and *R. exulans*; SGL, ZB, SBL, UMRL, HBL, HFL, and EL between *R. losea* and *R. tanezumi*; SGL, NBL, ZB, SBL, UTRL, UMRL, ML, BL, HBL, HFL, and EL between *R. losea* and *R. andamanensis*; SGL, NBL, ZB, SBL, UTRL, UMRL, ML, BL, and HFL between *R. losea* and *R. norvegicus*; ML, BL, and HFL between *R. losea* and *R. exulans*; in HBL, HFL, and EL between *R. losea* and *R. rattus*; UTRL between *R. tanezumi* and *R. andamanensis*; UTRL, ML, BL, HBL, HFL, and EL between *R. tanezumi* and *R. norvegicus*; SGL, NBL, ZB, SBL, UTRL, UMRL, ML, BL, HBL, HFL, and EL between *R. tanezumi* and *R. exulans*; HBL, HFL, and EL between *R. andamanensis* and *R. norvegicus*; SGL, NBL, ZB, SBL, UTRL, UMRL, ML, BL, HBL, HFL, and EL between *R. andamanensis* and *R. exulans*; UMRL between *R. andamanensis* and *R. rattus*; SGL, NBL, ZB, SBL, UTRL, UMRL, ABL, ML, and HFL between *R. norvegicus* and *R. exulans*; HBL and EL between *R. norvegicus* and *R. rattus*; and SGL, SBL, BL, HBL, HFL, and EL between *R. exulans* and *R. rattus*. Thus, the 12 morphological characters separated the seven species of *Rattus* and validated their occurrence in China.

When all individuals of the two subspecies of *R. nitidus* were subjected to an independent sample t-test for each variable, significant differences appeared in UTRL, UMRL, ML, and TL between *R. nitidus nitidus* and *R. nitidus* from Xizang.

Molecular analysis

We obtained cyt *b* sequences for 78 specimens of *Apodemus* and 106 specimens of *Rattus*. *De novo* sequences were deposited in GenBank under accession Nos. MG748165–MG748348 (Supplementary Table S3).

Cyt *b* K2P interspecies distances for *Apodemus* ranged from 5.4% to 20.7% (Supplementary Table S4). The smallest distance occurred between *A. uralensis* and *A. pallipes*, and largest between *A. sylvaticus* and *A. latronum*. The distances for *Rattus* ranged from 2.1% to 16.5% (Supplementary Table S5). The smallest distance occurred between *R. baluensis* and *R. tiomanicus*, and the largest between *R. leucopus* and *R. argentiventer*. The K2P distance of *R. nitidus* from Xizang and *R. nitidus nitidus* was 0.019.

Matrilineal genealogy (haplotype phylogeny) of *Apodemus*

Matrilineal genealogy using the mitogenome and cyt *b* data for *Apodemus* (n=569) did not fully resolve the higher relationships (Figure 4), as in previous studies (see Discussion). Representative animals from China fell into nine clades that corresponded to nine species. Notably, *A. uralensis* from Xinjiang, China, fell into a clade (BS=100) comprised of *A. pallipes* from Xizang, China, and a sequence from GenBank (origin unknown), thus rendering *A. pallipes* paraphyletic (BS=69). A sole mitogenome representing "*A. chejuensis*" from Jeju Island was embedded in a clade containing *A. agrarius*. *Apodemus draco*, *A. ilex*, and *A. semotus* fell together in a well-supported clade (BS=100), but the relationships among the three species were not resolved (BS<50). *Apodemus* chevrieri, *A. draco*, *A. ilex*, *A. latronum*, and *A. peninsulae* also comprised subclades.

Table 3 Measurement statistics of *Rattus*

	SGL					NBL				ZB				SBL			
	n	**Mean**	***SD***	**Minimum**	**Maximum**	**Mean**	***SD***	**Minimum**	**Maximum**	**Mean**	***SD***	**Minimum**	**Maximum**	**Mean**	***SD***	**Minimum**	**Maximum**
R. nitidus	46	41.93	3.22	28.40	47.05	16.13	1.68	10.54	19.00	19.87	1.16	17.64	22.30	38.30	2.36	32.82	43.00
R. nitidus nitidus	31	41.62	3.53	28.40	47.05	15.90	1.75	10.54	18.66	19.66	1.11	17.64	21.75	37.96	2.30	32.82	41.82
R. nitidus thibetanus	15	42.56	2.44	38.39	45.85	16.62	1.47	14.02	19.00	20.31	1.15	18.63	22.30	38.99	2.40	35.19	43.00
R. losea	31	37.12	3.32	31.24	46.53	13.51	1.77	10.06	18.35	17.99	1.38	15.02	21.12	34.37	2.61	29.72	40.55
R. tanezumi	34	40.11	2.06	33.98	43.27	14.50	1.26	11.69	16.57	19.57	1.03	16.73	21.67	36.50	1.96	30.75	39.80
R. andamanensis	44	41.49	3.06	34.87	46.80	15.13	1.75	11.25	17.84	20.33	1.63	16.88	24.05	37.69	2.93	31.76	42.72
R. norvegicus	69	41.63	3.52	31.75	52.13	15.33	1.69	10.79	20.22	20.42	1.88	15.33	25.63	38.16	3.30	29.95	48.56
R. exulans	4	32.86	2.15	31.09	35.88	11.33	1.64	9.91	13.14	15.77	0.73	15.15	16.79	30.49	1.22	29.15	32.04
R. rattus	5	39.86	2.10	37.96	43.15	14.11	1.24	12.93	16.02	18.83	0.71	17.93	19.58	37.75	2.18	35.75	41.03
	UTRL					**UMRL**				**ABL**				**ML**			
	n	**Mean**	***SD***	**Minimum**	**Maximum**	**Mean**	***SD***	**Minimum**	**Maximum**	**Mean**	***SD***	**Minimum**	**Maximum**	**Mean**	***SD***	**Minimum**	**Maximum**
R. nitidus	46	21.29	1.38	18.62	24.36	7.39	0.54	6.15	8.92	7.36	0.56	6.03	8.32	21.70	2.02	16.41	26.17
R. nitidus nitidus	31	20.96	1.25	18.62	23.02	7.29	0.53	6.15	8.35	7.28	0.59	6.03	8.32	21.08	1.85	16.41	24.65
R. nitidus thibetanus	15	21.97	1.45	19.56	24.36	7.62	0.51	6.66	8.92	7.54	0.42	6.86	8.11	22.96	1.78	19.81	26.17
R. losea	31	18.95	1.62	15.86	21.97	6.53	0.42	5.79	7.63	7.17	0.40	6.54	7.84	19.85	1.66	15.76	22.69
R. tanezumi	34	20.13	1.22	16.76	22.47	7.38	0.38	6.39	8.18	7.45	0.51	6.22	8.62	20.76	1.09	17.81	22.59
R. andamanensis	44	21.36	1.73	17.89	24.02	7.55	0.62	6.11	8.70	7.39	0.52	6.25	8.89	21.70	1.84	17.70	24.65
R. norvegicus	69	21.66	1.93	17.01	27.14	7.35	0.47	6.32	8.55	7.40	0.56	6.51	8.68	22.02	2.33	17.02	29.63
R. exulans	4	16.87	0.87	15.73	17.84	6.12	0.45	5.56	6.51	6.51	0.26	6.15	6.73	16.24	0.94	15.21	17.49
R. rattus	5	19.61	0.83	18.83	20.88	6.73	0.38	6.41	7.39	7.41	0.48	6.99	8.24	19.48	0.98	18.43	20.70
	HBL					**TL**				**HFL**				**EL**			
	n	**Mean**	***SD***	**Minimum**	**Maximum**	**Mean**	***SD***	**Minimum**	**Maximum**	**Mean**	***SD***	**Minimum**	**Maximum**	**Mean**	***SD***	**Minimum**	**Maximum**
R. nitidus	46	164.59	18.34	123.00	205.00	168.09	18.38	131.00	210.00	34.14	2.12	30.00	40.00	23.25	2.21	18.00	28.00
R. nitidus nitidus	31	161.32	19.18	123.00	205.00	161.81	16.71	131.00	192.00	33.79	1.89	30.00	37.00	22.96	2.16	18.00	27.00
R. nitidus thibetanus	15	171.33	14.84	155.00	205.00	181.07	14.81	162.00	210.00	34.87	2.45	31.00	40.00	23.87	2.26	19.00	28.00
R. losea	31	152.07	20.82	103.00	192.00	145.58	15.64	110.00	192.00	28.58	2.04	24.00	32.00	19.12	2.95	12.00	27.00
R. tanezumi	34	162.91	10.46	128.00	180.00	173.09	16.06	144.00	205.00	31.25	1.72	28.00	35.00	21.72	2.24	18.00	26.00
R. andamanensis	44	173.02	19.54	126.00	212.00	186.89	24.45	115.00	231.00	31.65	1.87	27.00	36.00	23.15	2.29	19.00	32.00
R. norvegicus	69	182.62	24.50	120.00	274.00	152.67	20.80	82.00	222.00	34.42	3.59	26.00	41.00	17.72	2.23	11.00	21.00
R. exulans	4	115.50	14.27	101.00	135.00	138.00	8.17	126.00	144.00	23.70	1.39	22.00	26.00	16.75	0.50	16.00	17.00
R. rattus	5	170.80	16.99	150.00	194.00	190.60	11.80	180.00	210.00	33.00	2.24	30.00	36.00	22.60	1.82	20.00	25.00

Abbreviations are explained in the Materials and Methods section. All measurements are in mm.

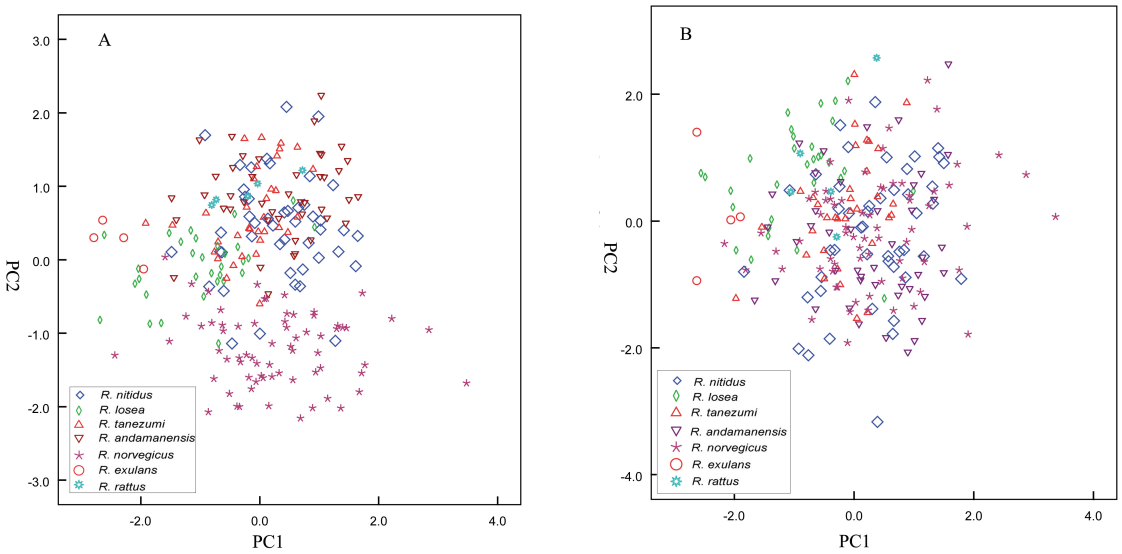

Figure 3 Principal component analysis of the first three principal components among the seven species of *Rattus* based on both external and craniomandibular variables (A) and craniomandibular variables only (B)

Matrilineal genealogy of *Rattus*

The interspecific relationships of *Rattus* using the mitogenome and cyt *b* sequences (*n*=396) were well-resolved (BS=95–100) or moderately resolved (BS=55–77) (Figure 5). Sequences representing animals from China fell into seven lineages that corresponded with *R. nitidus*, *R. norvegicus*, *R. exulans*, *R. andamanensis*, *R. losea*, *R. rattus*, and *R. tanezumi*. The clade of *R. nitidus* had two subclades, one from southern Xizang and the other from southeastern China (Figure 5). The tree depicted GenBank sequences deposited under different names within a shallow clade, most commonly with *R. andamanensis*. However, some specimens were also associated with *R. losea*, *R. nitidus*, *R. tanezumi* as well as *R. nitidus* from southern Xizang.

DISCUSSION

Genealogy and taxonomy

Species of *Apodemus* are among the most destructive of all animal pests, yet little attention has been paid to their evolutionary relationships. Our trees were consistent with those from the robust study of Steppan & Schenk (2017), indicating the repeatability of both. However, the created molecular phylogenetic tree of *Rattus* was inconsistent with that of Aplin et al. (2011), which may be due to the different ways in which the trees were constructed (ML phylogeny here, but BI and NJ methods in Aplin et al. (2011)), different number of species, or different sequences of the cyt *b* gene (only two individuals of *R. pyctoris* (GenBank accession No. JN675511 and JN675512) from Aplin et al. (2011)). The unresolved relationships within *Apodemus* were not surprising and are likely due to early radiation in the evolution of this genus, as indicated by the saturation of the mitochondrial gene (Serizawa et al., 2000). Similar problems likely also occur in *Rattus* due to hybridization and introgression. Previously, *Rattus* was recovered as a paraphyletic genus (Steppan & Schenk, 2017). Fully resolved phylogenies require many slowly evolving and unlinked genes, which is not within the scope of the current study.

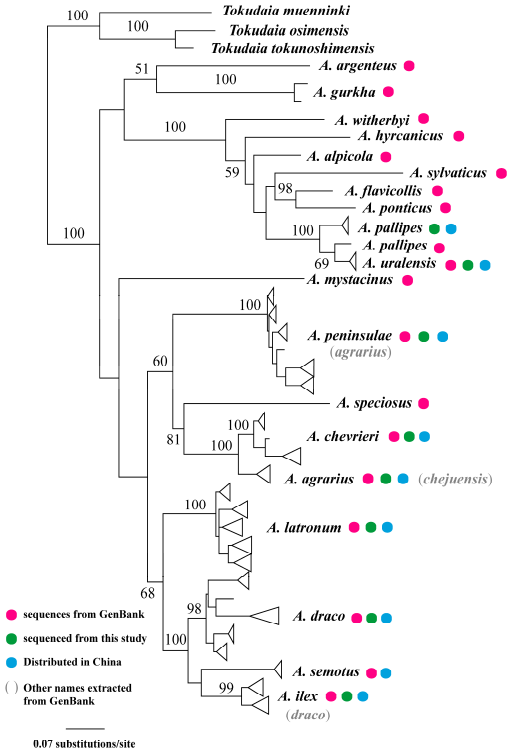

Figure 4 ML matrilineal genealogy of *Apodemus* derived from cyt *b* (Numbers above branches refer to bootstrap probabilities)

Despite uncertainty in phylogenetic relationships, questions regarding taxonomy in both genera remain. The differences between *A. pallipes* and *A. uralensis* have been discussed

previously in depth (Musser & Carleton, 2005). Our carefully identified specimens of *A. pallipes* were from southern Xizang (Pulan County). The average cyt *b* genetic distance between *A. uralensis* and *A. pallipes* was 5.4%, which was the smallest interspecific genetic distance in *Apodemus*. All our specimens of *A. pallipes* matched the original description and holotype (Musser & Carleton, 2005). Thus, *A. pallipes* undoubtedly occurs in China. The sequences of *A. pallipes* in GenBank were from Afghanistan and Pakistan, near the type locality of *A. pallipes* in Pamir Alta. However, as we had no access to these specimens, it was not possible to determine if they matched the morphological description of *A. pallipes*.

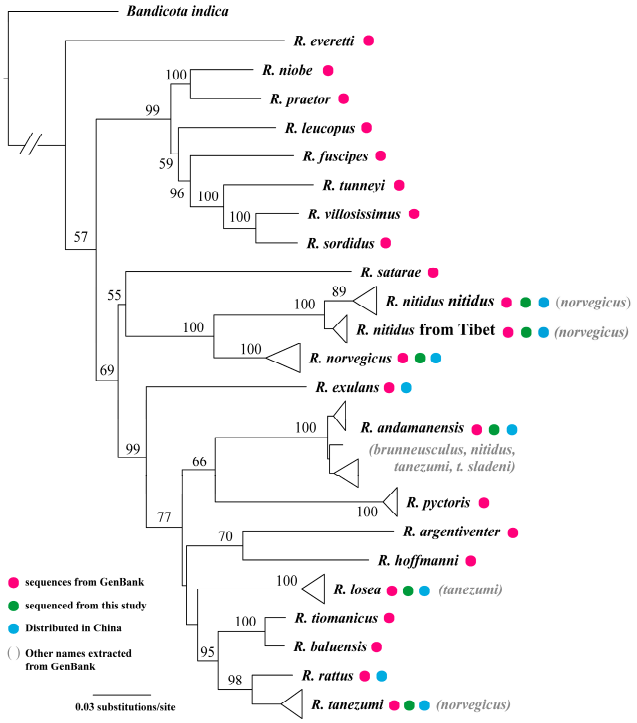

Figure 5 ML matrilineal genealogy of *Rattus* derived from cyt *b* (Numbers above branches refer to bootstrap probabilities)

Johnson & Jones (1955) described *A. chejuensis*. Koh (1991) also recognized the species based on its large body size and mtDNA genotype. Corbet (1978) assigned it as a synonym of *A. agrarius* ningpoensis, whereas Musser & Carleton (2005) treated it as a synonym of *A. agrarius*. Our phylogeny embedded *A. chejuensis* in *A. agrarius*, and thus our results agree with the assignment of Musser & Carleton (2005).

The taxonomic statues of *A. draco* remains uncertain. *Apodemus ilex* and *A. semotus* are close relatives to each other (Figure 4). Kaneko (2011) suggested that *A. semotus* did not differ significantly from *A. draco*. However, this endemic species of Taiwan was characterized by a dark gray pelage rather than the reddish-brown color of all other Asian species of *Apodemus*. Further, our ANOVA results demonstrated significant differences in TL and HFL between *A. ilex* and *A. draco*. Thus, we recognize all three as full species to better reflect their long evolutionary histories and distinct distribution patterns. Nevertheless, future comprehensive morphological diagnosis is desirable.

Hodgson described *R. pyctoris* in 1845 from Nepal (Hodgson, 1845). This name was later replaced by *R. rattoides* or *R. turkestanicus*. Musser & Carleton (1993) resurrected the oldest name and it has been reported to occur in China (Allen, 1940; Corbet, 1978; Ellerman & Morrison-Scott, 1951; Musser & Carleton, 1993, 2005; Wang, 2003). Feng et al. (1986) identified a series of specimens of *R. pyctoris* from Xizang and claimed that *R. pyctoris* closely resembled *R. rattus* but with a pale underbelly, relatively long nasal bone, and cusp t3 on M^1. Our series of specimens from Xizang coincide with the characteristics of *R. pyctoris* described by Feng et al. (1986). However, phylogenetic analysis associated the species with *R. nitidus*. The original description and comments of Musser & Carleton (2005) on *R. pyctoris* point to its diagnostic characters as a very small cusp t3 on M^1, a wide and short rostrum (narrow and slender in *R. nitidus*), and chunky wide molars (thinner and gracile in *R. nitidus*). Except for the morphology of M^1, the Xizang specimens differed from *R. pyctoris*. Furthermore, many characters of the Xizang specimens also differed from *R. nitidus*, including the cusp t3 being present, gray-white underbelly, and larger measurements. The molecular phylogeny also placed the Xizang specimens and *R. nitidus* in different clades. Accordingly, we assign the Xizang specimens to a new, undescribed subspecies of *R. nitidus*.

Peale (1848) described *R. exulans* from Society Island. Nevertheless, its existence in Taiwan, China has been recognized for a long time (Motokawa et al., 2001). The Guangdong Insects Institute collected specimens of *R. exulans* from Yongxing Island in 1975. *Rattus exulans* is the smallest Asian species in its genus. The specimens from Yongxing Island conformed to the characteristics of *R. exulans*. Thus, we confirm that *R. exulans* occurs in China in Yongxing Island and Taiwan.

The earliest Chinese specimen of *R. rattus* (black type) was collected by A. B. Howell from Kuliang, Fukien in 1929 (Allen, 1940). In 1955 and 1956, the Fujian Epidemic Prevention Station collected specimens from Fujian, which were confirmed by Shou (1962) as being *R. rattus*. Our examination of these specimens and one specimen from Guangdong Province resulted in the same conclusion. Thus, we confirm that *R. rattus* occurs in Fujian and Guangdong.

Morphometrics- and molecular-based species identifications

Regardless of skull and external measurements being similar between species, many interspecies measurements differed significantly. Species of *Apodemus* were easier to identify than *Rattus*. Furthermore, the different species of *Apodemus* exhibited stronger geographic distribution. For example, although measurements could not discriminate between *A. draco* and *A. ilex* (current study) or *A. semotus* (Kaneko, 2011), all three were found to be allopatric: *A. ilex* occurs in Hengduan Mountains, south of the Yangtze River and west of the Jinsha River; *A. semotus* occurs in Taiwan only; and *A. draco* occurs

in the middle and lower reaches of the Yangtze River and in eastern China. *Apodemus chevrieri*, *A. draco*, and *A. latronum* co-occur in western Sichuan, but they were separated by the third upper molar and certain measurements (Figure 2A, B). Only one sequence of *A. peninsulae* in GenBank was likely misidentified (assuming no other error). Thus, the confusion between *A. draco* and *A. ilex* appears to be due to out-of-date taxonomy rather than misidentification.

Identification of *Rattus* species using either morphometrics or molecular data requires caution. Unlike for the species of *Apodemus*, most species of *Rattus* are invasive in China and have likely experienced strong selection resulting in morphological modification to adapt to local habitats. Notwithstanding, it was possible to identify some species based on morphology alone, such as, *R. andamanensis*, which has a unique white belly, *R. norvegicus*, which has very short ears, and *R. nitidus* and *R. norvegicus*, which do not have the cusp t3 on M^1, with the former also having distinctly larger ears. The Chinese population of *R. rattus* is black all over its body, whereas *R. exulans* only occurs in islands of the South China Sea, including Taiwan, and has a very small head and body length. However, *R. losea* and *R. tanezumi* occur sympatrically in southern China. They are easily confused due to similar appearances and overlapping measurements. Most species showed significant overlap in the PCA plots (Figure 3A, B). Perhaps due to challenges in identification, GenBank contains many misidentifications. For example, sequences under the name of *R. norvegicus* occur in almost all clades (Figure 5).

Our new sampling and survey of sequences supported the occurrence of nine species of *Apodemus* and seven species of *Rattus* in China. However, it is necessary to be cautious with morphometric and molecular analyses for species identification due to considerable intraspecific variation and considerable errors in GenBank.

Alpha diversity of *Apodemus* and *Rattus*

We determined that *A. agrarius, A. chevrieri, A. draco, A. ilex, A. latronum, A. pallipes, A. peninsulae, A. semotus*, and *A. uralensis* occur in China. In addition, considerable intraspecific diversity occurs in several species. Future comprehensive and integrative analyses can determine if further splitting is necessary and/or desirable.

We determined that *R. andamanensis, R. exulans, R. losea*, *R. nitidus*, *R. norvegicus*, *R. rattus*, and *R. tanezumi* occur in China. Future research into the occurrence of *R. pyctoris* in China is not necessary. A new subspecies of *R. nitidus* is described as follows:

Subspecies description

***Rattus nitidus thibetanus* subsp. nov**

Holotype: Adult female, collected by Liao Rui on 15 January 2011. The specimen was prepared as a skin with cleaned skull and deposited in the Sichuan Academy of Forestry (MT11197).

Type locality: Motuo County, Xizang, China, N29.24344° and E95.169920°, 783 m a.s.l..

Measurements of holotype: Weight: 179.6 g; HBL: 205 mm; TL: 200 mm; HFL: 40 mm; EL: 23 mm; SGL: 45.49 mm; SBL: 43.00 mm; ZB: 19.98 mm; MB: 17.06 mm; ABL: 8.08 mm; LMxT: 7.38 mm; NBL: 19.00 mm.

Paratypes: 5 specimens, with skins and skulls: XCY01001, ♀, 28.5048, 97.01045; XZ16259, ♀; 27.47033, 88.91450; XZ16258, ♂; 27.47033, 88.91450; MT020, ♂; MT035, ♂, 29.25491, 95.21331.

Additional specimens: 15 specimens (9 juveniles, 6 adults with skulls broken). Adults: XZ16260, ♀; XZ16253, ♂; XZ11280, ♀; XZ11262, ♂; XZ11177, ♂; and XZ11173, ♀. Juveniles: XZ11207, ♀; MT11174, ♀; XZ11176, ♀; XZ11207, ♀; XZ11208, ♀; XZ11232, ♀; XZ11175, ♀; XZ11196, ♂; and XZ11028, ♀.

Geographic distribution: The new subspecies is recorded from Yadong, Motuo, Nielamu, and Jilong counties, southern Xizang, China.

Etymology: The name is derived from the type locality, southern Xizang (Tibet), China.

Diagnosis: Cusp t3 present on M^1 in first transverse loop, but very small; head and body relatively large; tail length usually larger than head plus body length; belly gray-white; transition between darker dorsal and lighter ventral pelage abrupt; dorsum of feet white, not glossy.

Description: Summer pelage from neck to hip uniform brown-black. Ventral hairs with gray-black base and gray-white tip, transition between darker dorsal and lighter ventral pelage relatively abrupt. Dorsal and ventral tail uniform brown-black; hairs on dorsal and venter of feet white, not glossy.

Skull sturdy (Figure 6), in dorsal profile straight and brain case flattened; highest point of skull in middle of parietal bone. Nasal broad anteriorly narrowing posteriorly. Posterior margin of nasals irregular and protruding in front of maxilla. Posterior and anterior of frontal broad, middle narrower. Interparietal broad, anterior part triangle-shaped and posterior margin arc-shaped (Figure 6). Interorbital and temporal ridges present. Zygomatic arches medium in size, front part slightly broader. Auditory bullae moderately sized. Incisory foramen broad. Mandibles medium-sized (Figure 6).

Upper incisors medium in size vertically downward and orange. Molars rooted; 1st upper molar with three transverse dental loops, first dental loop with 3 cusps, t3 present but small; 2nd upper molar with three transverse dental loops, first dental loop only on lingual cusp; 3rd upper molar with three transverse dental loops, first dental loop only on lingual cusp, third loop only single semicircle and second loop rectangular; mandibular condyle and coronoid process large, but lower molar same as in other species of *Rattus*.

Habitat: Specimens were collected from an abandoned farmland, along the footpath of a rice field where highland barley was grown, forest edge, shrubland, surrounding a house, and salvage station.

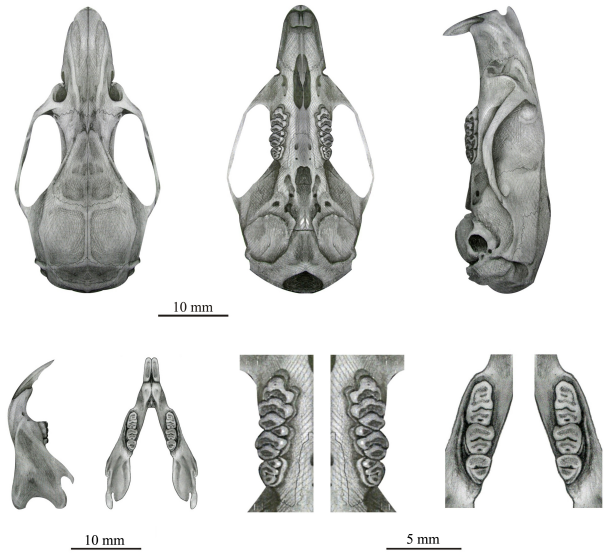

Figure 6 Skull of new subspecies of *Rattus nitidus*

Comparison with other subspecies: Compared with *R. n. nitidus*, t3 of the first dental loop present in *Rattus nitidus thibetanus* **subsp. nov** (vs. t3 absent or just vestigial; belly gray-white, and transition between darker dorsal and lighter ventral pelage relatively abrupt in *Rattus nitidus thibetanus* **subsp. nov** (vs. belly gray-white or yellow-gray, and transition vague in *R. n. nitidus*); dorsum of feet white, not glossy in *Rattus nitidus thibetanus* **subsp. nov** (vs. dorsum of feet white and shiny pearl in *R. n. nitidus*). The independent sample *t*-test demonstrated significant differences in UTRL, UMRL, ML, and TL between *R. n. nitidus* and *R. n. thibetanus*. The K2P distance for *R. n. thibetanus* and *R. n. nitidus* was 0.019, smaller than the smallest interspecies distance known in *Rattus*.

COMPETING INTERESTS

The authors declare that they have no competing interests.

AUTHORS' CONTRIBUTIONS

S.Y.L. and K.H. conceived and designed the study. S.D.C, W.J, M.K T, R.L, and F.J.L conducted data collection. S.Y.L, K.H., and S.D.C analyzed the data and wrote the manuscript. R.W.M revised the manuscript. All authors read and approved the final version of the manuscript.

ACKNOWLEDGEMENTS

We thank Qing Zhang for help in morphological data collection. We thank Qi Zhang for assistance in the molecular lab work. We also thank the editor and the two anonymous reviewers for comments and suggestions.

REFERENCES

Allen GM. 1940. The Mammals of China and Mongolia: Natural History of Central Asia. New York: American Museum of Natural History, 621–1350.

Aplin KP, Suzuki H, Chinen AA, Chesser RT, Ten Have J, Donnellan SC, Austin J, Frost A, Gonzalez JP, Herbreteau V, Catzeflis F, Soubrier J, Fang YP, Robins J, Matisoo-Smith E, Bastos ADS, Maryanto I, Sinaga MH, Denys C, Van Den Bussche RA, Conroy C, Rowe K, Cooper A. 2011. Multiple geographic origins of commensalism and complex dispersal history of Black Rats. *PLoS One,* **6**(11): e26357.

Barnett SA. 2001. The Story of Rats: Their Impact on Us, and Our Impact on Them. Sydney: Allen & Unwin.

Bousbouras D. 1999. Study of *Apodemus sylvaticus* and *Apodemus flavicolis* habitat occupation at the Dadia forest reserve. Contribution to issues concerning the conservation of raptors. *Biologia Gallo Hellenica,* **25**(1): 3–14.

Corbet GB. 1978. The Mammals of the Palaearctic Region: A Taxonomic Review. London: British Museum (Natural History).

Duplantier JM, Catalan J, Orth A, Grolleau B, Britton-Davidian J. 2003. Systematics of the black rat in Madagascar: consequences for the transmission and distribution of plague. *Biological Journal of the Linnean Society,* **78**(3): 335–341.

Ellerman JR, Morrison-Scott TCS. 1951. Checklist of Palaearctic and Indian Mammals 1758 to 1946. London: British Museum (Natural History), 563–576.

Feng ZJ, Cai GQ, Zheng CL. 1986. The Mammals of Xizang. Beijing: Science Press, 1–396. (in Chinese)

Filippucci MG. 1992. Allozyme variation and divergence among European, Middle Eastern, and North African species of the genu *Apodemus* (Rodentia, Muridae). *Israel Journal of Zoology,* **38**(3–4): 193–218.

Galan M, Pagès M, Cosson JF. 2012. Next-generation sequencing for rodent barcoding: species identification from fresh, degraded and environmental samples. *PLoS One*, **7**(11): e48374.

Huang P, Yang ZN, Liu Y, Yao PP, Hu JL, Wang XC, Yu JJ, Li J, Han YP, Jin K, Yang L, Zhang Y, Yue M. 2017. The molecular characteristics and epidemiological analysis of Hantavirus in southeast coastal area of China from 1980 to 2015. *Chinese Journal of Vector Biology and Control*, **28**(4): 354–358. (in Chinese)

Hodgson BH. 1845. On the rat, mice, and shrews of the central region of Nepal. *The Annals and Magazine of Natural History*, **15**: 266–270.

Irwin DM, Kocher TD, Wilson AC. 1991. Evolution of the cytochrome *b* gene of mammals. *Journal of Molecular Evolution*, **32**(2): 128–144.

Johnson DH, Jones JK. 1955. Three new rodents of the genera *Micromys* and *Apodemus* from Korea. *Proceedings of the Biological Society of Washington*, **68**: 167–172.

Kaneko Y. 2010. Identification of *Apodemus peninsula*, *draco* and *A. latronum* in China, Korea, and Myanmar by cranial measurements. *Mammal Study*, **35**(1): 31–55.

Kaneko Y. 2011. Taxonomic status of *Apodemus* semotus in Taiwan by morphometrical comparison with *A. draco*, *A. peninsulae* and *A. latronum* in China, Korea and Myanmar. *Mammal Study*, **36**(1): 11–22.

Kimura M. 1980. A simple method for estimating evolutionary rates of base substitutions through comparative studies of nucleotide sequences. *Journal of Molecular Evolution*, **16**(2): 111–120.

Klein SL, Calisher CH. 2007. Emergence and persistence of Hantaviruses. In Wildlife and Emerging Zoonotic Diseases: The Biology, Circumstances and Consequences of Cross-Species Transmission. Berlin Heidelberg, 217–252.

Koh HS. 1991. Morphometric analyses with eight subspecies of striped field mice, *Apodemus agrarius* Pallas (Rodemtia, Mammalia), in Asia: the taxonomic status of subspecies chejuensis at Cheju iland in Korea. *The Korean Journal of Systematic Zoology*, **7**(2): 179–188.

Liu SY, Sun ZY, Liu Y, Wang H, Guo P, Murphy RW. 2012. A new vole from xizang, China (Cricetidae: Arvicolinae) and the molecular phylogeny of the genus *Neodon*. *Zootaxa*, **3235**(3235): 1–22.

Liu XM, Wei FW, Li M, Feng ZJ. 2002. A review of the phylogenetic study on the genus *Apodemus* of China. *Acta Theriologica Sinica*, **22**(1): 46–51. (in Chinese)

Liu XM, Wei FW, Li M, Jiang XL, Feng ZJ, Hu JC. 2004. Molecular phylogeny and taxonomy of wood mice (genus *Apodemus* Kaup, 1829) based on complete mtDNA cytochrome *b* sequences, with emphasis on Chinese species. *Molecular Phylogenetics and Evolution*, **33**(1): 1–15.

Macholán M, Filippucci MG, Benda P, Frynta D, Sádlová J. 2001. Allozyme variation and systematics of the genus *Apodemus* (Rodentia: Muridae) in Asia Minor and Iran. *Journal of Mammalogy*, **82**(3): 799–813.

Martin Y, Gerlach G, Schlötterer C, Meyer A. 2000. Molecular phylogeny of European Muroid Rodents based on complete cytochrome *b* sequences. *Molecular Phylogenetics and Evolution*, **16**(1): 37–47.

Meerburg BG, Singleton GR, Kijlstra A. 2009. Rodent-borne diseases and their risks for public health. *Critical Reviews in Microbiology*, **35**(3): 221–270.

Menachery VD, Yount BL Jr, Debbink K, Agnihothram S, Gralinski LE, Plante JA, Graham RL, Scobey T, Ge XY, Donaldson EF, Randell SH, Lanzavecchia A, Marasco WA, Shi ZL, Baric RS. 2015. A SARS-like cluster of circulating bat coronaviruses shows potential for human emergence. *Nature Medicine*, **21**(12): 1508–1513.

Mezhzherin SV, Zykov AE. 1991. Genetic divergence and allozymic variability in mice of the genus *Apodemus* s. lato (Muridae, Rodentia). *Tsitologiia I Genetika*, **25**(4): 51–59.

Michaux JR, Filippucci MG, Libois RM, Fons R, Matagne RF. 1996. Biogeography and taxonomy of *Apodemus sylvaticus* (the woodmouse) in the Tyrrhenian region: enzymatic variations and mitochondrial DNA restriction pattern analysis. *Heredity*, **76**(Pt 3): 267–277.

Moritz C, Cicero C. 2004. DNA barcoding: promise and pitfalls. *PLoS Biology*, **2**(10): e354.

Motokawa M, Lu KH, Harada M, Lin LK. 2001. New records of the Polynesian rat *Rattus exulans* (Mammalia: Rodentia) from Taiwan and the Ryukyus. *Zoological Studies*, **40**(4): 299–304.

Musser GG, Carleton MD. 1993. Family muridae. *In*: Wilson DE, Reeder DM. Mammal Species of the World: A Taxonomic and Geographic Reference. Washington: Smithsonian Institution Press, 501–755.

Musser GG, Brothers EM, Carleton MD, Hutterer R. 1995. Taxonomy and distributional recors of Oriental and European *Apodemus*, with a review of the *Apodemus*-Sylvaemus problem. *Bonner Zoologische Monographien*, **46**(1–4): 143–190.

Musser GG, Carleton MD. 2005. Superfamily muroidea. *In*: Wilson DE, Reeder DM. Mammal Species of the World: A Taxonomic and Geographic Reference. 3rd ed. Baltimore: Johns Hopkins University Press, 894–1531.

Nowak MR. 1999. Walker's Mammals of the World. 6th ed. Baltimore and London: The Johns Hopkins University Press, 1499–15011.

Peale TR. 1848. United States Exploring Expedition, during the year 1838, 1839, 1940, 1841, 1842, under the command of Charles Wilkes U. S. N: Mammalogy and Ornithology. Philadelphia.

Serizawa K, Suzuki H, Tsuchiya K. 2000. A phylogenetic view on species radiation in *Apodemus* inferred from variation of nuclear and mitochondrial genes. *Biochemical Genetics*, **38**(1–2): 27–40.

Shankardass MK. 2000. Book reviews and notices: ELLEN R. GIRDEN, Evaluating research articles: from start to finish. Thousand Oaks: Sage Publications, 1996. xi + 290 pp. Tables, bibliography. $55.00 (hardback)/$24.95 (paperback). *Contributions to Indian Sociology*, **34**(1): 160–161.

Shou ZH. 1962. Chinese Economical Fauna: Mammals. Beijing: Chinese Academic Press.

Sambrook J, Russell DW. 2001. Molecular Clonning: A Laboratory Manual. New York: Cold Spring Harbor Laboratory Press.

Simpson GG. 1945. The Principles of Classification and a Classification of Mammals. New York: American Museum of Natural History, 515–527.

Smith AT, Xie Y, Hoffmann R, Lunde D, MacKinnon J, Wilson DE, Wozencraft WC, Gemma F. 2008. A Guide to the Mammals of China. Princeton: Princeton University Press, 671.

Steppan SJ, Schenk JJ. 2017. Muroid rodent phylogenetics: 900-species tree reveals increasing diversification rates. *PLoS One*, **12**(8): e0183070.

Suzuki H, Sato JJ, Tsuchiya K, Luo J, Zhang YP, Wang YX, Jiang XL. 2003. Molecular phylogeny of wood mice (*Apodemus*, Muridae) in East Asia. *Biological Journal of the Linnean Society*, **80**(3): 469–481.

Tamura K, Peterson D, Peterson N, Stecher G, Nei M, Kumar S. 2011. MEGA5: molecular evolutionary genetics analysis using maximum likelihood, evolutionary distance, and maximum parsimony methods. *Molecular Biology and Evolution*, **28**(10): 2731–2739.

Wang YX. 2003. A Complete Checklist of Mammal Species and Subspecies in China: A Taxonomic and Geographic Reference. Beijing: China Forestry Publishing House, 19–197.

Wu HX, Lu L, Meng FX, Guo YH, Liu QY. 2017. Reports on national surveillance of rodents in China, 2006–2015. *Chinese Journal of Vector Biology and Control*, **28**(6): 517–522. (in Chinese)

Xia WP. 1984. A study on Chinese *Apodemus* with a discussion of its relations to Japanese species. *Acta Theriologica Sinica*, **4**(2): 93–98. (in Chinese)

Zimmermann K. 1962. Die Untergattungen der gattung *Apodemus Kaup*. *Bonner Zoologische Beiträge*, **13**: 198–208.

A new genus of Asiatic short-tailed shrew (Soricidae, Eulipotyphla) based on molecular and morphological comparisons

Kai He[1,2,#], Xing Chen[1], Peng Chen[1], Shui-Wang He[1], Feng Cheng[1], Xue-Long Jiang[1,*], Kevin L. Campbell[2,*]

[1] *Kunming Institute of Zoology, Chinese Academy of Sciences, Kunming Yunnan* 650223*, China*
[2] *Department of Biological Sciences, University of Manitoba, Winnipeg, Manitoba* R3T 2N2*, Canada*

ABSTRACT

Blarinellini is a tribe of soricine shrews comprised of nine fossil genera and one extant genus. Blarinelline shrews were once widely distributed throughout Eurasia and North America, though only members of the Asiatic short-tailed shrew genus *Blarinella* currently persist (mostly in southwestern China and adjacent areas). Only three forms of *Blarinella* have been recognized as either species or subspecies. However, recent molecular studies indicated a strikingly deep divergence within the genus, implying the existence of a distinct genus-level lineage. We sequenced the complete mitochondrial genomes and one nuclear gene of three Asiatic short-tailed and two North American shrews and analyzed them morphometrically and morphologically. Our molecular analyses revealed that specimens ascribed to *B. griselda* formed two deeply diverged lineages, one a close relative to *B. quadraticauda*, whereas the other—comprised of topotype specimens from southern Gansu—diverged from other *Blarinella* in the middle Miocene (ca. 18.2 million years ago (Ma), 95% confidence interval=13.4–23.6 Ma). Although the skulls were similarly shaped in both lineages, we observed several diagnostic characteristics, including the shape of the upper P^4. In consideration of the molecular and morphological evidence, we recognize *B. griselda* as the sole species of a new genus, namely, *Pantherina* **gen. nov.** Interestingly, some characteristics of *Pantherina griselda* are more similar to fossil genera, suggesting it represents an evolutionarily more primitive form than *Blarinella*. Recognition of this new genus sheds light on the systematics and evolutionary history of the tribe Blarinellini throughout Eurasia and North America.

Keywords: Blarinellini; Capture-hybridization; Mitogenome; Molecular phylogeny; Next-generation sequencing; *Pantherina*

INTRODUCTION

Asiatic short-tailed shrews, currently classified as species in the genus *Blarinella*, are small insectivorous mammals distributed mainly in central and southwestern China, adjacent Myanmar, and northern-most Vietnam. These small- to middle-sized shrews are uniformly black or dark brown and have large incisors, heavy tooth pigmentation, and a short tail that is typically 40%–60% of the head-body length. The fore claws are enlarged, suggesting adaptation for a semi-fossorial lifestyle (Wilson & Mittermeier, 2018).

The taxonomy of *Blarinella* has been studied since the

Received: 30 May 2018; Accepted: 06 June 2018; Online: 28 June 2018

Foundation items: This work was supported by a Natural Sciences and Engineering Research Council (NSERC) of Canada Discovery Grant (RGPIN/238838-2011), NSERC Discovery Accelerator Supplement (RGPAS/412336-2011), and University of Manitoba Research Grants Program Award (#41342) to K.L.C. K. H. was supported by the Youth Innovation Promotion Association, Chinese Academy of Sciences, and a JSPS Postdoctoral Fellowship for Overseas Researchers (P16092)

[#]Present address: The Kyoto University Museum, Kyoto University, Kyoto, Japan

[*]Corresponding authors, E-mail: jiangxl@mail.kiz.ac.cn; Kevin.Campbell@umanitoba.ca

DOI: 10.24272/j.issn.2095-8137.2018.058

late 19th century. The first recognized species was *Sorex quadraticauda*, described by Milne-Edwards & Milne-Edwards (1872) based on a specimen from Baoxing (=Mouping), northwestern Sichuan, China (the same type locality as the giant panda, *Ailuropoda melanoleuca* (David, 1869)). Milne-Edwards & Milne-Edwards (1872) documented the shrew's relatively short and somewhat square-shaped tail, well-developed incisors, and intensively dark pigmentation on the teeth. This species typically has five upper unicuspids, although the holotype specimen has only four (with the fifth one missing) on one side of its skull and five on the other, as discussed by Thomas (1911). When Thomas (1911) examined new specimens from Mt. Emei (Omi-San, 100 km south of Baoxing) in western Sichuan, *S. quadraticauda* was determined to be more closely related to the North American short-tailed shrews *Blarina* and *Cryptotis* (tribe Blarinini), than to the Old World *Sorex*, and thus assigned to its own genus *Blarinella* (literally "small *Blarina*").

Thomas himself recognized additional two *Blarinella* species. One (*Blarinella griselda*) was based on specimens from Lintan (=Taochou), Gansu, which were differentiated by their smaller size, grayer color, and shorter tails (Thomas, 1912). Thomas (1915) later recognized specimens from Pianma (=Hpimaw), Yunnan, as a third species, *Blarinella wardi*, based on their small size, dark color, and narrow skull. Since then, specimens collected across southern China and northern-most Vietnam have been assigned to one of these three groupings, though their taxonomic status has varied. For example, Allen (1938) and Hutterer (1993) placed *B. griselda* and *B. wardi* as subspecies in *B. quadraticauda*, whereas Corbet (1978) and Hutterer (2005) recognized all three as distinct species.

Jiang et al. (2003) reviewed the taxonomy and distribution of the group and, based on multivariate and univariate morphometric analyses of skulls, recognized the three as distinct species but assigned only a few populations from northwestern Sichuan to *B. quadraticauda*. This three-species division has been widely accepted (Hutterer, 2005; Smith & Xie, 2008). Chen et al. (2012) was the first to apply molecular phylogenetic approaches to samples collected mostly from western Sichuan and Shaanxi. Their study revealed *B. wardi* as a distinct lineage at a basal position of the genus, confirming its species status, and found *B. quadraticauda* was a well-supported clade embedded within *B. griselda*, making the latter a paraphyletic group. The authors suggested that either this represented an incipient speciation event for *B. quadraticauda,* or the taxonomy of the genus was incorrect. It is worth noting that no holotype or topotype specimens of *B. griselda* from southern Gansu were included in either study, so the populations from Chongqing, Hubei, and eastern Yunnan were tentatively assigned to *B. griselda* based on their intermediate size between *B. quadraticauda* and *B. wardi*.

All the studies mentioned above examined *Blarinella* taxonomy at the species/subspecies levels, implicitly accepting the monophyly of the genus. More recently, however, He (2011) discovered two genetically distinct, but sympatrically distributed, lineages from Mt. Qinling, Shaanxi, China, that called this into question. One lineage clustered with previously sequenced *Blarinella griselda*, whereas the other formed a cryptic lineage that appears to have diverged from other *Blarinella* more than 10 million years ago (Ma), suggesting that an undescribed genus may exist. However, because the Mt. Qinling and southern Gansu mountains (including Lintan, the type locality of *B. griselda*) are on the same tectonic Qinling belt, and because no specimen from Gansu has ever been included in morphometric or genetic study, it was uncertain whether the cryptic lineage represented *B. griselda* or an unrecognized taxon. Despite efforts to explore the southern Gansu mountains (see He et al., 2013), no *Blarinella* species have been captured, and the question remains unresolved. Based on sequences from a single specimen from Gansu and a handful of specimens from Vietnam, Bannikova et al. (2017) confirmed the existence of two clades in the genus *Blarinella*. Because their sample locality in Gansu was near the type locality of *B. griselda*, their specimen is likely to be the "true" *B. griselda*. Based on the results of these two studies, we hypothesized that *B. griselda* occurs only in Gansu and Shaanxi. We further hypothesized that this distinct evolutionary lineage may represent a separate genus, and that "*B. griselda*" from central and southern China, northern Vietnam, and Mt. Qinling is likely to be more closely related to *B. quadraticauda*. Thus, a revision of the taxonomic status of *B. griselda* is warranted.

The systematic position of *Blarinella* has been revised by paleontologists based on craniodental characteristics and revisited by mammalogists using molecular data. Repenning (1967) firstly included the genus in the tribe Soricini, despite acknowledging the similarity between *Blarinella* and Blarinini (North American *Blarina* and *Cryptotis*). Reumer (1998) established the new tribe Blarinellini to include the extant *Blarinella* plus eight fossil genera. A close relationship between Blarinini and Blarinellini is supported by molecular phylogenetic analyses (Dubey et al., 2007; He et al., 2010). These lines of evidence together point to *Blarinella* as a relict genus of Blarinellini.

The craniodental characteristics of *Blarinella* were first described by Repenning (1967) based on *B. quadraticauda* and fossil species *B. kormosi* (=*Zelceina kormosi*; Storch, 1995). Several characters recognized by Repenning (1967) were adopted by Reumer (1998) for defining the tribe Blarinellini, such as breadth of the interarticular area on the mandibular condyle, reduced posterior emargination on the upper molariform teeth, presence of entoconid crests on M_1 and M_2, and reduction of the talonid of M_3.

In the current study, we sequenced five complete mitochondrial genomes and seven partial *ApoB* genes of two *Blarinella* and five *Blarina* specimens and also compared their craniodental morphology. We used these data to update the taxonomy of *Blarinella*, focusing on the distinctiveness of *B. griselda* from Gansu and Shaanxi.

MATERIALS AND METHODS

Sampling and experiments

All specimens and tissue samples were obtained following locally approved animal care procedures under the auspices

of authorized collection permits. *Blarinella* specimens from China were collected by the Mammal Ecology and Evolution Group of the Kunming Institute of Zoology, Chinese Academy of Sciences, from Mts. Ailao, Gongshan, and Qinling (Figure 1). *Blarina brevicauda* was collected near Bird Lake in Nopiming Provincial Park, Manitoba, Canada, while conducting research under Manitoba Conservation Permit WB12563. A tissue sample of *Blarina hylophaga* was obtained from the National Museum of Natural History, Smithsonian Institution, Washington DC, USA (USNM 568994) under transaction No. 2073785 (Supplementary Table S1). DNA was extracted using a DNA extraction kit (Qiagen DNeasy Blood & Tissue Kits, China) or the phenol/proteinase K/sodium dodecyl sulphate method (Sambrook et al., 2001). For each specimen, we sequenced the complete mitochondrial cyt *b* gene and a nuclear *ApoB* gene segment using Sanger sequencing. The primers were developed in previous studies (Dubey et al., 2007; He et al., 2010) and are given in Supplementary Table S2. Each PCR product was sequenced using both the sense and anti-sense primers and were assembled using Lasergene SeqMan v7 (DNASTAR).

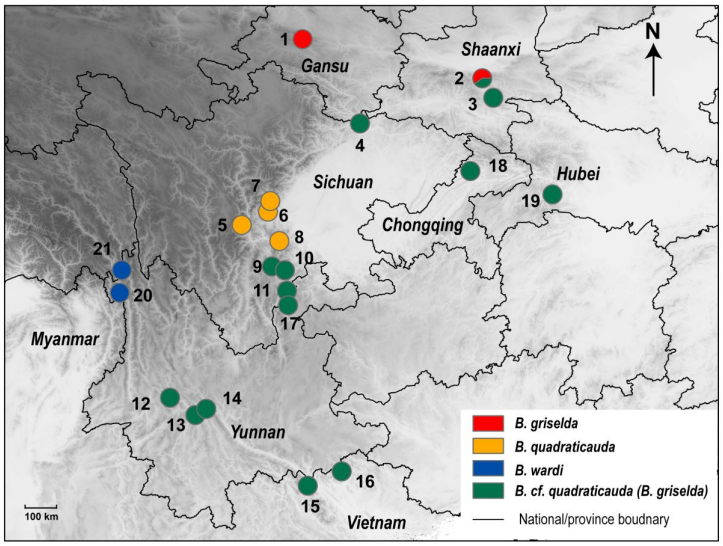

Figure 1 Sample localities of specimens used for molecular analyses

Blarinella cf. *quadraticauda* (green dots) represents localities for specimens previously identified as *B. griselda*. Numbers refer to sample localities provided in the supplementary file.

We selected one sample per species for *Blarina brevicauda*, *Blarina hylophaga*, and *Blarinella wardi*, and one for each of the two distinct lineages of *B. griselda* for sequencing of the complete mitochondrial genomes (mitogenome(s) hereafter) using next-generation sequencing (NGS). We used two approaches to obtain the mitogenomes, that is, long-range PCR and cross-species hybridization capture. Our full protocol has been described and published separately (Chen et al., 2018). In short, we first amplified the mitogenomes using Phusion High-Fidelity DNA Polymerase (New England Biolabs, Canada) with two pairs of primers (Supplementary Table S2) designed within conserved regions of *12s rRNA*, *16s rRNA*, *COX3*, and *ND1*. The amplicons (~8 000 and 10 000 bp in length) were purified using Serapure magnetic beads (Rohland & Reich, 2012) sheared to small fragments using NEBNext dsDNA Fragmentase (New England Biolabs, Canada) and ligated with barcode adapters (NEXTflex DNA Barcodes for Ion Torrent, BIOO Scientific, USA) using a NEBNext Fast DNA Library Prep Set for Ion Torrent (New England Biolabs, Canada) to construct DNA libraries. After ligation, the libraries were purified using Serapure magnetic beads and size-selected using a 2% E-gel on an E-Gel Electrophoresis System (Invitrogen, Canada). Libraries within the 450–500 bp size range were selected and re-amplified using a NEBNext High-Fidelity 2X PCR Master Mix (New England Biolabs, Canada). We then purified the libraries using Serapure magnetic beads and measured the DNA concentration of the purified libraries using Qubit Fluorometric Quantitation (Thermo Fisher Scientific, Canada).

In cases where the sample could not be amplified successfully using the primers, we used an in-solution capture-hybridization approach to enrich mitochondrial DNA (Horn, 2012; Mason et al., 2011). Briefly, this approach uses mitochondrial probes and DNA libraries constructed using genomic DNA to capture mitochondrial-like sequences. To make the probes, we first amplified and purified two amplicons of the *Blarinella griselda* mitogenome. We then measured the DNA concentration of each amplicon using a Nanodrop 2000 spectrophotometer (Thermo Fisher Scientific, Canada) and mixed the two amplicons to ensure the amount of DNA was

in proportion to their relative lengths. The mixed DNA was used to make mitogenome probes (hereafter termed baits) using a Biotin-Nick Translation mix kit (Roche, Germany) according to the manual. The baits were stored at –20 °C before hybridization.

We constructed 450–500 bp-size libraries for each sample from previously extracted genomic DNA (each with a unique barcode as described above) using a NEBNext Fast DNA Library Prep Set for Ion Torrent (New England Biolabs, Canada). The libraries were re-amplified and purified (see above). We mixed the baits and each DNA library at a ratio of approximately 1:10 and then incubated them for 24–48 h at 65 °C (Chen et al., 2018). The enriched libraries were reamplified and quantified using a Qubit as described above. Finally, we pooled the samples to ensure that each had a similar amount of DNA. We sequenced the samples using a v318 chip with the Ion Torrent Personal Genome Machine (PGM).

Molecular data processes and analyses

After sequencing, we first binned the samples based on their sample-specific barcode adapters and converted the raw reads to FASTQ format using the Torrent Suite v4.0.2 (Thermo Fisher Scientific, Canada). We filtered out reads shorter than 60 bp and trimmed off adapter sequences before assembly. We used MIRA4 for *de novo* assemblies (Chevreux et al., 1999), during which we used a strategy (technology=iontor) specifically suitable for ion torrent data to better resolve the homopolymer insertions-deletions problem (Bragg et al., 2013). We also used the Geneious iterative approach (up to 100 iterations) to map the reads to a reference mitogenome of *Blarinella quadraticauda* from Baoxing, Sichuan, China (GenBank accession No. KJ131179.1). These assemblies were conducted using Geneious v8.1 (Kearse et al., 2012). We repeated both the MIRA4 and Geneious assemblies at least twice for each sample, aligned the assemblies for each sample using MUSCLE (Edgar, 2004), and generated a 50% consensus sequence in Geneious v8.1. We also compared the assembled mitogenome with the cyt *b* sequence of the same sample conducted using Sanger sequencing to ensure the mismatch between the two was $\leq$1 bp per 1 000 bp for quality control. Finally, we annotated the mitogenomes using the annotation function in Geneious v8.1. We removed the repeat region of the D-loop region assuming the short NGS reads were not long enough to correctly assemble.

For phylogenetic analyses, we downloaded available mitogenomes of 13 soricine and one crocidurine (*Crocidura attenuata*) shrew from GenBank. We also included *16S rRNA* and cyt *b* fragments of *Blarinella*, most of which were collected in one previous study (Chen et al., 2012), for a mitochondrial gene tree estimation. We aligned the mitogenomes with partial *16S rRNA* and cyt *b* using MUSCLE and removed all tRNAs, the *ND6* gene (which is on the light chain), and the D-loop region from the alignment. The remaining 13 375-bp alignment, which included all coding genes on the heavy chain and two rRNA genes, was used for maximum-likelihood (ML) tree estimation using RAxML (Stamatakis, 2014) and implemented in CIPRES (Miller et al., 2010). We subdivided the alignment by genes (15 partitions) and employed a GTR+G model for each gene. We conducted rapid bootstrapping and searched for the best-scoring ML tree, allowing the program to halt bootstrapping automatically under an extended majority rule criterion (autoMRE). We also subdivided the alignment by gene and codon positions (for coding genes) into 38 data blocks and conducted an additional analysis for comparison.

We estimated an *ApoB* gene tree to ensure the mitogenomic tree was not strongly affected by incomplete lineage sorting or mitochondrial introgression. To accompany our newly collected sequences, we obtained sequences from previous studies (Dubey et al., 2007; He, 2011) and downloaded sequences of 10 soricid shrews as outgroups (Supplementary Table S1). We estimated the RAxML *ApoB* gene tree as described above. The *ApoB* gene was considered as a single partition because few mutations were observed in *Blarinella* sequences of the alignment.

We estimated lineage divergence times from the mitogenome data. While we recognize that mitochondrial genes may overestimate true divergence times, this effect can be mitigated using appropriate calibrations. We applied a second calibration following Springer et al. (2018), which focused on the divergence times of eulipotyphlans, and estimated that the divergence between Crocidurinae and Soricinae occurred 36 Ma (95% confidence interval (CI)=28.6–44.0 Ma). This is much older than fossil calibration used in previous studies (Dubey et al., 2007; He et al., 2010), which was based on the assumption that Crocidosoricinae was the ancestor of Crocidurinae, Myosoricinae, and Soricinae. Crocidosoricinae is now recognized as a tribe of Myosoricinae (Crocidosoricini), thereby invalidating that assumption (Furio et al., 2007). Fossils of both crocidurines and soricines are known from the Oligocene (<34 Ma), with the oldest soricid fossil, *Soricolestes soricavus*, found from Middle Eocene strata, Khaychin Formation (Lopatin, 2002). Thus, the estimated divergence time in Springer et al. (2018) is congruent with fossil records. We estimated divergence times using BEAST v2.5 (Bouckaert et al., 2014). We first estimated the best partition scheme and evolutionary model for each partition using PartitionFinder v2.1.1 (Lanfear et al., 2017). A four-partition scheme (Supplementary Table S3) was selected and the GTR+G model was supported as the best-fitting model for each partition. The monophyly of Soricinae was constrained so that *Crocidura* was fixed at the root of the tree. We employed the Birth-Death model as the tree prior and relaxed lognormal as the clock model prior. We used lognormal distribution for the prior of the divergence time of Soricidae. We set the mean to 36 Ma, with a standard deviation of 0.135, so that the median of the prior was 35.7 Ma and the 95% CI was 28.6–44.5 Ma. We set 4×10^8 generations for each analysis and sampled every 4 000 generations. Convergence was assessed using Tracer v1.7 (Rambaut et al., 2018). We repeated the analyses twice and combined the tree files using LogCombiner v2.5 and estimated the maximum clade credibility tree using Tree Annotator v2.5, both in the BEAST v2.5 package.

Specimen examination and morphometric analyses

We recorded morphological measurements from five newly collected *Blarinella* specimens from Shaanxi (representing the two distinct lineages of *B. griselda*), and included specimens used in our previous study, which were mainly deposited in the American Museum of Natural History, Smithsonian National Museum of Natural History, and Kunming Institute of Zoology (Appendix I; Jiang et al., 2003). External measurements, including head and body length (HB), tail length (TL), and hind foot length (HF), were recorded from specimen labels or field notes. Nineteen craniomandibular variables were measured using a digital caliper graduated to 0.01 mm: condyloincisive length (CIL), interorbital breadth (IOB), cranial breadth (CB), cranial height (CH), maxillary breadth (MB), rostral length (RL), postrostral length (PRL), palatoincisive length (PIL), postpalatal length (PPL), upper toothrow length (UTR), maximum width across upper second molars (M2-M2), postpalatal depth (PPD), mandibular length (ML), lower toothrow length (LTR), length of lower incisor (LLI), zygomatic plate breadth (ZP), condyle-glenoid length (CGT), and breadth of coronoid process (BCP). We analyzed morphometric variation using craniomandibular variables for 88 intact skulls by principal component analyses (PCA). We $\log_{10}$-transformed each variable prior to conducting the PCA in SPSS v17.0 (SPSS Inc, Chicago, Illinois, USA). Based on the results of our molecular analyses (see Results), we assigned the single individual from Gansu and three of the Shaanxi specimens to *B. griselda*; the two other Shaanxi specimens previously identified as *B. griselda* were tentatively identified as *B.* cf. *quadraticauda*.

Morphological comparison and diagnosis

We examined the morphology of the specimens as per Jiang et al. (2003), Repenning (1967), Reumer (1984), and Storch (1995), and followed their terminology for morphological descriptions. We took photos of skulls and teeth using a digital microscope VHX-2000C (KEYENCE).

RESULTS

Phylogenetic relationships

Regardless of the partitioning scheme, each of our mitochondrial datasets revealed the same relationships with similar bootstrap values (BS); thus, only the tree partitioned by genes is presented (Figure 2). Nectogaline (*Episoriculus*, *Neomys*, and *Nectogale*) + anourosoricine (*Anourosorex*) shrews were strongly supported as a clade (BS=88) placed sister to the Soricini with moderate support (BS=75). Species of the genus *Episoriculus* were recovered as paraphyletic (BS=87). The Blarinellini (*Blarinella*) and Blarinini (*Blarina*) were strongly supported as a clade (BS=100), but, within Blarinellini, *Blarinella* formed two distinct sister clades (BS=95), the branch lengths of which were as long as those between Anourosoricini and Nectogalini. One of the two *Blarinella* clades contained the three specimens from Shaanxi and the single specimen from Gansu that we identified as *B. griselda*. Within the second major *Blarinella* clade, four specimens of *B. wardi* from northwestern Yunnan (Gongshan and Zhongdian) formed a distinct branch (BS=100) sister to the subclade consisting of the remaining specimens from Sichuan, Shaanxi, Yunnan, Chongqing, Hubei, and North Vietnam, previously identified as either *B. quadraticauda* or *B. griselda* (BS=100). There were several strongly supported subdivisions in the latter subclade. For example, samples from southern Shaanxi and northeastern-most Sichuan (Qingchuan, adjacent to Shaanxi; Figure 1) formed a basal position, sister to other members of this subclade (BS=73). Samples from Vietnam were placed in two distinct lineages (BS=100).

In our *ApoB* nuclear gene tree, the same interspecific relationships were recovered in Blarinini-Blarinellini (Figure 3). A sister relationship between Blarinini and Blarinellini was strongly supported (BS=100), and two deeply diverged clades were recovered within *Blarinella* (BS=81). One comprised *B. griselda* from Shaanxi and Gansu. In the other clade, *B. wardi* again occupied a position (BS=97) sister to the remaining samples (i.e., *B. quadraticauda*).

Our BEAST analyses recovered the same topology (Figure 4) as our mitochondrial and nuclear gene trees. All relationships were strongly supported with posterior probabilities $\geq$0.98, except for the sister-relationship between *Episoriculus caudatus* and *E. macrurus*, which was 0.90. The divergence time between Blarinini and Blarinellini was estimated to be 21.9 Ma (95% CI=16.5–27.6 Ma), close to that estimated for Anourosoricini and Nectogalini (21.4 Ma, 95% CI=19.2–30.8 Ma). The estimated divergence time between *B. griselda* and other *Blarinella* species was 18.2 Ma (95% CI=13.4–23.6 Ma). The most recent common ancestor of *B. quadraticauda* and *B. wardi* was estimated at 5.8 Ma (95% CI=3.8–8.2 Ma).

Morphometric comparison

External morphology and skull measurements are given in Table 1. Based on the PCA using craniomandibular measurements of intact skulls, the 1st principal component (PC1) accounted for 72.2% of the variation (eigenvalue=13.7), being positively correlated with all variables (loading >0.69), thus reflecting a size effect. The 2nd principal component (PC2) accounted for 7.3% of the variation (eigenvalue=1.4) and was positively correlated with condyle-glenoid length (CGT), postpalatal length (PPL), and postrostral length (PRL), and negatively correlated with interorbital breadth (IOB), thus indicating strong correlation with the shape of the posterior cranium. On the PC1 and PC2 plot (Figure 5), *B. griselda* overlaps with *B.* cf. *quadraticauda* specimens (i.e. those previously identified as *B. griselda*), suggesting they do not differ from each other by size or overall shape of the skull. When looking at the remaining specimens, *B. quadraticauda* occurs along the positive regions of PC1 and PC2, whereas *B. wardi* plots on the negative regions of both PC1 and PC2. Furthermore, *B.* cf. *quadraticauda* exhibits geographic variations. For example, the specimens from Chongqing are closest to *B.* cf. *quadraticauda* on the plot, being distinguishable from the specimens from Yunnan, Sichuan, and

Shaanxi. In addition, *B. wardi* from Yunnan and northern Myanmar also diverge, although they still overlap on the plot.

Morphological diagnosis

Because of the deep genetic divergence between *B. griselda* and the other *Blarinella* taxa, it is necessary to describe the morphology at higher taxonomic levels. *Blarinella griselda* exhibits entoconid crests on the lower M_1 and M_2 (Figure 6A), which are missing in Blarinini; its mandibular condyle also has a broad interarticular area (Figure 7A), which differs from Anourosoricini and Nectogalini, both of which have a narrow interarticular area; *B. griselda* has large but not fissident upper incisors (Figure 7B), which differs from Beremendiini with strongly fissident upper incisors. Finally, the M_3 of *B. griselda* has a highly reduced talonid (Figure 7C), which differs from Soricini and Notiosoricini.

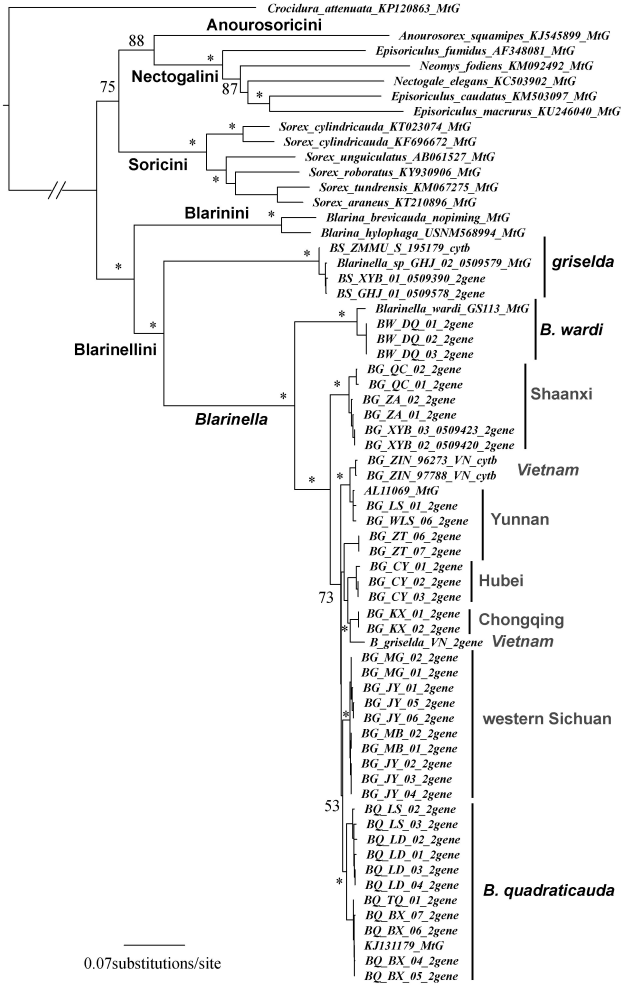

Figure 2 Mitochondrial gene tree

Branch lengths represent substitutions per site. Numbers above branches are bootstrap values supporting the relationship. Asterisks indicate bootstrap value is higher than 90. Key to type of gene data: 18MtG: mitogenome; 42 2 gene:16S rRNA and cyt *b*; 3 cyt *b*: only cyt *b* gene.

The craniodental morphology of *B. griselda* closely matches descriptions given by Reumer (1998) for the tribe Blarinellini (see Systematic Biology section) with a single exception regarding the position of the entoconid and shape of the entoconid crest on the lower M_1 and M_2, which are variable in *Blarinella* (Figure 6), as discussed in a previous study (Storch, 1995).

Though *B. griselda* does not differ from *B.* cf. *quadraticauda* morphometrically (see Figure 5), there are several characters of the skull and teeth that differentiate *B. griselda* from *B. quadraticauda*, *B.* cf. *quadraticauda*, and *B.* w*ardi*. For example, the tip of the coronoid of *B. griselda* is bent anteriorly relative to its position in the other species (Figure 8). The lambdoid crest (dorsal view) of *B. griselda* is triangle-shaped, whereas in the other species the crest is arcuate, extending

more anteriorly (Figure 8). The lower P_4 of *B. griselda* is small, whereas P_4 extends anteriorly in other species (Figure 9A). On the lower molars of the other species, the paraconids extend anteriorly and the protoconids extend buccally, so that the trigonid basin area is large. Conversely, the paraconids and protoconids of *B. griselda* are not extended, and thus the trigonid basin is smaller (Figure 9A). In *B. griselda*, the entoconid and metaconid on M_1 and M_2 are close to each other but well separated, while the entoconid crests are present but distinctly lower than these two cusps (Figure 6A). In the other species, the entoconid and metaconid are either close to one another, connected by a high crest (*B. quadraticauda*; Figure 6B, C), or the entoconid is inconspicuous (*B. wardi*; Figure 6D), although there are some exceptions in *B. quadraticauda*. On unworn upper incisors, the apex of *B. griselda* extends more anteriorly, whereas the apex extends downward in the other species (Figure 8). The upper P^4 of *B. griselda* has a triangular occlusal outline (Figure 9C), whereas P^4 in the other species has a quadrangular occlusal outline (Figure 9D). These nuanced but stable characteristics distinguish *B. griselda* from *B. quadraticauda*, *B.* cf. *quadraticauda,* and *B. wardi.* In consideration of the deep genetic divergence and morphological distinctions, we elevate *B. griselda* to a new genus, as described below.

Systematic biology

Family Soricidae G. Fischer, 1814

Subfamily Soricinae G. Fischer, 1814

Tribe Blarinellini Reumer, 1998

The tribe was defined by Reumer (1998) basically based on dental morphology: "*horizontal ramus of mandible short and high, making the lower dentition compressed anteroposteriorly, and giving the lophs and lophids a compressed W-shaped appearance, mandibular condyle large, with a broad interarticular area; coronoid spicule of mandible well developed; teeth heavily pigmented; upper incisor protruding but not fissident; upper molariform teeth with a reduced posterior emargination, showing a tendency to develop a continuous endoloph; occlusal surface of M_1 nearly square; M_3 with a reduced talonid*". The "lower molars with the entoconid close to the metaconid so that the entoconid crest is short and high" are variable in *Blarinella* (Figure 6), as observed in a previous study (Storch, 1995).

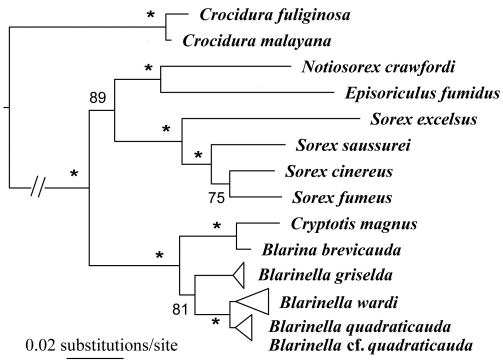

Figure 3 *ApoB* gene tree

Branch lengths represent substitutions per site. Numbers above branches are bootstrap values supporting the relationship. Asterisks indicate bootstrap value is higher than 90. We collapsed each species branch because of low intra-specific variation.

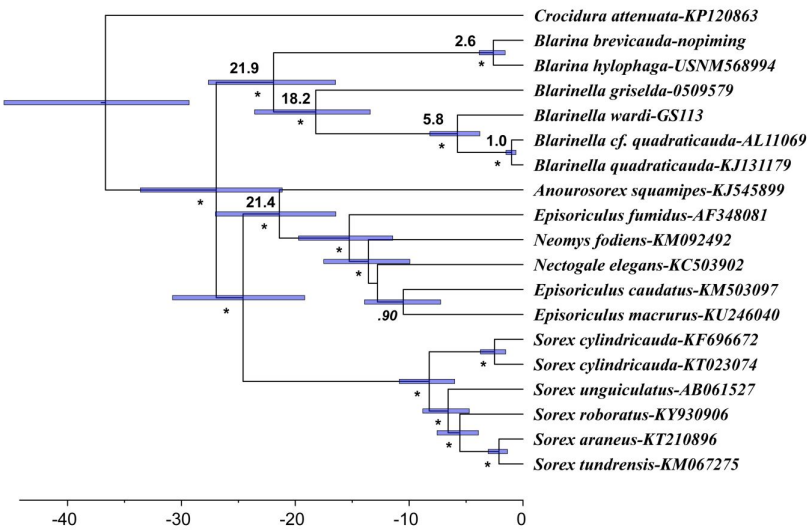

Figure 4 Divergence times estimated using BEAST based on mitogenome data

Branch lengths represent time. Number below each node denotes posterior probabilities (PP). Asterisks indicate PP is higher than 0.98. Numbers above branches refer to divergence time in millions of years.

Table 1 External and craniomandibular measurements, including mean values, standard deviations (top line), together with range and sample sizes (bottom line) of species included in the current study

Variable	*B. griselda*	B. *quadraticauda*	B. cf. *quadraticauda*	B. *wardi*
HB	66.33±0.47	72.21±4.01	65.19±4.32	64.04±2.77
	66–67; 3	65–81; 19	52–73; 47	60–69; 23
TL	36.67±1.7	45.63±4.13	36.37±2.38	37.57±3.14
	35–39; 3	40–60; 19	31–39; 46	32–43; 21
HF	11±0	14.53±0.99	11.04±1.53	11.83±0.52
	11–11; 3	13–16; 19	8.5–13; 46	10.5–13; 23
CIL	19.52±0.34	21.32±0.18	19.97±0.42	19.15±0.38
	19.14–19.96; 4	21–21.69; 19	19.13–20.93; 47	18.54–19.91; 23
IOB	4.33±0.13	4.45±0.15	4.39±0.2	4.04±0.09
	4.2–4.52; 4	4.13–4.66; 19	4.06–4.83; 47	3.89–4.33; 23
CB	9.08±0.26	9.5±0.1	9.12±0.22	8.33±0.22
	8.85–9.48; 4	9.34–9.7; 19	8.57–9.63; 46	7.84–8.72; 22
CH	5.52±0.52	5.38±0.15	4.98±0.22	4.58±0.2
	4.62–5.89; 4	5.11–5.82; 19	4.43–5.15; 46	4.12–4.93; 23
RL	6.51±0.15	7.68±0.25	7.25±0.35	6.64±0.2
	6.32–6.73; 4	7.19–8.05; 19	6.79–7.96; 47	6.25–7.11; 23
PRL	11.49±0.28	12.59±0.2	11.81±0.31	11.58±0.29
	11.2–11.96; 4	12.28–12.94; 19	11.26–12.51; 46	11.06–12.11; 23
MB	5.78±0.18	6.14±0.12	5.91±0.15	5.39±0.15
	5.57–6.05; 4	5.91–6.36; 19	5.62–6.26; 46	5.04–5.77; 23
PIL	8.62±0.19	9.49±0.09	8.93±0.24	8.42±0.22
	8.42–8.9; 4	9.33–9.66; 19	8.26–9.45; 47	7.93–8.78; 23
PPL	9.15±0.29	9.95±0.17	9.28±0.23	9.15±0.25
	8.76–9.5; 4	9.54–10.25; 19	8.7–9.76; 46	8.67–9.63; 23
UTR	8.34±0.16	8.74±0.11	8.34±0.24	7.63±0.24
	8.16–8.59; 4	8.37–8.88; 19	7.79–8.64; 47	6.98–7.97; 23
M^2-M^2	5.25±0.11	5.51±0.13	5.29±0.12	4.81±0.11
	5.15–5.44; 4	5.34–5.77; 19	5.08–5.58; 47	4.56–5.03; 23
ML	10.27±0.21	10.7±0.15	10.06±0.32	9.52±0.29
	10.04–10.61; 4	10.37–11; 19	9.39–10.86; 46	8.91–9.95; 22
LTR	7.83±0.16	8.6±0.1	8.1±0.2	7.5±0.16
	7.66–8.07; 4	8.41–8.77; 19	7.55–8.47; 46	7.08–7.74; 22
LLI	4.49±0.07	5.21±0.14	4.73±0.2	4.39±0.18
	4.4–4.6; 4	4.84–5.49; 19	4.2–5.04; 46	4.13–4.79; 22
CGT	8.69±0.17	9.27±0.14	8.74±0.18	8.61±0.2
	8.54–8.96; 4	9.04–9.55; 19	8.36–9.14; 46	8.13–8.96; 23
BCP	1.19±0.01	1.34±0.05	1.2±0.09	1.11±0.09
	1.18–1.2; 4	1.24–1.45; 19	1.03–1.4; 46	0.98–1.34; 22
MTL	4.73±0.15	5.23±0.08	5.03±0.11	4.68±0.11
	4.58–4.92; 4	5.12–5.41; 19	4.8–5.29; 47	4.37–4.87; 23
PPL	3.32±0.08	3.64±0.08	3.47±0.1	3.21±0.08
	3.23–3.44; 4	3.48–3.78; 19	3.29–3.65; 47	3.07–3.34; 23
ZP	2.03±0.09	2.28±0.09	2.14±0.1	1.97±0.11
	1.91–2.14; 4	2.16–2.44; 19	1.86–2.38; 47	1.7–2.2; 23

B. cf. *quadraticauda* represents specimens originally identified as *B. griselda*. Abbreviations of variable names are explained in the Materials and Methods. All measurements are in mm.

***Pantherina* He Kai, gen. nov**.

Type species: *Pantherina griselda* (Thomas, 1912)

Etymology: The genus name derives from the feminine Latin noun *Panthera* ("panther") + the diminutive suffix *-ina*, hence, "little panther". The name indicates animals in this genus are small but as black and aggressive as a panther. Griselda is a feminine given name.

Suggested common name: Panther shrew; 豹鼩属.

Included species: Type species only.

Diagnosis: External morphology and overall shape of skull very similar to *Blarinella*. Tip of coronoid process slightly bends anteriorly, differs from *Blarinella* (continuing vertically). Lambdoid crest angular in dorsal view (more rounded in *Blarinella*). Five upper unicuspids (four upper unicuspids in *Petenyia*). I_1 bicuspulate, with minute third posterior cuspule present (tricuspulate in *Alloblarinella* and *Zelceina*). Lower P_4 small, not extending anteriorly (larger and extending anteriorly in *Blarinella*). Trigonid occlusal outline of lower molars trapezoidal-shaped (V-shaped or U-shaped in *Blarinella*). Apex of upper incisors extends anteriorly (directly downward in *Blarinella*). Upper P^4 with triangular occlusal outline; protocone low, forming antero-lingual corner on ventral outline (trapezoidal-shaped in *Blarinella*).

Description: Skull and mandible: Skull stout and robust. Rostrum short. Braincase dome-shaped but low. Occipital bone small, lambdoid crest triangle-shaped from dorsal view. Entoglenoid processes well developed. Horizontal ramus high. Coronoid process broad and spatulate-shaped, tip of coronoid bends anteriorly, anterior edge of coronoid concave. Coronoid spicule high and strongly pronounced, external temporal fossa shallow. Articular facets of condyle close to each other, with angle of intersection approximately 45°, upper facet narrow and cylinder-shaped, interarticular area broad.

Lower teeth: Lower incisor (I_1) obviously bicuspulate, with minute third posterior cuspule present. On buccal side, posterior end reaches level of anterior part of M_1. On lingual side, slender groove obviously presents along I_1 toward tip. First lower unicuspid very small, larger part of tooth squeezed between I_1 and P_4. Occlusal outline of P_4 bulbous-shaped. Trigonids of M_1 and M_2 trapezoidal-shaped. On M_1, M_2, entoconids high and close to metaconid, with two cusps connected by low entoconid crest. M_3 with trigonid unreduced in size but with talonid reduced to single, low, nearly conical, slightly blade-like hypoconid, with no trace of entoconid crest.

Upper teeth: Upper I^1 noticeably extends anteriorly. Apex of upper I^1 moderately long and broad, spatulate, not fissident; talon lower than first upper unicuspid. Five upper unicuspids (U) present. From occlusal view, U^1–U^5 decreases in size of total area in order. U^1 twice as large as U^2, and U^4 and U^5 extremely small. U^1–U^4 visible in lateral view of skull. P^4 with no posterior emargination; protocone small, forming antero-lingual corner in outline of tooth; hypocone absent, hypoconal flange extends to approximately level of metacone; occlusal outline of P^4 triangular in shape. M^1 and M^2 similar in shape: protocone low, forming antero-lingual corner in ventral outline, hypocone absent, hypoconal flange extends posteriorly; occlusal outline square-shaped. M^3 small, with well-developed paracone, lingual part consists of basin surrounded by U-shaped ridge.

Remarks: Some characters observed in *P. griselda* are more similar to fossil genera related to extant *Blarinella* species. For example, the anterior projection of the tip of the coronoid process in *P. griselda* has also been observed in *Petenyia hungarica* and *Zelceina kormosi* (Reumer, 1984; Storch, 1995). The entoconid and entoconid crest on the lower M_1 and M_2 of *P. griselda* have been observed in *Petenyia hungarica* (Reumer, 1984). Of note, this is a variable character in *Blarinella*, with some *B. quadraticauda* also having a similar structure. The triangular-shaped P^4 of *P. griselda* is somewhat similar to that of *Alloblarinella sinica* and *Petenyia hungarica* and quite similar to that of *Petenyia bubia* (Reumer, 1984).

Pantherina griselda

Blarinella griselda (Thomas, 1912)

Blarinella quadraticauda griselda (Allen, 1938)

Type locality: 68 km SE Taochou (=Lingtan), 3 048 m a.s.l., Gansu, NW China.

Holotype: Natural History Museum (British) No. 12.8.5.23, collected by J.A.C. Smith

Suggested common name: Gray panther shrew; 淡灰豹鼩

Measurements: Table 1

Figure 6A, Figure 7, Figure 8 left, Figure 9A, C, E

Distribution: Currently known from two localities in southern Gansu and southern Shaanxi (Figure 1).

Description: As for the genus.

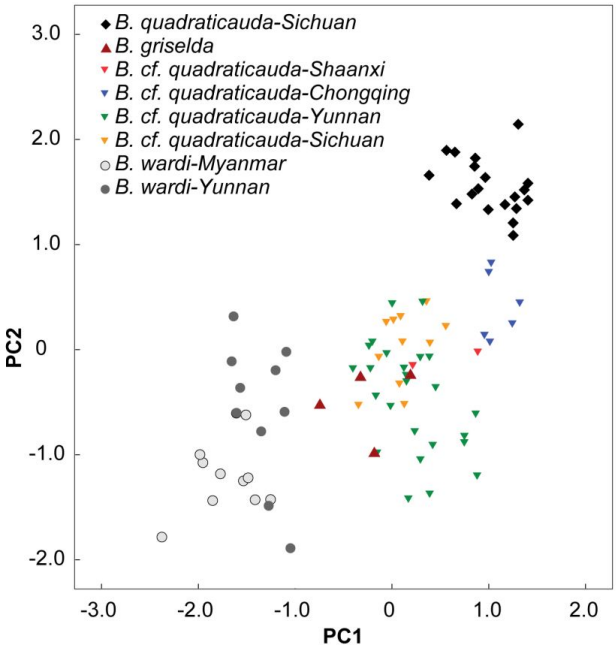

Figure 5 Plot of PC1 and PC2 scores from principal component analyses (PCA) of 19 $\log_{10}$-transformed cranial measurements from 87 *Blarinella* specimens

Most specimens were previously examined by Jiang et al. (2003). Specimens identified as *B.* cf. *quadraticauda* were originally identified as *B. griselda* in Jiang et al. (2003).

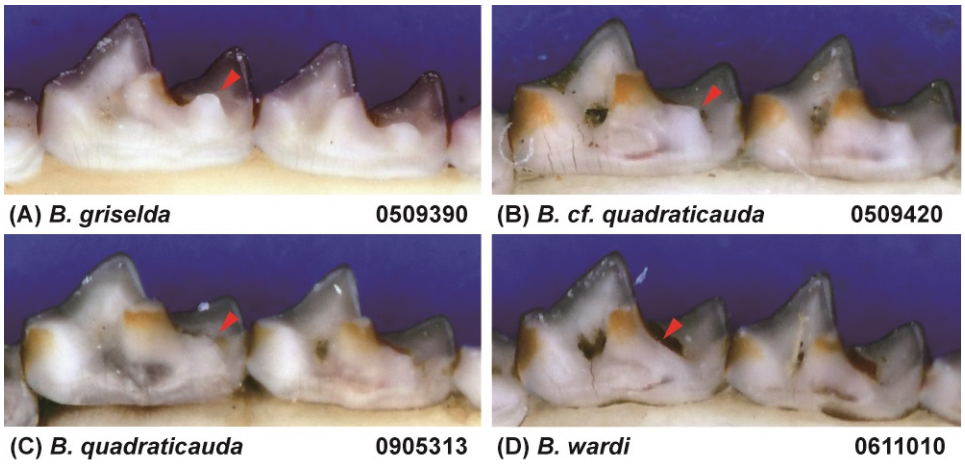

Figure 6 Buccal view of lower M_1 and M_2 of four Blarinellini specimens

Interspecific variations among entoconids and entoconid crests. The arrows point at the entoconids of M_1. In *B. wardi*, entoconid does not present.

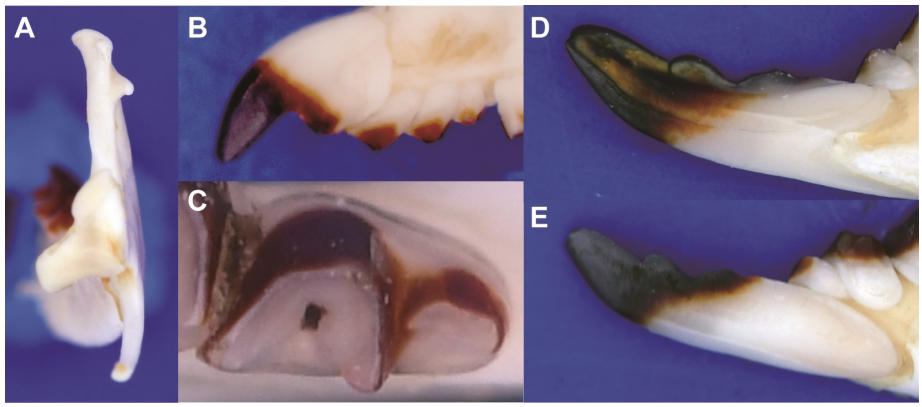

Figure 7 Craniodental characters of *B. griselda*

Articular facets of mandibular condyle (A), first upper incisor (B), lower M_3 (C), buccal view (D) and lingual view (E) of lower incisor.

Comparison: Specimens of *Pantherina griselda* from Shaanxi are superficially similar to *Blarinella* in gross morphology; however, a number of characters distinguish the two taxa. In *P. griselda*, the lambdoid crest is angular in dorsal view, whereas in species of *Blarinella*, the occipital bone extends anteriorly, resulting in a more rounded lambdoid crest (Figure 8B). The tip of the coronoid process projects anteriorly rather than continuing vertically, as in *Blarinella*. The groove on the buccal side of I_1 is narrow, rather than broad in *Blarinella*. In the labial view, P_4 of *P. griselda* does not extend anteriorly, so the tooth and trigonid basin are smaller than that of *Blarinella*, in which the P_4 extends anteriorly. In *P. griselda*, the paraconids of M_1 and M_2 do not extend anteriorly, the trigonid occlusal outline is trapezoidal, and the trigonid basin area is small, whereas in *Blarinella*, the paraconids of M_1 and M_2 extend anteriorly, the metaconid extends posteriorly, the trigonid has a V-shaped or U-shaped occlusal outline, and the trigonid basin area is large. In *P. griselda*, the entoconid and metaconid on M_1 and M_2 are high and connected by distinctly lower entoconid crest. *Blarinella wardi* has no entoconid or entoconid crest on M_1 or M_2, but the posterior faces of its metaconids extend posteriorly forming a posterior ridge, which is not present in *Pantherina.* In *B. quadraticauda* (including *B.* cf. *quadraticauda*), the entoconid crest is variable, depending on the locality. For example, some specimens from the type locality (i.e., northwestern Sichuan) have a low, moderately-developed entoconid located close to the metaconid, resulting in a short and moderately-high entoconid crest; in a few populations from northeastern Yunnan (*B.* cf. *quadraticauda*), the entoconid and entoconid crest are more similar to those of *P. griselda,* although the height of the entoconid is lower; in other samples, the entoconid is not obviously present and is more similar to *B. wardi*. The upper I^1 of *P. griselda* extend anteriorly, with a long apex, whereas, in *Blarinella*, the apex is shorter and typically directed ventrally. The occlusal outline of P^4 in *P. griselda* is triangular and the protocone is small, forming an antero-lingual corner in the outline of the tooth, whereas in *Blarinella*, the occlusal outline of P^4 is mostly trapezoidal, and the protocone is more robust, not forming an antero-lingual corner in the outline. On the M^1 and M^2 of *P. griselda,* the hypoconal flange extends posteriorly, whereas in *Blarinella*, the hypoconal flange extends anteriorly.

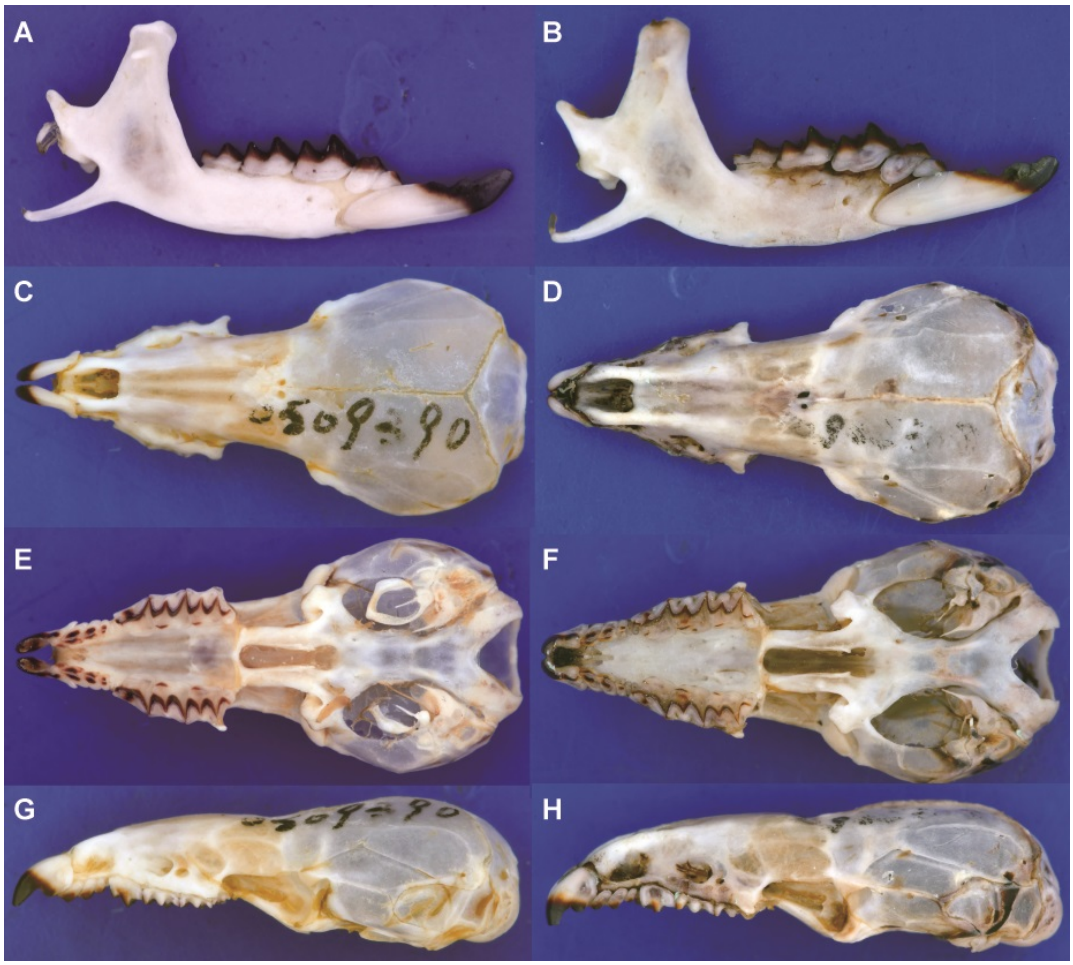

Figure 8 Mandibles and skulls of *B. griselda* (KIZ0509390; A,C,E,G) and *B. quadraticauda* (KIZ0905313; B,D,F,H)

DISCUSSION

Taxonomic implications

Our results strongly support the conclusion that specimens ascribed to *Blarinella griselda* are paraphyletic; one is a close relative to *B. quadraticauda*, whereas the other presents an anciently diverged lineage of Blarinellini. The divergence time estimation (18.2 Ma) suggests a divergence more ancient than the ancestor of Nectogalini, and close to that between Anourosoricini and Nectogalini. Morphometric analyses could not differentiate the two forms, indicating that phenotypic evolution was not strongly associated with quantitative characters. However, several nuanced but stable diagnostic characters on the skull and dentition distinguish *B. griselda* from other species of *Blarinella*. Some of these craniodental differences were observed for several fossil genera of the tribe. In other words, the difference between *B. griselda* and members of the genus *Blarinella* is at the same level as that between currently recognized genera. Because the two extant lineages showed marked genetic divergence from one another (Figures 2, 3), and because of the observation of inter-generic level morphological variation (Figures 6–9), we recognize *B. griselda* as a distinct genus, namely *Pantherina*.

It should be noted that *Pantherina* shares several characters with fossil taxa, such as a triangle-shaped P^4 on occlusal view, indicating that the genus represents a more primitive form of the tribe and may have closer affinities with fossil taxa within Blarinellini. We have not attempted to fully revise the systematic paleontology in the current study, but taxonomic revision that includes fossils is warranted. We do not currently recognize *Pantherina* as one of the fossil genera based on the obvious differences in the skull and dentation. For example, it should not be assigned to *Alloblarinella* or *Zelceina* whose lower incisor is tricuspulate (bicuspulate in *Pantherina*). It should not be assigned to *Petenyia* which has only four unicuspids (*Pantherina* has five). Its small M_3 also differs from that of *Alloblarinella* which has a large M_3 with complete trigonid and talonid.

The new monotypic genus *Pantherina* is known currently only from southern Gansu (Lintan) and southern Shaanxi (Ningshaan). Despite extensive recent surveys (Chen et al., 2012; K.H., unpublished data), members of this genus have

not been found in southern areas of China such as Chongqing, Hubei, or northwestern Sichuan—areas that are, however, occupied by *B. quadraticauda*. *Pantherina* is unlikely to be distributed in more northern areas due to absence of suitable habitat, and thus presumably has a restricted distribution in southern Shaanxi and southern Gansu. Because *Pantherina* has similar morphology to *B. quadraticauda*, and because they co-occur in Shaanxi, they might compete for the same habitat.

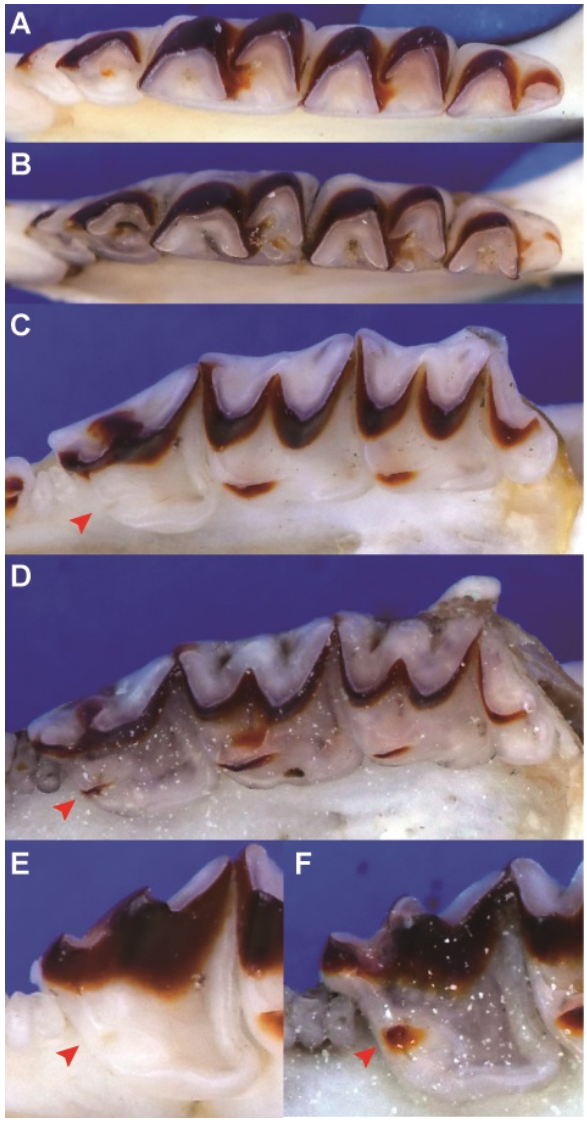

Figure 9 Occlusal views of lower teeth and upper teeth, and occlusal view of upper P^4 of *B. griselda* (A,C,E) and *B. quadraticauda* (B,D,F). Arrows point at the protocone of upper P^4

We tentatively assign the remaining specimens previously identified as *B. griselda* from China and Vietnam to *B.* cf. *quadraticauda* because they clustered together with *B. quadraticauda* in a well-supported clade in both the mitochondrial (Figure 2) and nuclear gene trees (Figure 3), with the latter forming a lineage well embedded within this clade (Figure 2). This placement does not mean that a two-species scenario (*B. quadraticauda* and *B. wardi*) is sufficient to cover the species diversity of this genus. Instead, we believe that species diversity is still underestimated, as implied in our morphometric and phylogenetic analyses. For example, on the PCA plot, the animals from Chongqing are clearly distinguished from other *B. quadraticauda* (Figure 5). The mitogenomic gene tree supports multiple fine-supported subclades within *B. quadraticauda* (i.e., BS≥70), which also show a strong geographic pattern. The animals from Shaanxi and northeastern-most Sichuan cluster together, forming a basal divergence within *B. quadraticauda* (BS=73). The specimens from Vietnam are also of two different originations (BS=100). Whether these distinguishable clades or morphometric groups represent undescribed species/subspecies or geographic populations remain open questions.

Implications for systematics and macroevolution

Recognition of a new genus of Blarinellini is especially interesting, not only because it is the second extant genus of the tribe, but because it could provide clues to fill the evolutionary relationship gaps among living and fossil taxa of this genera-rich tribe. Reumer (1998) assigned *Blarinella* together with eight fossil genera into Blarinellini, and *Tregosorex*, previously assigned to Blarinini, has also been assigned recently based on diagnosis of newly discovered fossil material (Doby, 2015). With the addition of *Pantherina*, 11 genera can be recognized, which is the largest number for the Soricinae. The genus boundaries of Blarinellini shrews were established exclusively based on morphological diagnosis and comparison, and some species have been moved from one genus to another. The current classification and systematic hypotheses for the tribe Blarinellini are difficult to test using molecular-based approaches because there are no available resources. Although it is possible to use a morphological matrix, the results may be affected by homoplasy, especially when the number of characters is not large and molecular data are not integrated. Indeed, phylogenic analysis was carried out for Eurasian soricine shrews to include six genera of Blarinellini but revealed five polyphyletic lineages (Rofes & Cuenca-Bescos, 2009). Because all characters were equally weighted (which is usually not a good assumption for morphological characters), the topology was not constrained, and molecular data were not incorporated, high-level relationships among extant taxa were very different from the well-known molecular phylogenies: *Blarinella* was grouped with Anourosoricini (which is closely related with Nectogalini; see Figure 2), and *Neomys* (a nectogaline genus) was not grouped with the other Nectogalini shrews (see Figure 2). As acknowledged by the authors, the homoplasy index was high, so it may suffer convergence in morphology (Springer et al., 2013), which is very common in semi-fossorial small mammals (He et al., 2015). These

previous studies suggest that a systematic relationship exclusively based on morphological data may be biased. The time-calibrated tree accomplished by a morphological matrix could provide a scaffold for analyzing craniodental evolution in the tribe, thereby assisting in examining hypotheses of systematic relationships. The latter could be especially true because *Pantherina* seems to represent a more primitive lineage than *Blarinella*, as some characteristics of *Pantherina* are also observed in fossil taxa. These include a more triangle-shaped P^4, which is similar to that of *Petenyia bubia* from the Miocene. The presence of entoconids and entoconid crests on the lower M_1 and M_2 also seem to be pleiomorphic, which has been observed in many primitive fossil shrews, including Heterosoricinae from the Eocene (Repenning, 1967). Among the fossil genera of Blarinellini, four were exclusively distributed in Eurasia (*Alloblarinella*, *Cokia*, *Hemisorex*, and *Paenepetenyia*) and four were exclusively from North America (*Alluvisorex*, *Anchiblarinella*, *Parydrosorex*, and *Tregosorex*). In addition, *Petenyia* was distributed throughout both North America and Eurasia. Finely-resolved phylogenetic and systematic relationships could help to illustrate the pattern of transcontinental migrations through time (Dubey et al., 2007).

COMPETING INTERESTS

The authors declare that they have no competing interests.

AUTHORS' CONTRIBUTIONS

K.H., X.L.J., and K.L.C. designed the study. K.H. and X.C. conducted the NGS experiments, K.H., P.C., and S.W.H conducted the Sanger sequencing, X.L.J. measured specimens. K.H. conducted the morphological analyses. F.C. took all skull photos. K.H. drafted the manuscript with assistance from K.L.C. All authors read and approved the final manuscript.

ACKNOWLEDGEMENTS

We are grateful to Esther Langan and Darrin Lunde, National Museum of Natural History, Smithsonian Institution, and Robert Voss and Guy Musser, American Museum of Natural History, for allowing us to access the specimens under their care. We are also grateful to Esther Langan and Darrin Lunde for providing the tissue samples of *Blarina hylophaga*. We are grateful to Margaret Docker for allowing us to use ION Torrent PGM in her lab. We thank the anonymous reviewers for positive comments and suggestions and thank Neal Woodman for his suggestions and extensive editing for improvement. We also thank Qiang Li and Yi-Kun Li from the Institute of Vertebrate Paleontology and Paleoanthropology, Chinese Academy of Sciences for sharing literature.

REFERENCES

Allen GM. 1938. The Mammals of China and Mongolia. Part I. New York: American Society of Mammalogists.

Bannikova AA, Abramov AV, Lebedev VS, Sheftel BI. 2017. Unexpectedly high genetic diversity of the Asiatic short-tailed shrews *Blarinella*(Mammalia, Lipotyphla, Soricidae). *Doklady Biological Sciences*, **474**(1): 93–97.

Bouckaert R, Heled J, Kühnert D, Vaughan T, Wu CH, Xie D, Suchard MA, Rambaut A, Drummond AJ. 2014. BEAST 2: A software platform for Bayesian evolutionary analysis. *PLoS Computational Biology*, **10**(4): e1003537.

Bragg LM, Stone G, Butler MK, Hugenholtz P, Tyson GW. 2013. Shining a light on dark sequencing: Characterising errors in ion torrent PGM data. *PLoS Computational Biology,* **9**(4): e1002031.

Chen S, Liu S, Liu Y, He K, Chen W, Zhang X, Fan Z, Tu F, Jia X, Yue B. 2012. Molecular phylogeny of Asiatic short-tailed shrews, genus *Blarinella* Thomas, 1911(Mammalia: Soricomorpha: Soricidae) and its taxonomic implications. *Zootaxa*, **3250**: 43–53.

Chen X, Ni G, He K, Ding ZL, Li GM, Adeola AC, Murphy RW, Wang WZ, Zhang YP. 2018. Capture hybridization of long-range DNA fragments for high-throughput sequencing. *In*: Huang T. Computational Systems Biology: Methods and Protocols. New York, NY: Springer New York, 29–44.

Chevreux B, Wetter T, Suhai S. German Conference on Bioinformatics. 1999.

Corbet GB. 1978. The Mammals of the Palaearctic Region: A Taxonomic Review. British Museum (Natural History) Publication, 1–314.

Doby J. 2015. A Systematic Review of the Soricimorph Eulipotyphla (Soricidae: Mammalia) from the Gray Fossil Site (Hemphillian). East Tennessee State University, Tennessee.

Dubey S, Salamin N, Ohdachi SD, Barrière P, Vogel P. 2007. Molecular phylogenetics of shrews(Mammalia: Soricidae) reveal timing of transcontinental colonizations. *Molecular Phylogenetics and Evolution*, **44**(1): 126–137.

Edgar RC. 2004. MUSCLE: Multiple sequence alignment with high accuracy and high throughput. *Nucleic Acids Research,* **32**(5): 1792–1797.

Furio M, Santos-Cubedo A, Minwer-Barakat R, Agusti J. 2007. Evolutionary history of the African soricid Myosorex(Insectivora : Mammalia) out of Africa. *Journal of Vertebrate Paleontology*, **27**(4): 1018–1032.

He K. 2011. Phylogeny and Phylogeography of Some Taxa in Soricomorpha in Southwest China. Ph D. dissertation. Kunming Institute of Zoology, Chinese Academy of Sciences, Kunming. (in Chinese with English abstract)

He K, Li YJ, Brandley MC, Lin LK, Wang YX, Zhang YP, Jiang XL. 2010. A multi-locus phylogeny of Nectogalini shrews and influences of the paleoclimate on speciation and evolution. *Molecular Phylogenetics and Evolution*, **56**(2): 734–746.

He K, Wang WZ, Li Q, Luo PP, Sun YH, Jiang XL. 2013. DNA barcoding in surveys of small mammal community: a case study in Lianhuashan, Gansu Province, China. *Biodiversity Science*, **21**(2): 197–205.

He K, Woodman N, Boaglio S, Roberts M, Supekar S, Maldonado JE. 2015. Molecular phylogeny supports repeated adaptation to burrowing within small-eared shrews genus of Cryptotis(Eulipotyphla, soricidae). *PLoS ONE*, **10**(10): e0140280.

Horn S. 2012. Target enrichment via DNA hybridization capture. *In*: Shapiro B, Hofreiter M. Ancient DNA. Springer, 177–188.

Hutterer R. 1993. Order Insectivora. *In*: Wilson DE, Reeder DM. Mammal Species of the World: A Taxonomic and Geographic Reference. Washington & London: Smithsonian Institution Press, 69–130.

Hutterer R. 2005. Order Erinaceomorpha. *In*: Wilson DE, Reeder DM. Mammal Species of the World: A Taxonomic and Geographic Reference. Baltimore: The Johns Hopkins University Press, 212–219.

Jiang XL, Wang YX, Hoffmann RS. 2003. A review of the systematics and distribution of Asiatic short-tailed shrews, genus *Blarinella(*Mammalia:

Soricidae). *Mammalian Biology*, **68**(4): 193–204.
Kearse M, Moir R, Wilson A, Stones-Havas S, Cheung M, Sturrock S, Buxton S, Cooper A, Markowitz S, Duran C, Thierer T, Ashton B, Meintjes P, Drummond A. 2012. Geneious Basic: an integrated and extendable desktop software platform for the organization and analysis of sequence data. *Bioinformatics*, **28**(12):1647–1649.
Lanfear R, Frandsen PB, Wright AM, Senfeld T, Calcott B. 2017. Partitionfinder 2: New methods for selecting partitioned models of evolution for molecular and morphological phylogenetic analyses. *Molecular Biology and Evolution*, **34**(3): 772–773.
Lopatin AV. 2002. The earliest shrew (Soricidae, Mammalia) from the Middle Eocene of Mongolia. *Paleontological Journal*, **36**(6):650–659.
Mason VC, Li G, Helgen KM, Murphy WJ. 2011. Efficient cross-species capture hybridization and next-generation sequencing of mitochondrial genomes from noninvasively sampled museum specimens. *Genome Research*, **21**(10): 1695–1704.
Miller MA, Pfeiffer W, Schwartz T. 2010. Creating the CIPRES Science Gateway for Inference of Large Phylogenetic Trees in SC10: Workshop on Gateway Computing Environments (GCE10).
Milne-Edwards H, Milne-Edwards A. 1872. Recherches pour servir à l'histoire naturelle des mammifères. Paris.
Wilson DE, Mittermeier RA. 2018. Handbook of the Mammals of the World - Volume 8: Insectivores, Sloths and Colugos. Barcelona: Lynx Edicions.
Rambaut A, Drummond AJ, Xie D, Baele G, Suchard MA. 2018. Posterior summarisation in Bayesian phylogenetics using Tracer 1.7. *Systematic Biology*, syy032. https://doi.org/10.1093/sysbio/syy032.
Repenning CA. 1967. Subfamilies and genera of the Soricidae: Geological Survey Professional Paper 565. United States Government Printing Office, https://pubs.usgs.gov/pp/0565/report.pdf.
Reumer JWF. 1984. Ruscinian and early Pleistocene Soricidae(Insectivora, Mammalia) from Tegelen(The Netherlands) and Hungary. *Scripta Geologica,* **73**: 1–173
Reumer JWF. 1998. A classification of the fossil and recent shrews. *In*: Wojcik JM, Wolsan M. Evolution of Shrews. Bialowieza: Mammal Research Institute, 5–22.
Rofes J, Cuenca-Bescos G. 2009. A new genus of red-toothed shrew(Mammalia, Soricidae) from the Early Pleistocene of Gran Dolina(Atapuerca, Burgos, Spain), and a phylogenetic approach to the Eurasiatic Soricinae. *Zoological Journal of the Linnean Society,* **155**(4): 904–925.
Rohland N, Reich D. 2012. Cost-effective, high-throughput DNA sequencing libraries for multiplexed target capture. *Genome Research,* **22**(5): 939–946.
Sambrook J, Russell DW, Maniatis T. 2001. Molecular Cloning: a Laboratory Manual. Cold Spring Harbor, New York: Cold Spring Harbor Laboratory Press.
Smith AT, Xie Y. 2008. A Guide to the Mammals of China. Princeton, New Jersey: Princeton University Press.
Springer MS, Murphy WJ, Roca AL. 2018. Appropriate fossil calibrations and tree constraints uphold the Mesozoic divergence of solenodons from other extant mammals. *Molecular Phylogenetics and Evolution,* **121**: 158–165.
Springer MS, Meredith RW, Teeling EC, Murphy WJ. 2013. Technical comment on "The placental mammal ancestor and the post–K-Pg radiation of placentals". *Science*, **341**(6146): 613.
Stamatakis A. 2014. RAxML version 8: A tool for phylogenetic analysis and post-analysis of large phylogenies. *Bioinformatics*, **30**(9): 1312–1313.
Storch G. 1995. The Neogene mammalian faunas of Ertemte and Harr Obo in Inner Mongolia(Nei Mongol), China. - 11. Soricidae(Insectivora). *Senckenbergiana Lethaea*, **75**: 221–251.
Thomas O. 1911. The Duke of Bedford's zoological exploration of Eastern Asia.- XIII. On Mammals from the provinces of Kan-su and Sze-chwan, western China. *Proceedings of the Zoological Society of London*, **81**(1): 158–180.
Thomas O. 1915. XXIX.—A new shrew of the genus Blarinella from Upper Burma. *Annals and Magazine of Natural History*, **15**(87):335–336.
Thomas O. 1912. LI. —On a collection of small Mammals from the Tsin-ling Mountains, Central China, presented by Mr. G. Fenwick Owen to the National Museum. *Annals and Magazine of Natural History*, **10**(58): 395–403.

Appendix I

Specimens examined.

Abbreviations: KIZ: Kunming Institute of Zoology, Chinese Academy of Sciences, AMNH: American Museum of Natural History, USNM: National Museum of Natural History, Smithsonian Institution.

B. quadraticauda (*n*=19)

Baoxin, Sichuan (KIZ820495, KIZ820588, KIZ820625, KIZ820626),

Qionglai, Sichuan (AMNH111121, AMNH111125, AMNH111126, AMNH111127, AMNH111128, AMNH111130, AMNH111136)

Wenchuan, Sichuan (AMNH111112, AMNH111114, AMNH111119, AMNH111137, AMNH111138, AMNH111140, AMNH111142, AMNH111145)

B. cf. quadraticauda (identified as *B. griselda* in Jiang et al., 2003; *n*=45)

Jingdong, Yunnan (KIZ640068, KIZ640105, KIZ640128, KIZ640129, KIZ640133, KIZ640134, KIZ640152, KIZ640191, KIZ640199, KIZ640200, KIZ640418, KIZ640429, KIZ640430, KIZ640431, KIZ640432, KIZ96180, KIZ98069, KIZ98107, KIZ98114, KIZ98151, KIZ98152, KIZ98313, KIZ98335, KIZ98378, KIZ98553, KIZ72053), Luchun, Yunnan (KIZ72053), Mt. Qinling, Shaanxi (KIZ0509420, KIZ0509423), Nanchuan, Sichuan (KIZ88126, KIZ88127, KIZ88252), Shimian, Sichuan (KIZ820742, KIZ820743, KIZ820744, KIZ820752, KIZ820753, KIZ820754, USNM574289, USNM574290, USNM574291, USNM574292, USNM574293), Wulong, Sichuan (KIZ88320, KIZ88321, KIZ88395)

B. griselda (*n*=4)

Gansu (AMNH60449), Mt. Qinling, Shaanxi (KIZ0509390, KIZ0509578, KIZ0509579)

B. wardi (*n*=25)

Bijiang, Yunnan (KIZ820280), Deqin, Yunnan (KIZ820280), Gongshan, Yunnan (KIZ73863, KIZ73889, KIZ73910, KIZ73920, KIZ73927, KIZ73928, KIZ73929), Lijiang, Yunnan (USNM241403), Myanmar (AMNH114720, AMNH114721, AMNH114722, AMNH114723, AMNH114739, AMNH114740, AMNH114741, AMNH114748, AMNH114757, AMNH114758, AMNH114760), Pianma, Yunnan (KIZ74176), Weixi, Yunnan (KIZ810669), Yinjiang, Yunnan (KIZ76286), Zhongdian, Yunnan (KIZ810147)

Taxonomic revision of the genus *Mesechinus* (Mammalia: Erinaceidae) with description of a new species

Huai-Sen Ai[1,#], Kai He[2,3,#,*], Zhong-Zheng Chen[2,4,#], Jia-Qi Li[5], Tao Wan[2], Quan Li[2], Wen-Hui Nie[2], Jin-Huan Wang[2], Wei-Ting Su[2], Xue-Long Jiang[2,*]

[1] *Gaoligongshan National Nature Reserve, Baoshan Yunnan* 678000*, China*
[2] *Kunming Institute of Zoology, Chinese Academy of Sciences, Kunming Yunnan* 650223*, China*
[3] *The Kyoto University Museum, Kyoto University, Kyoto* 606-8501*, Japan*
[4] *College of Life Sciences, Anhui Normal University, Wuhu Anhui* 241000*, China*
[5] *Nanjing Institute of Environmental Sciences, Ministry of Environmental Protection, Nanjing Jiangsu* 210042*, China*

ABSTRACT

Hedgehogs in the genus *Mesechinus* (Family Erinaceidae), which include two currently recognized species (*M. dauuricus* and *M. hughi*), are distributed from northeast Mongolia to the upper Amur Basin in Russia and adjacent areas in northeast and northern China. In recent years, a population of *Mesechinus* hedgehogs was discovered from Mt. Gaoligong, southwestern Yunnan, China, far from the known distribution range of the genus. Furthermore, these hedgehogs are the only known population to be distributed at elevations higher than 2 100 m and in sympatry with gymnures. To evaluate the taxonomic status of these hedgehogs, we examined specimens representing *Mesechinus* taxa in China and further conducted morphometric and karyotypic analyses. Our results supported the existence of four species in China. Specifically, we identified the hedgehogs from Mt. Gaoligong as a new species, *Mesechinus wangi* **sp. nov.**, and recognized *M. miodon*, previously considered as a synonym of either *M. dauuricus* or *M. hughi*, as a distinct species. Interestingly, we observed a supernumerary M^4 on all specimens of *Mesechinus wangi* **sp. nov.**, which is an extremely rare event in the evolution of mammalian dentition.

Keywords: *Mesechinus*; Taxonomy; Morphometrics; Inhibitory cascade; Karyotype; New species; Supernumerary molar

INTRODUCTION

Extant erinaceids, including spiny hedgehogs (Erinaceinae) and silky-skinned gymnures and moonrats (Galericinae), are found within the family Erinaceidae (Hutterer, 2005). The monophyly of each subfamily, as well as their sister-relationships, are well supported in various morphological and molecular studies (Corbet, 1988; Frost et al., 1991; He et al., 2012). These molecular studies also suggest that the living gymnures diverged from the ancestor of hedgehogs 40 million years ago (Ma), which is far older than the most recent common ancestor of living hedgehogs (Bannikova et al., 2014). Members in the two subfamilies are not only morphologically and genetically distinct but also characterized by different geographic distributions and habitats (Corbet, 1988). The living species in Galericinae are mainly distributed in humid montane forests of subtropical and tropical Southeast Asia (*Echinosorex*, *Hylomys* and *Podogymnura*), Southern China (*Hylomys* and *Neotetracus*),

Received: 06 October 2017; Accepted: 02 April 2018; Online: 25 April 2018

Foundation items: This study was supported by the National Key Research and Development Program of China (2017YFC0505200), Fundamental Research Funds for NIES in 2017(GYZX170308) and Biodiversity Conservation Program by MEP of China, K. H. was supported by a JSPS Postdoctoral Fellowship for Overseas Researchers (P16092)

[#]Authors contributed equally to this work

[*]Corresponding authors, E-mail: hekai@mail.kiz.ac.cn; jiangxl@mail.kiz.ac.cn

DOI: 10.24272/j.issn.2095-8137.2018.034

and Hainan Island (*Neohylomys*). With their most recent common ancestor considered to be in the late Miocene (Bannikova et al., 2014), living hedgehogs have adapted to diverse habitats and are widely distributed throughout Africa (*Atelerix* and *Paraechinus*) and Eurasia (*Erinaceus*, *Hemiechinus*, *Mesechinus* and *Paraechinus*) in deciduous woodland, coniferous forest, forest steppe, grasslands, savanna, dry steppes, semi-desert, and even arid desert (Corbet & Hill, 1992); until recently, however, they have never been found in tropical or subtropical rainforest. In 2003, Ai (2007) discovered a small population of hedgehogs from the southern-most edge of Mt. Gaoligong in Yunnan Province at approximately 2 200–2 600 m a.s.l., near the border between China and Myanmar. These hedgehogs are characterized by the absence of a spineless section on their head and by ears of similar length to the surrounding spines, suggesting that they are members of the genus *Mesechinus* (Figure 1). The discovery was unexpected and of interest because: (1) the location is at least 1 000 km from the known distribution of any other hedgehog species; (2) the elevations are higher than that of any known hedgehog habitat; (3) the habitat is subtropical montane evergreen broad-leaved forest, which is typical habitat of the gymnures but differs from any known hedgehog habitat; and (4) the animals are sympatrically distributed with gymnures (*Neotetracus sinensis*), which is also the first ever record. While these clues indicate that the population represents a distinct taxon, its taxonomic status has yet to be resolved.

Figure 1 Living *Mesechinus wangi* sp. nov. (KIZ 034115)

Mesechinus hedgehogs are mainly distributed in northern China and Mongolia, as well as the Transbaikalia region and upper Amur Basin in Russia (Figure 2). Two species (*M. dauuricus* and *M. hughi*) were recognized in Mammal Species of the World (Hutterer, 2005). After Sundevall described the type species *Erinaceus* (*Mesechinus*) *dauuricus* in 1842, another five forms were recognized, including *przewalskii* Satunin, 1907, *hughi* Thomas, 1908, *miodon* Thomas, 1908, *manchuricus* Mori, 1927, and *sylvaticus* Ma, 1964. Subsequently, however, *manchuricus*, *przewalskii*, and *sibiricus* were recognized as synonyms of *M. dauuricus* (Corbet, 1988), and *miodon* and *sylvaticus* as synonyms of *M. hughi*. The most debated species continues to be *miodon*, which was originally described together with *hughi* by Thomas (1908). Based on successive morphological research, some authors have included it in *M. dauuricus* (Corbet, 1978; Corbet & Hill, 1992), whereas others have included it in *M. hughi* (Hoffmann & Lunde, 2008; Hutterer, 2005). Furthermore, karyotypic study of *miodon* from its type locality demonstrated variable chromosomal numbers ranging from 2*n*=44 to 48 (Lin & Min, 1989; Kong et al., 2016a) due to the existence of B-chromosomes (Kong et al., 2016a), which has been interpreted as evidence of full species status (Kong et al., 2016a, 2016b). However, B-chromosomes are rarely used for delimiting species and as its craniodental morphology has not yet been fully diagnosed, the species status of *M. miodon* remains suspicious.

In this study, we integrated morphometric and karyotypic approaches to revisit the taxonomy of *Mesechinus*. We examined whether *M. miodon* is distinguishable from other species and were particularly interested in the taxonomic status of the hedgehog population found from Mt. Gaoligong.

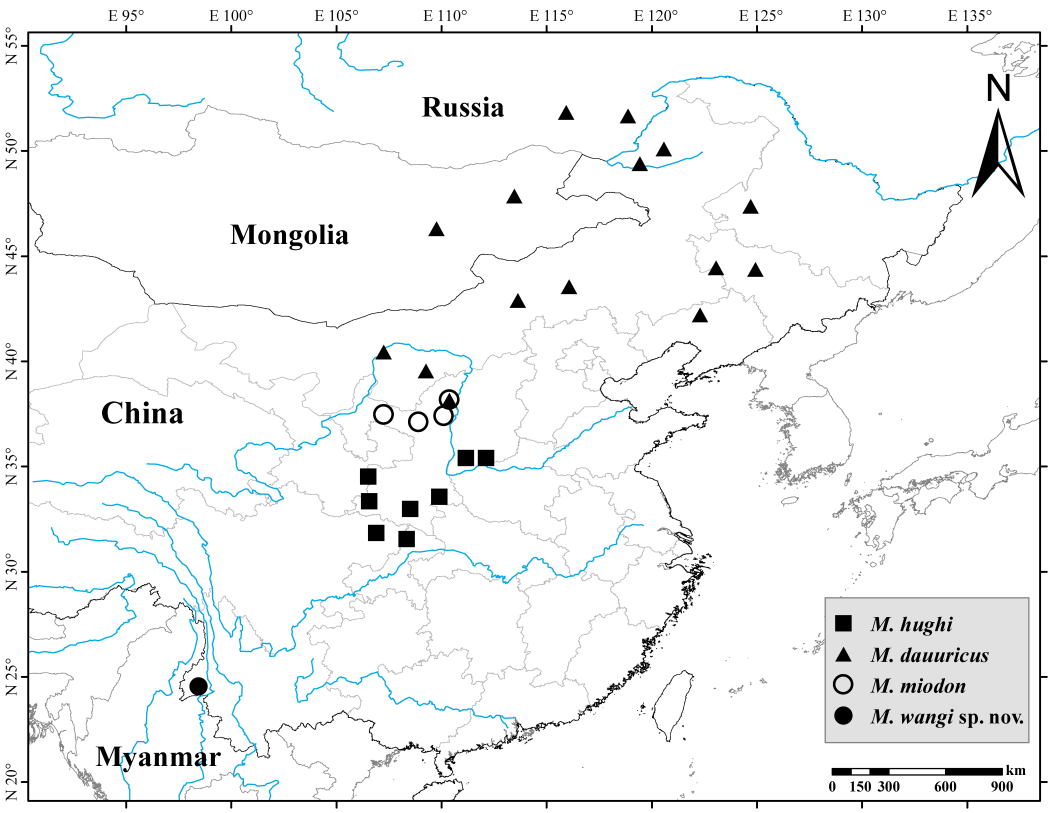

Figure 2 Distribution of genus *Mesechinus*

MATERIALS AND METHODS

Specimens examined

We examined 59 specimens (skins and skulls) of *Mesechinus* deposited in the Institute of Zoology (IOZ) and Kunming Institute of Zoology (KIZ) of the Chinese Academy of Sciences (CAS), Shaanxi Institute of Zoology (SXIZ), Northwest University (NWU), and China West Normal University (CWNU) (see Supplementary Appendix I). These specimens included the *M. hughi sylvaticus* holotype. Photo images of the *M. miodon* holotype were also obtained for examining diagnosable characters and for morphological description and comparison with other named species. Morphology was examined and described following Corbet (1988), Frost et al. (1991), Gould (1995), and Thomas (1908). Based on our diagnosis and comparison of external and craniodental morphology, we recognized four species/putative species, including *M. dauuricus* (to include *M. dauuricus dauuricus* (*n*=8) and *M. dauuricus manchuricus* (*n*=5)), *M. hughi* (to include *M. hughi hughi* (*n*=28) and *M. hughi sylvaticus* (*n*=3)), and *M. miodon* (*n*=9). We recognized the animals from Mt. Gaoligong as a new species, which we name herein as *Mesechinus wangi* **sp. nov.** (*n*=6).

Morphological measurement and analysis

External measurements, including body weight (W), head and body length (HB), tail length (TL), length of hind foot (HF), and ear length (EL), were recorded from specimen tags. Spine length (SL) was measured from specimens. Twelve cranial characters were measured in millimeters with a digital caliper graduated to 0.01 mm (Table 1) following Pan et al. (2007): greatest length of skull (GLS), condylobasal length (CBL), basal length (BL), cranial height (CH), palatal length (PL), zygomatic breadth (ZMB), interorbital breadth (IOB), mastoid width (MTW), greatest width of nasal (GWN), breadth of first upper molar (BM^1), length of upper tooth row (LUTR), and length of below tooth row (LBTR). We extracted measurements from Allen (1938) for the eight specimens of *M. miodon* deposited in the Natural History Museum.

Morphometric variation was analyzed using principal component analysis (PCA) in SPSS v19.0 (SPSS Inc., Chicago, IL, USA). Only the 12 cranial measurements were used for PCA. All variables were $\log_{10}$-transformed before PCA. One-way analysis of variance (ANOVA) was used to test significant differences in external and cranial variables among species.

Table 1 External and cranial measurements (mm) of *Mesechinus* specimens examined in this study (mean±*SD* and range for each measurement and numbers of specimens measured (*n*) are given)

	Mesechinus wangi	*Mesechinus miodon*	*Mesechinus hughi*	*Mesechinus dauuricus*
	n=6	*n*=18*	*n*=31	*n*=13
W	411.20±48.66	505.00±168.73	341.39±127.82	562.41±130.37
	336.00–451.00; 5	230.00–750.00; 6	112.00–750.00; 31	423.00–840.00; 11
HB	202.40±26.10	195.22±24.26	189.71±24.20	206.21±22.30
	177.00–240.00; 5	120.00–220.00; 17	148.00–232.00; 31	175.00–261.00; 12
TL	17.26±1.82	33.22±5.22	19.23±3.32	24.08±3.65
	14.00–18.20; 5	25.00–43.00; 17	12.00–24.00; 27	17.00–30.30; 12
HF	47.20±1.20	58.80±85.13	37.97±4.36	34.74±7.39
	45.30–48.00; 5	35.00–378.00; 16	30.00–47.00; 31	18.00–41.00; 12
EL	29.60±1.74	28.81±3.13	22.94±3.99	31.19±3.44
	28.00–31.80; 5	24.00–34.50; 17	16.00–33.00; 31	22.30–34.00; 11
GLS	54.75±0.81	54.10±2.18	49.39±1.58	55.18±3.21
	53.70–55.60; 4	49.30–57.20; 14	45.10–52.40; 23	50.20–58.40; 12
CBL	54.55±0.68	53.18±2.47	48.46±1.61	54.72±2.94
	53.60–55.20; 4	48.50–56.30; 11	44.40–51.20; 23	49.40–57.40; 13
CH	17.13±0.69	18.67±0.72	16.14±0.97	18.37±0.58
	16.10–17.60; 4	17.80–19.70; 6	14.90–18.20; 21	17.20–19.10; 9
BL	50.00±1.58	49.64±2.12	45.55±1.32	51.83±2.02
	47.70–51.30; 4	44.70–52.30; 14	43.20–48.80; 21	48.10–54.50; 13
PL	30.25±0.58	28.82±1.46	26.58±0.63	28.60; 1
	29.50–30.80; 4	27.00–32.18; 14	25.70–28.40; 21	
ZMB	33.97±0.23	32.77±2.17	28.90±1.72	32.62±2.93
	33.70–34.10; 3	28.70–37.08; 14	25.70–32.00; 22	28.40–36.40; 13
IOB	14.68±0.38	13.87±0.83	12.51±0.52	13.86±0.72
	14.20–15.10; 4	12.90–15.10; 6	11.70–13.60; 23	13.00–15.10; 9
MTW	25.60±0.73	25.93±1.23	21.67±1.60	25.58; 1
	24.70–26.20; 4	24.30–28.30; 14	19.50–24.50; 21	
GWN	4.30±0.00	2.70±0.23	2.97±0.30	2.96; 1
	4.30–4.30; 3	2.37–2.94; 6	2.60–3.60; 23	
BM[1]	21.43±0.31	21.08±0.69	17.38±0.77	20.20; 1
	21.10–21.70; 3	20.30–22.30; 14	16.50–19.50; 21	
LUTR	27.90±1.18	27.25±1.03	24.65±1.15	27.85; 13
	26.70–29.10; 4	25.70–29.02; 14	21.40–26.10; 23	
LBTR	24.85±0.51	24.91±0.73	21.19±0.80	24.30; 1
	24.20–25.30; 4	23.40–25.70; 14	20.20–23.70; 21	

*: Includes measurement of nine specimens measured by Allen (1938). Abbreviations are given in the Materials and Methods section.

Cell culture and cytological preparation

One specimen representing *Mesechinus wangi* **sp. nov.** (museum catalog number: KIZ 034115) was used for cell cultures. We followed Hungerford (1965) for cell culture and metaphase preparation. The fibroblast cell cultures derived from skin fibroblasts and bone marrow are stored in the Kunming Cell Bank, Kunming, Yunnan, China. Images were captured using the Genus System (Applied Imaging Corp., USA) with a CCD camera mounted on a Zeiss Axioplan 2 microscope. Chromosomes of *Mesechinus wangi* **sp. nov.** were arranged based on their relative length in order from longest to shortest.

RESULTS

Morphological comparison and diagnosis

As mentioned previously, the hedgehogs from Mt. Gaoligong could be assigned to *Mesechinus* unambiguously based on external morphology. These animals lack a spineless area on their heads, which is distinct from *Atelerix*, *Erinaceus*, and *Paraechinus* (Figures 2, 3), and their ears are similar to the surrounding spines in length, which is distinguishable from *Hemiechinus*. The skull and teeth are also characterized by several typical *Mesechinus* features, including a robust jugal reaching the lacrimal (Figure 4), shallow suprameatal fossa, and narrowly separated anterior and posterior borders of the

suprameatal fossa (Figure 4), which distinguish it from all other genera (see Frost et al., 1991 for discussion). We compared the external and craniodental morphology of our specimens. It is worth noting that the sample size for some species/subspecies was small and may not reflect intra-specific variation, especially that of teeth (see discussion in Frost et al., 1991; Gould, 2001), which needs to be verified in future study.

All specimens examined in the current study showed few wholly white spines (Corbet, 1988; Figure 3). Spine lengths from longest to shortest were: *M. miodon* (~26 mm), *M. dauuricus* and *Mesechinus wangi* **sp. nov.** (~21–24 mm), and *M. hughi* (~21 mm). Spine color pattern was used by Thomas (1908) as a distinguishing feature for describing *M. hughi* and *M. miodon* (Figure 3). We found that *M. hughi* from Shaanxi (including topotype of *M. hughi hughi*) and Shanxi (holotype of *M. h. sylvaticus*) and *M. dauuricus* shared similar characters: that is, white for two-thirds of length, followed by black ring, narrow light ring, and black tip (Figure 3C, D). *Mesechinus miodon* was distinguished by spine light brown (rather than wholly white) for two-thirds of its length, followed by broad blackish-brown rings (rather than wholly black), light brown terminal (3–4 mm), and non-black tip (Figure 3D). *Mesechinus wangi* **sp. nov.** was differentiated from *M. hughi* by dark ring extending to tip on most spines, with narrow white ring near tip (Figure 3A).

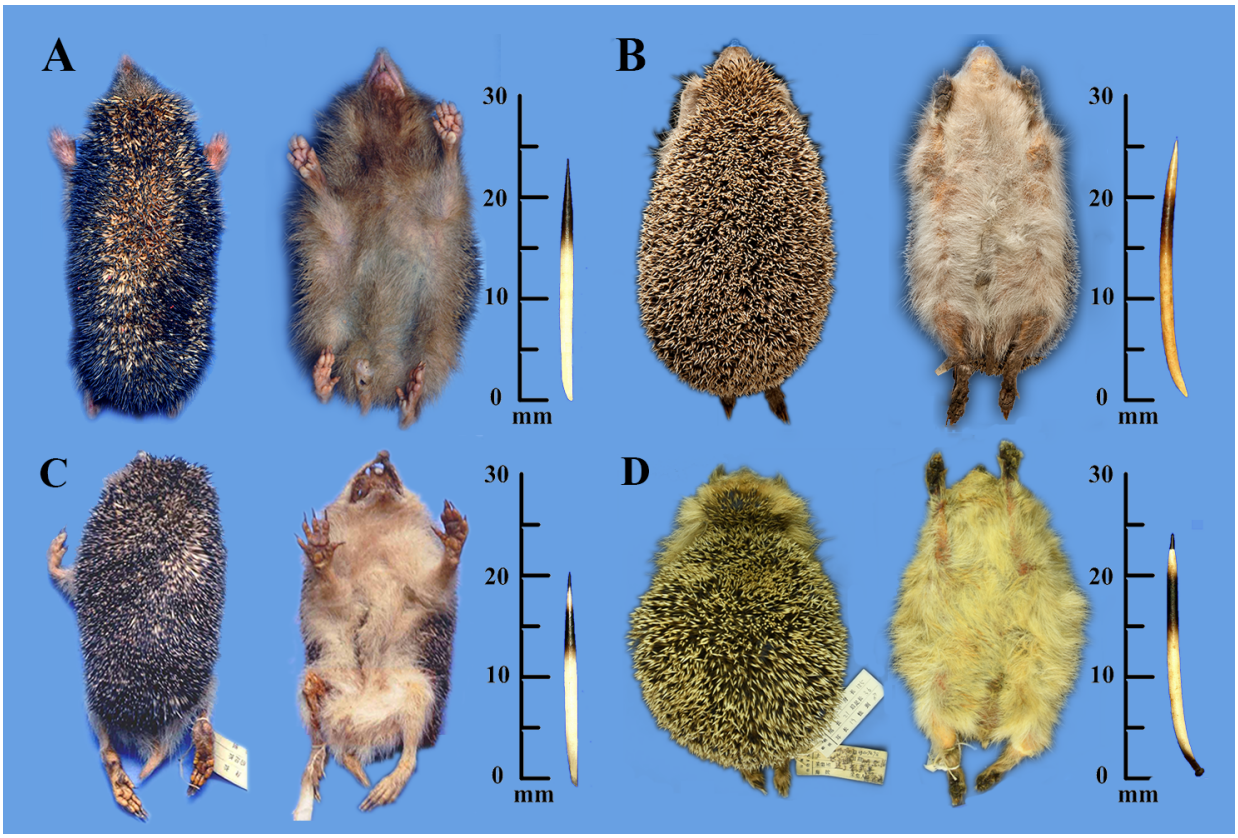

Figure 3 External morphs and spines of *Mesechinus wangi* sp. nov. (Type KIZ 022028) (A), *M. miodon* (Type BM 9.1.1.9) (B), *M. h. hughi* (KIZ 027029) (C), and *M. d. dauuricus* (KIZ 027005) (D)

Based on skull morphology, frontals were relatively higher than parietals in *M. hughi* and *Mesechinus wangi* **sp. nov.**, whereas parietals were higher than frontals in *M. dauuricus* and *M. miodon* (Figure 4). On the ventral side of the skulls, a posterior palatal shelf and well-developed spine were present on all specimens examined (Figure 4). *Mesechinus miodon* showed longer spines than other species (Figure 4B). An epipterygoid process was present in all specimens (Figure 4; Frost et al., 1991). In *M. miodon* this process was well developed, extending labially (Figure 4B), but only slightly or moderately developed in other taxa (Figure 4). The basisphenoid of *M. dauuricus* was previously considered to be uninflated, intermediate between the condition of *Hemiechinus* and that of *Atelerix* and *Erinaceus* (Frost et al., 1991). According to our examination, however, the basisphenoid was inflated in *M. dauuricus*, *M. hughi*, and *M. miodon* (Figure 4B, C), similar to the condition observed in *Hemiechinus auritus*, whereas the basisphenoid was uninflated in *Mesechinus wangi* **sp. nov.** (Figure 4A), similar to that of *Atelerix* and *Erinaceus*.

On the dorsal side of the skull, the nasal-maxilla relationship

was used in Corbet (1988) and Ma (1964), though Frost et al. (1991) determined that the relationship exhibited too much inter-specific variation. Nevertheless, nasal breadth was obviously and significantly (see below) different between *Mesechinus wangi* **sp. nov.** and other species. More specifically, *Mesechinus wangi* **sp. nov.** was characterized by: nasal broad, premaxilla extending only slightly posteriorly and frontal extending only slightly anteriorly on dorsal side, premaxilla not touching frontal, and nasal and maxilla sharing long common sutures (Figure 4A). All other species exhibited much narrower nasal (Figure 4B–D). *Mesechinus hughi* could be characterized by: premaxilla extending posteriorly, frontal extending anteriorly, not touching premaxilla, with nasal and maxilla sharing short sutures (Figure 4C). *Mesechinus d. manchuricus* and *M. miodon* could be diagnosed by: premaxilla extending posteriorly, frontal extending anteriorly, premaxilla and frontal touching on dorsal side of skull (or nearly so), with nasal and maxilla not sharing common suture (Figure 4B, D).

As *M. miodon* was named based on its small P^3 (triangular (equal-sided) in shape; Thomas, 1908)), examination of teeth was unavoidable here. *Mesechinus dauuricus* could be diagnosed by P^3 similar to P^2 in size; *M. miodon* could be diagnosed by P^3 smaller than P^2 (and smaller than that of *M. dauuricus*); *Mesechinus wangi* **sp. nov.** and *M. hughi* could be diagnosed by P^3 small, though similar to *M. miodon* (Figure 4). All species showed reduced upper M^3 and small trigonid (Figure 4). Most notably, *Mesechinus wangi* **sp. nov.** could be further distinguished by consistent presence of single-rooted M^4 on all specimens examined (Figure 5), much smaller than M^3.

Morphometric analyses

External and cranial measurements of each species are given in Table 1. Thirty intact skulls were used for PCA, including specimens of *M. dauuricus manchuricus* (*n*=1), *M. hughi hughi* (*n*=20), *M. miodon* (*n*=6), and *Mesechinus wangi* **sp. nov.** (*n*=3).

The first principal component (PC1) accounted for 74.24% of variation (eigenvalue=8.91) and was positively correlated with all variables, reflecting a size effect (Table 2). The second principal component (PC2) accounted for 9.40% of variation (eigenvalue=1.13) and was dominated by MTW (loading=0.93), but was also positively correlated with PL, BM^1, LBTR, BL, and LUTR (loading>0.53). The third principal component (PC3) represented 4.90% of variation (eigenvalue=0.59) and was correlated primarily with GWN (loading=0.97).

As shown in Figure 6A, *M. dauuricus*, *M. miodon*, and *Mesechinus wangi* **sp. nov.** plotted closely in the positive region of PC1 and PC2, indicating that these taxa had larger skulls. Further, *M. hughi* plotted in the negative region of PC1, indicating this species had a smaller skull. In the PC1 and PC3 figure (Figure 6B), *Mesechinus wangi* **sp. nov.** plotted in the positive region of PC3 against all other species, indicating this species had the widest nasal.

We employed one-way ANOVA for all external and cranial variables. The results showed that all variables were significantly different among the four species (P<0.001), except for HB (F=2.080, P=0.134), HF (F=0.522, P=0.596), and PL (F=7.561, P=0.002).

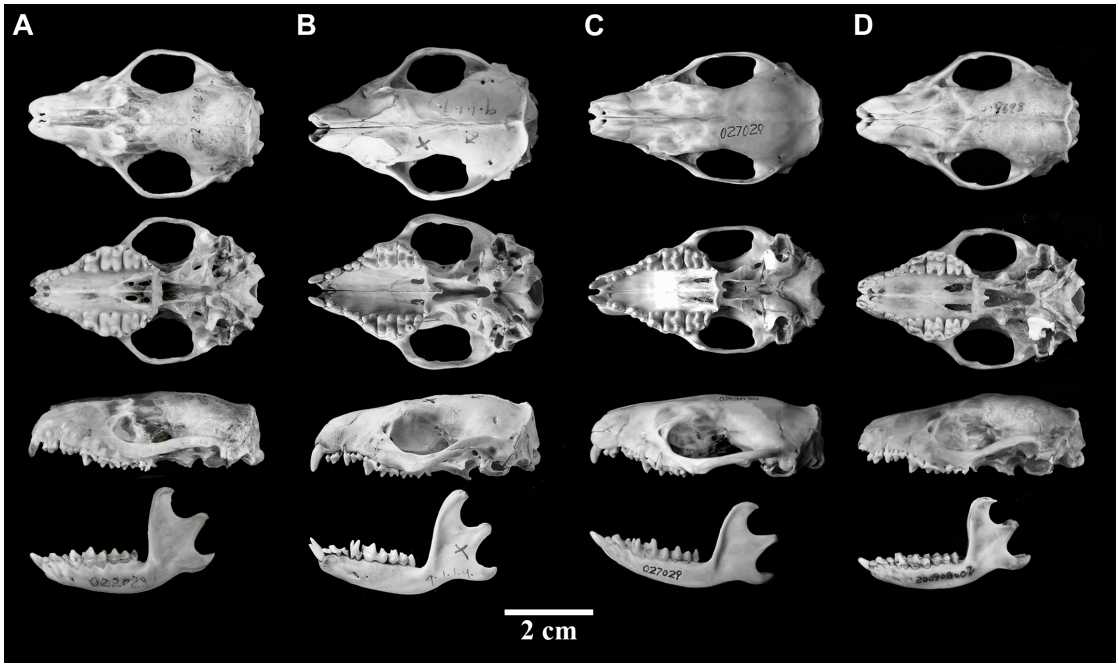

Figure 4 Dorsal ventral and lateral views of skull and mandible of *Mesechinus wangi* sp. nov. (Type KIZ 022028) (A), *M. miodon* (Type BM 9.1.1.9) (B), *M. h. hughi* (KIZ 027029) (C), and *M. d. dauuricus* (KIZ 027005) (D)

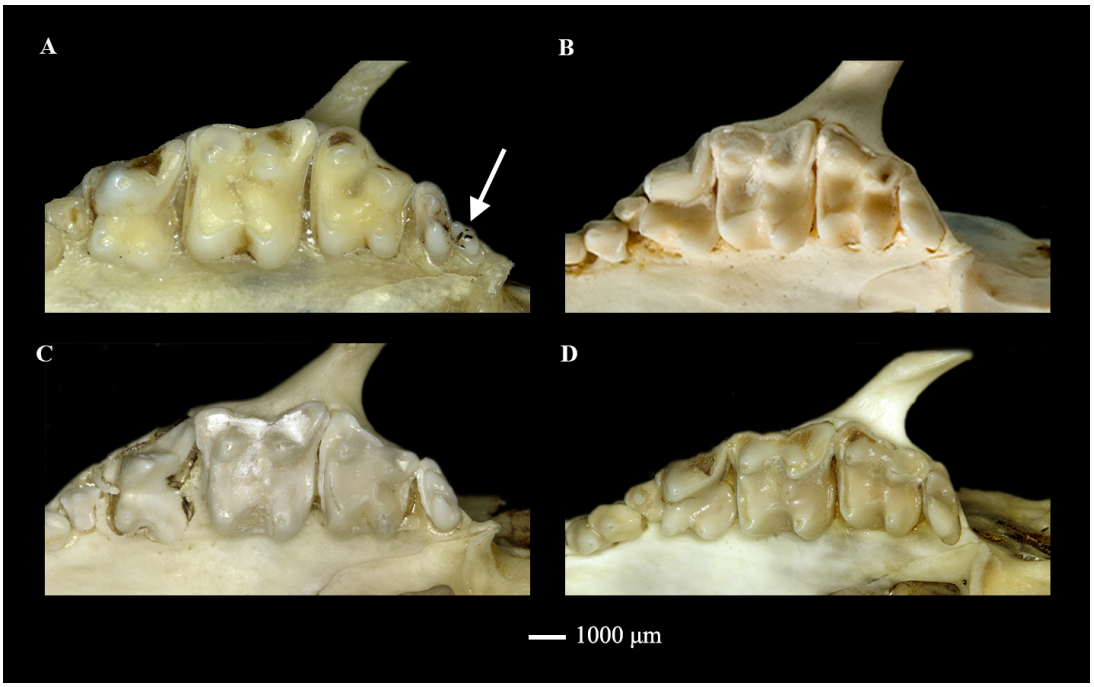

Figure 5 Right upper molars of *Mesechinus wangi* sp. nov. (Type KIZ 022028) (A), *M. miodon* (Type BM 9.1.1.9) (B), *M. h. hughi* (KIZ 027029) (C), and *M. d. dauuricus* (KIZ 027005) (D)

Table 2 Factor loading eigenvalues and percentage of variance explained for PC1, PC2, and PC3 from principal component analysis

Variables	Component		
	1	2	3
CH	0.916	0.200	−0.136
CBL	0.836	0.461	0.221
GLS	0.830	0.483	0.160
BL	0.800	0.541	0.141
LUTR	0.720	0.538	0.236
ZMB	0.632	0.450	0.288
IOB	0.542	0.480	0.458
MTW	0.293	0.928	0.026
PL	0.523	0.721	0.292
BM[1]	0.623	0.696	0.216
LBTR	0.631	0.683	0.155
GWN	0.034	0.093	0.970
Eigenvalues	8.909	1.128	0.588
Total variance explained (%)	74.241	9.403	4.899

Abbreviations are given in the Materials and Methods section.

Karyotypic characteristics of *Mesechinus wangi* sp. nov.

The karyotypes of *Mesechinus wangi* **sp. nov.** are shown in Figure 7. The diploid number (2*n*) and autosomal fundamental number (FNa) were 48 and 92, respectively (Figure 7A). The autosomes and X chromosomes were biarmed; however, we could not determine whether the Y chromosome was biarmed as it was too small. In total, 22 metacentric + 24 submetacentric autosomes were found in the karyotype. Both the X and Y chromosomes were metacentric, with the Y chromosome being smallest. G-banded karyotypic analysis identified homologous chromosomes (Figure 7B).

Compared with other species in the genus *Mesechinus*, *Mesechinus wangi* **sp. nov.** had the same 2*n* and FNa as *M. dauuricus* and *M. hughi*, but differed from the reported karyotype of *M. miodon*, which is characterized by the presence of 0–4 B-chromosomes (2*n*=44–48; FNa=82–92; Table 3). The numbers of metacentric chromosomes (M), submetacentric chromosomes (SM), and subtelocentric chromosomes (ST) also differed among species.

DISCUSSION

Taxonomic implications

We compared the morphology and karyotypes among *Mesechinus* taxa in China. Although sample sizes were small for several forms, the patterns detected in the morphological and karyotypic analyses helped clarify the taxonomy of this genus. It is worth noting, as well discussed in Gould (2001), that dental structures in hedgehogs can exhibit considerable intraspecific variation, and all dental characters should be treated with caution.

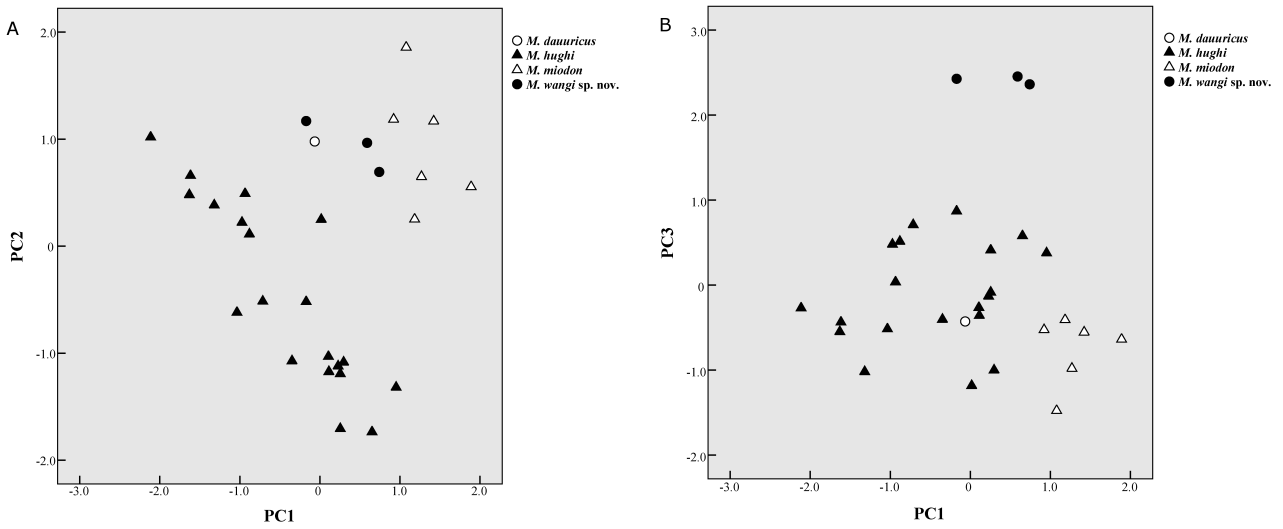

Figure 6 Plot of *Mesechinus* spp. for principal component factors 1 and 2 (A) and 1 and 3 (B)

Mesechinus miodon is still recognized as a subspecies of either *M. dauuricus* (Corbet & Hill, 1992) or *M. hughi* (Hutterer, 2005). Here, however, we recognized *M. miodon* as a distinct species based on morphometric and karyotypic analyses (Figure 6; Table 3). Thomas (1908) named *M. miodon* and *M. hughi* but did not compare either with *M. dauuricus*. In the current study, *M. miodon* was easily distinguished from *M. hughi* (Figure 6A), with its obviously larger cranial measurements (Table 1). *Mesechinus miodon* and *M. dauuricus* exhibited similar overall skull shape and size (Table 1, Figure 6), but *M. miodon* was distinguishable based on different spine color pattern and smaller P^3.

The implications of the karyotypic evidence are two-fold. On the one hand, *M. miodon* had a smallest number of metacentric chromosomes in the genus, and the numbers of submetacentric and subtelocentric chromosomes were also different from that of *M. dauuricus*, indicating that these two morphologically similar forms were distinct species. On the other hand, the existence of B chromosomes in the topotype of *M. miodon* (from Yulin), as reported in previous studies (Lin & Min, 1989; Kong et al., 2016a), should be treated with caution. Although B chromosomes are heterochromatic and can be verified easily using the C-banding karyotypic approach (e.g., Badenhorst et al., 2009), this was not adopted in the original studies mentioned above. The number of B-chromosomes is usually stable, rather than highly variable as reported for *M. miodon* (0–4), and is usually an odd number, rather than an even number (Table 3) as reported in other mammals (e.g., Badenhorst et al., 2009). Thus, reexamination of the C-banding karyotype using additional samples is warranted. Finally, B-chromosomes are considered adaptive characters that can vary between populations and may be a poor characteristic for distinguishing species.

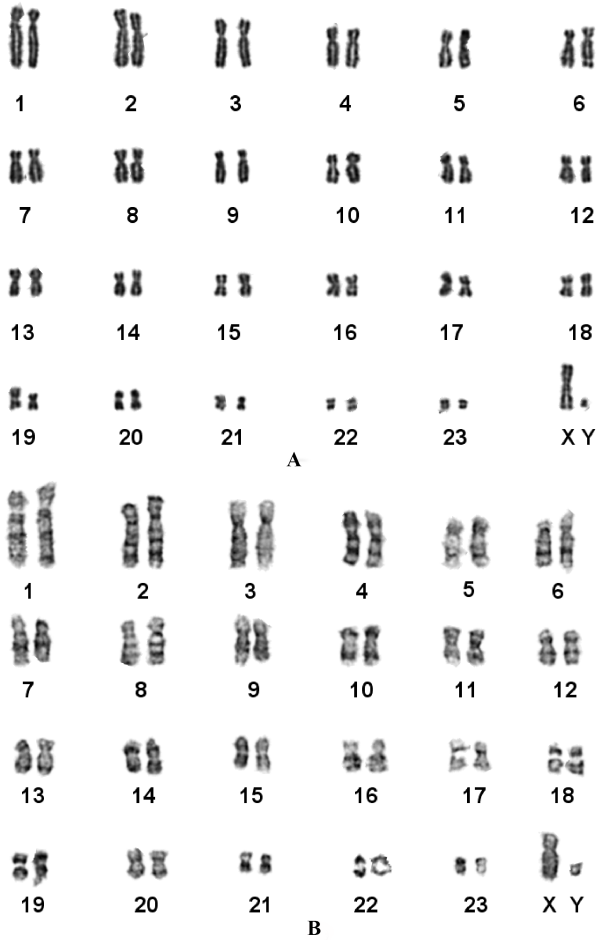

Figure 7 Karyotypes of *Mesechinus* sp. (KIZ 034115)

A: Conventional karyotype; B: G-banding karyotype.

We recognized the hedgehogs from Mt. Gaoligong as a distinct new species due to their many unique features. This new species is the first known hedgehog to be found at elevations higher than 2 100 m (*Erinaceus europaeus* and *M. hughi* are distributed no higher than 2 100 m), while also inhabiting subtropical evergreen broad-leaved forests (Figure 8) and co-occurring with gymnures. The color pattern of its spine is distinguishable from other *Mesechinus* species due to the lack of a narrow white ring (Figure 3A). It has a broad nasal that shares a long common suture with the maxilla (Figure 4A), which differs from all other taxa. The presence of a supernumerary M^4 is also highly distinctive (Figure 5A). We propose the name of *Mesechinus wangi* **sp. nov.** for the new species, in memory of the late Prof. Ying-Xiang Wang, a highly respected mammologist from the Kunming Institute of Zoology, Chinese Academy of Sciences.

Table 3 Karyotypes of the four recognized *Mesechinus* species

Species	2*n*	NFa[1]	Autosomes	X/Y chromosomes	Locality	Reference
M. dauuricus	48	92	22M+14SM+10ST	SM/T	Chita, Russia	Korablev et al., 1996
M. hughi	48	92	30M+12SM+4ST	M/T	Yulin, China	Lin & Min, 1989
M. miodon	44	82	18M+24SM	ST/T	Yulin, China	Lin & Min, 1989[2]
	44–48[3]	84–92	18M+24SM+0–4B(M/SM)	ST/T	Yulin, China	Kong et al., 2016
M. wangi **sp. nov.**	48	92	22M+24SM	M/M[4]	Baoshan, China	This study

[1]: Diploid chromosomes classified into metacentric (M), submetacentric (SM), subtelocentric (ST), and telocentric chromosomes (T). [2]: Animals were identified as *M. dauuricus* in the original article. Kong et al. (2016a) argued that the specimens should be *M. miodon*. [3]: Because of the existence of 0–4 B-chromosomes (M or SM; Kong et al., 2016a), the 2*n* could be 44–48 and NFa could be 84–92. [4]: Y chromosome most likely biarmed (see Figure 6B), but was too small to be confirmed.

Figure 8 Habitats of *Mesechinus wangi* sp. nov. within Gaoligongshan National Nature Reserve

Supernumerary upper molar

During the evolution of mammalian dentition, changes in tooth number are very common between taxa and within species, including in the eulipotyphlan mammals. Differences in number of teeth can be used as diagnostic characteristics in shrews (e.g., between *Crocidura* and *Suncus*) and talpid moles (e.g., between *Euroscaptor Mogera*, and *Parascaptor*), especially the number of incisors and premolars (or unicuspids in Soricidae). These differences are often triggered by geographic isolation and speciation, such as observed in the Persian mole (*Talpa davidiana*; Kryštufek et al., 2001) and Japanese mole (*Mogera wogura*; Asahara et al., 2012). Nevertheless, an increased number of molars is an extremely rare event observed in only a few taxa, such as the bat-eared fox (*Otocyon megalotis*), and can be impacted by the evolution of different feeding behaviors and explained using an inhibitory cascade model (Asahara, 2013; Asahara, 2016; Asahara et al., 2016). For example, adaptation toward an increased bite force in the hypercarnivorous bush dog (*Speothos venaticus*) resulted in an enlarged M_1, thus prohibiting the development of M_3 dentition (Damasceno et al., 2013). Although erinaceids are characterized by highly variable dentition and tooth structure (Gould, 2001), M_4 and M^4 have never been observed in either living or fossil species. Loss of M_3 has been observed

in short-faced hedgehogs, an extinct subfamily of gymnures (Brachyericinae), following remarkable shortening of the skull (Rich & Rich, 1971). Based on teeth features, Lopatin (2006) hypothesized that brachyericines from Asia underwent adaptation toward carnivory. If the inhibitory cascade model is valid in Erinaceidae, the presence of a supernumerary M^4 in *Mesechinus wangi* **sp. nov.** could be attributed to a combination of genetic bottleneck and isolation (hypothetically after long-distance dispersal from northern China) as well as adaptive selection from an omnivorous-insectivorous diet toward a highly omnivorous one resulting in reduced inhibition during the development of the upper molars (Asahara, 2016; Asahara et al., 2016).

Taxonomic accounts

***Mesechinus dauuricus* (Sundevall, 1842) Daurian Hedgehog**

Erinaceus dauuricus Sundevall, 1842: 237. Type locality: Dauuria, Transbaikalia, USSR.

Hemiechinus przewalskii Satunin, 1907: 181. Type locality: North China.

Hemiechinus manchuricus Mori, 1927: 108–109. Type locality: "Koshurei, South Manchuria" (=Gongzhuling, Jilin, China).

Hemiechinus dauuricus (Sundevall), Satunin, 1907: 185.

Erinaceus (*Mesechinus*) *dauuricus* (Sundevall), Ognev, 1951: 8–14.

Mesechinus dauuricus (Sundevall), Frost et al., 1991: 30.

Hedgehog of genus *Mesechinus* (GLS=55.18 mm; Table 1). Length of ear similar to surrounding spines. Spines 21–23 mm in length, white for two-thirds of length, followed by black ring, light narrow ring, and black tip (Figure 3); premaxilla extending posteriorly to frontal (Figure 4); P^3 triangular (equal-sided) in shape, similar to P^2 in size (Figure 4).

Distribution: Widely distributed in eastern Inner Mongolia, Shaanxi, Ningxia, Heilongjiang, Jilin, and Liaoning, China; NE Mongolia; Transbaikalia and upper Amur Basin, Russia (Figure 1).

Comments: Because *M. miodon* has been recognized previously as a synonym or subspecies of this species, the distribution boundary between these two species is unclear and the specimens from the southern-most distributions (especially in northwestern China Ningxia and Shaanxi) need to be carefully re-examined.

***Mesechinus hughi* (Thomas, 1908) Hugh's Forest Hedgehog**

Erinaceus hughi Thomas, 1908: 966. Type locality: Paochi (=Baoji), Shaanxi, China.

Hemiechinus sylvaticus Ma, 1964: 31–36. Type locality: Qin-Shui District, Northern slope of Mt. Lishan, Shanxi, China.

Hemiechinus dauuricus (Sundevall), Corbet, 1978: 15.

Mesechinus hughi (Thomas), Frost et al., 1991: 30–31 (including *M. sylvaticus*).

Smallest species of *Mesechinus* (GLS=48.46 mm; Table 1). Ears not longer than surrounding spines; ventral pelage light brown; spines 19–21 mm in length, color pattern same as *M. dauuricus* (Figure 3); frontal relatively higher than parietal; short spine on posterior palatal shelf moderately developed; epipterygoid process moderately developed; basisphenoid moderately inflated; nasal narrow, premaxilla extending posteriorly, frontal extending anteriorly, not meeting premaxilla, nasal and maxilla sharing short suture; P^3 triangular (nearly equal-sided) in shape, smaller than P^2.

Distribution: Southern Shaanxi, southern Shanxi, and northern Sichuan in China (Figure 1).

Comments: We recognized *H. sylvaticus* (Ma, 1964) as a synonym of *M. hughi*. To date, its taxonomic status has not been appropriately evaluated as it is only known from its holotype. Ma (1964) described *sylvaticus* as a new species but did not examine the specimens of *M. hughi*. Here, the characters used to define *sylvaticus*, such as spine color pattern and presence of sagittal ridge, were observed on all specimens of *M. hughi* examined. Therefore, we recognized *sylvaticus* as a synonym of *M. hughi*. This species inhabits mountainous broad-leaved forest, distinct from *M. dauuricus* and *M. miodon*, and its overall dark color may be an adaptation to such environments.

***Mesechinus miodon* (Thomas, 1908) Small-toothed Forest Hedgehog**

Erinaceus miodon Thomas, 1908: 965. Type locality: Yulinfu (=Yulin), Shaanxi, China.

Erinaceus europaeus miodon Thomas, Allen, 1938: 47–54.

Hemiechinus dauuricus (Sundevall), Corbet, 1978: 15.

Hemiechinus dauuricus (Sundevall), Min & Lin, 1989: 4.

Mesechinus dauuricus (Sundevall), Frost et al., 1991: 30.

Mesechinus miodon (Thomas), Wang, 2003: 4.

Large species of *Mesechinus* (GLS=54.10 mm; Table 1). Ventral pelage pale white; spines 22–29 mm long, first two-thirds light brown (ivory white in other species), then broadly ringed blackish-brown, terminal 3–4 mm of spine light brown; parietal higher than frontal; well-developed spine on posterior palatal shelf; epipterygoid processes well developed; nasal narrow, premaxilla extending posteriorly, frontal extending anteriorly on dorsal side, touching premaxilla, nasal and maxilla without common suture; P^3 triangular (nearly equal-sided) in shape, smaller than P^2.

Distribution: Northern Shaanxi and eastern Ningxia, China (Figure 1).

Comments: Named as *Erinaceus miodon* based on small P^3 (Thomas, 1908). Corbet (1978) considered it as a synonym of Hemiechinus dauuricus, which was subsequently followed by many researchers (e.g., Corbet, 1978, 1988; Corbet & Hill, 1992). Hutterer (2005) assigned it as a synonym of *M. hughi* (perhaps following a comment in Frost et al. (1991)). However, both the skull size and shape were very distinct from *M. hughi* in our morphometric analyses (Figure 6). Furthermore, it could be distinguished from *M. dauuricus* based on the different color patterns on the spine (Figure 3) and smaller P^3. The epipterygoid processes were also longer than those in *M.*

dauuricus, though the sample size was small (Figure 4). We therefore recognized it as a valid species.

The karyotype of animals from the type locality varied from 2*n*=44–48 due of the presence of B chromosomes (Lin & Min, 1989; Kong et al., 2016a). Kong et al. (2016b) reported both *M. miodon* and *M. dauuricus* as distributed in Yuling in northern-most Shaanxi; however, the distribution boundary remains unknown.

***Mesechinus wangi* sp. nov. HE, JIANG, and AI**

Common names: Gaoligong Forest Hedgehog (高黎贡林猬, Gaoligong Linwei) or Wang's Forest Hedgehog (王氏林猬, Wangshi Linwei)

Holotype: KIZ 022028 (field number: 201012001), adult female collected from Gaoligongshan National Nature Reserve (N24°50′, E98°45′), Baoshan, Yunnan, China, on 1 September 2010 at an altitude of 2 215 m a.s.l.. Alcohol-preserved and cleaned skull are deposited in KIZ, CAS.

Paratypes: KIZ 027001 (field number: 0907003), KIZ 027002 (field number: 0907001), KIZ 022027 (field number: 1102007), KIZ 034255 (field number: 201507001), and KIZ 034115 (field number: GLGS 20160601) collected from Gaoligongshan National Nature Reserve, southwestern Yunnan, China from 2003 to 2016 at elevations of 2 100 to 2 680 m. Except for KIZ 034115, which is preserved in fluid, all other specimens are preserved as dried skins with cleaned skulls. The skull of KIZ 027002 is broken and the skull of KIZ 034255 is missing.

Etymology: Named in memory of Prof. Ying-Xiang Wang (1938–2016), head of the mammal research group at the Kunming Institute of Zoology, Chinese Academy of Sciences. He undertook extensive research on the taxonomy, phylogeny, zoogeography, and conservation of mammals and made distinguished contributions to Mammalogy in China (Jiang, 2016).

Diagnosis: Body size larger than *M. hughi*, but similar to *M. dauuricus* and *M. miodon*. Most spines (>80%) lack white ring, in contrast to other *Mesechinus* species. Frontal higher than parietal, differing from *M. dauuricus* and *M. miodon* but similar to *M. hughi*. Spine on posterior palatal shelf short, similar to *M. hughi* but different from *M. dauuricus* and *M. miodon*. Epipterygoid processes longer than that on *M. dauuricus* and *M. hughi*, but shorter than that on *M. miodon*. Basisphenoid uninflated, distinct from other *Mesechinus* species with basisphenoids moderately inflated. Nasal (~4.30 mm) broader than all other *Mesechinus* species (<3.00 mm). P^3 smaller than that of *M. dauuricus*, but similar to *M. hughi* and *M. miodon*. Supernumerary M^4 consistently present after each M^3, unique among all living hedgehogs (Figure 5).

Description: Large *Mesechinus* species (HB=202.40 mm; GLS=54.75 mm; CBL=54.55 mm; Table 1). Absence of spineless area on scalp; length of ear equal to surrounding spines; ventral pelage dark brown; spines 22–25 mm long, most spines (>80%) white for two-thirds of length and black for other one-third, small number of spines (<20%) white for two-thirds of length, then ringed in black, followed by narrow white ring, tip black; frontal higher than parietal; short spine (~1 mm) present on posterior palatal shelf, extending only slightly posteriorly; epipterygoid processes extend labially (2–3 mm); basisphenoids uninflated, two basisphenoids on both sides touch medially, excavated into shallow spherical fossa (namely, nasopharyngeal fossa; see Frost et al., 1991), breadth of nasopharyngeal fossa ~1.5 mm, breadth of nasal ~4.3 mm; premaxilla extending slightly posteriorly and frontal extending slightly anteriorly on dorsal side of skull, not meeting each other, nasal and maxilla sharing suture (~5–8 mm); jugal large, reaching lacrimal, lacrimal/maxilla suture unfused in adults; I^2 small, I^3 with two roots, larger than I^2, P^2 rectangular shaped, similar to I^3 in size but larger than C^1, P^3 smaller than P^2, triangular (nearly equal-sided) in shape, M^3 heavily reduced, hypocone and metacone absent, M^4 single rooted, much smaller than M^3 (Figure 5).

Measurement: Measurements for *Mesechinus wangi* **sp. nov.** (KIZ 027028, 027001, 027002, 022027 and 034225) are presented in Table 4.

Comparisons: *Mesechinus wangi* **sp. nov.** can be characterized by many unique features within *Mesechinus*, including unique color pattern on spine, uninflated basisphenoid, broad nasal, long common suture shared by nasal with maxilla, and presence of M^4. It is similar to *M. dauuricus* and *M. miodon* in overall size (HB=202.40±26.10 mm) but is obviously larger than *M. hughi* (HB=189.71±24.20 mm; Table 1). *Mesechinus wangi* **sp. nov.** differs from *M. dauuricus* and *M. miodon* in relatively higher frontal than parietal in skull.

Distribution: To date, this species is known only from three counties (Tengchong, Longling, and Longyang) of Baoshan in Yunnan, China, at elevations ranging from 2 200 m–2 680 m. The habitat is subtropical evergreen broad-leaved forest formed by a variety of vegetation, including Fagaceae, Lauraceae, Ericaceae, and Theaceae (Figure 8).

Comments: Population size is currently unknown. However, the known distribution is extremely small and located only within the Gaoligong National Nature Reserve. The species hibernates from middle of October to the following early April.

Key of four species of *Mesechinus*

1. Ventral pelage dark brown; white for two-thirds and black for other one-third on most spines; greatest width of nasal≥4.00 mm; nasal shares long common suture with maxilla; basisphenoid uninflated; supernumerary M^4 present after M^3, occurs only in Mt. Gaoligong, Yunnan, China..... *Mesechinus wangi* **sp. nov.**

   Ventral pelage light brown or white; nasal narrower than 3.00 mm; premaxilla meets frontal on dorsal side of skull (or nearly), nasal does not share suture with maxilla; basisphenoid moderately inflated; M^4 not present; occurs outside of

Yunnan. 2

2. Overall small; GLS<53.00 mm, LUTR<27.00 mm; frontal relatively higher than parietal; occurs in southern Shaanxi, southern Shanxi, and northern Sichuan, China. . . . . *M. hughi*

   Overall large; GLS>53.00 mm, LUTR>27.00 mm; parietal relatively higher than frontal, spine on posterior palatal shelf well developed. 3

3. Spines 21–23 mm in length; tip of spines black, followed by narrow white ring; epipterygoid processes short; P^3 similar to P^2 in size; distributed in northern China, Mongolia, and Russia. . . . . *M. dauuricus*

   Spines 22–29 mm in length; tip of spine light brown; epipterygoid processes well developed; P^3 obviously smaller than P^2. . . . . *M. miodon*

Table 4 External and craniodental measurements for type specimens of *Mesechinus wangi* sp. nov.

Variable	Holotype	Paratypes			
	022028	022027	027001	027002	034255
W	449.00	336.00	390.00	430.00	451.00
HB	240.00	215.00	200.00	180.00	177.00
TL	18.20	18.00	14.00	18.10	18.00
HF	48.00	48.00	45.30	46.70	48.00
EL	31.10	28.90	31.80	28.20	28.00
GLS	55.10	55.60	53.70	54.60	–
CBL	54.80	55.20	53.60	54.60	–
CH	17.50	17.60	16.10	17.30	–
BL	50.50	51.30	50.50	47.70	–
PL	30.80	30.60	30.10	29.50	–
ZMB	34.10	33.70	34.10	–	–
IOB	15.10	14.80	14.20	14.60	–
MTW	26.20	26.20	25.30	24.70	–
GWN	4.30	4.30	4.30	–	–
BM^1	21.50	21.10	21.70	–	–
LUTR	29.10	28.70	27.10	26.70	–
LBTR	25.30	24.20	25.20	24.70	–

Abbreviations are explained in the Materials and Methods section.
–: Not available.

COMPETING INTERESTS

The authors declare that they have no competing interests.

AUTHORS' CONTRIBUTIONS

X.L.J., H.S.A., K.H., and Z.Z.C. designed the study. K.H. and Z.Z.C wrote the manuscript. T.W. and Q.L. contributed to field work. W.H.N., J.H.W., and W.T.S. extracted and analyzed the chromosomes of *Mesechinus wangi* **sp. nov.** All authors read and approved the final manuscript.

ACKNOWLEDGEMENTS

We are grateful to the curators of the Institute of Zoology, Chinese Academy of Sciences, Shaanxi Institute of Zoology (SXIZ), Northwest University (NWU), and China West Normal University (CWNU) for allowing us access to the specimens in their museums. We are grateful to Ms. Paula Jenkins (The Natural History Museum, UK) for taking photos of the holotype specimens of *M. miodon*. We thank Mr. Su Lin for taking photos of specimens.

REFERENCES

Ai HS. 2007. A short introduction of the cover photo for the current issue. *Zoological Research*, **28**(6): 633. (in Chinese)

Allen GM. 1938. The Mammals of China and Mongolia, Part I. New York: American Museum of Natural History, 1–620.

Asahara M, Kryukov A, Motokawa M. 2012. Dental anomalies in the Japanese mole *Mogera wogura* from Northeast China and the Primorsky region of Russia. *Acta Theriologica*, **57**(1): 41–48.

Asahara M. 2013. Unique inhibitory cascade pattern of molars in canids contributing to their potential to evolutionary plasticity of diet. *Ecology and Evolution*, **3**(2): 278–285.

Asahara M, Saito K, Kishida T, Takahashi K, Bessho K. 2016. Unique pattern of dietary adaptation in the dentition of Carnivora: its advantage and developmental origin. *Proceedings of the Royal Society B: Biological Sciences*, **283**(1832): 20160375.

Asahara M. 2016. The origin of the lower fourth molar in canids, inferred by individual variation. *PeerJ*, **4**: e2689.

Badenhorst D, Herbreteau V, Chaval Y, Pagès M, Robinson TJ, Rerkamnuaychoke W, Morand S, Hugot JP, Dobigny G. 2009. New karyotypic data for Asian rodents (Rodentia, Muridae) with the first report of B-chromosomes in the genus *Mus*. *Journal of Zoology*, **279**(1): 44–56.

Bannikova AA, Lebedev VS, Abramov AV, Rozhnov VV. 2014. Contrasting evolutionary history of hedgehogs and gymnures (Mammalia: Erinaceomorpha) as inferred from a multigene study. *Biological Journal of the Linnean Society*, **112**(3): 499–519.

Corbet GB. 1978. The Mammals of the Palearctic Region: A Taxonomic Review. London: British Museum (Natural History), 1–314.

Corbet GB. 1988. The family Erinaceidae: a synthesis of its taxonomy, phylogeny, ecology and zoogeography. *Mammal Review*, **18**(3): 117–172.

Corbet GB, Hill JE. 1992. The Mammals of the Indomalayan Region: A Systematic Review. Oxford: Oxford University Press, 1–488.

Damasceno EM, Hingst-Zaher E, Astúa D. 2013. Bite force and encephalization in the Canidae (Mammalia: Carnivora). *Journal of Zoology*, **290**(4): 246–254.

Frost DR, Wozencraft WC, Hoffmann RS. 1991. Phylogenetic Relationships of Hedgehogs and Gymnures (Mammalia: Insectivora: Erinaceidae). Washington, D.C: Smithsonian Contributions to Zoology, **518**: 1–69.

Gould GC. 1995. Hedgehog phylogeny (Mammalia, Erinaceidae): the reciprocal illumination of the quick and the dead. *American Museum Novitates*, **3131**: 1–45.

Gould GC. 2001. The phylogenetic resolving power of discrete dental morphology among extant hedgehogs and the implications for their fossil record. *American Museum Novitates*, **3340**: 1–52.

He K, Chen JH, Gould GC, Yamaguchi N, Ai HS, Wang YX, Zhang YP, Jiang XL. 2012. An estimation of Erinaceidae phylogeny: a combined analysis approach. *PLoS One*, **7**(6): e39304.

Hoffmann RS, Lunde D. 2008. Order Erinaceomorpha. *In*: Smith AT, Xie Y. A Guide to the Mammals of China. Princeton and Oxford: Princeton University Press, 292–297.

Hungerford DA. 1965. Leukocytes cultured from small inocula of whole blood and the preparation of metaphase chromosomes by treatment with hypotonic KCL. *Stain Technology*, **40**(6): 333–338.

Hutterer R. 2005. Subfamily Erinaceinae. *In*: Wilson DE, Reeder DM. Mammal Species of the World. 3rd ed. Baltimore: Johns Hopkins University Press, 212–217.

Jiang XL. 2016. Obituary: professor Ying-Xiang Wang (1938–2016). *Zoological Research*, **37**(2): 61–64.

Kong F, Guo JM, Wu JY. 2016a. Study on the Chromosome of *Mesechinus miodon*. *Sichuan Journal of Zoology*, **35**(2): 217–220. (in Chinese)

Kong F, Wu JY, Guo JM, Wu XM. 2016b. On classification and distribution of Erinaceinae in Shaanxi province. *Journal of Northwest Normal University* (*Natural Science*), **52**(6): 98–120. (in Chinese)

Korablev VP, Kirijuk VE, Golovuskin MI. 1996. Study of the karyotype of Daurian Hedgehog, *Mesechinus dauricus* (Mammalian. Erinaceidae) from its terra typical. *Zoologichestskii Zhurnal*, **75**: 558–564. (in Russian)

Kryštufek B, Spitzenberger F, Kefelioğlu H. 2001. Description, taxonomy, and distribution of *Talpa davidiana*. *Mammalian biology*, **66**(3): 135–143.

Lin W, Min ZL. 1989. A study on karyotypes of two species of genus *Hemiechinus* (*H. dauuricus* and *H. hughi*). *Journal of Northwest University*, **19**(1): 69–72. (in Chinese)

Lopatin AV. 2006. Early Paleogene insectivore mammals of Asia and establishment of the major groups of Insectivora. *Paleontological Journal*, **40**(S3): S205-S405.

Ma Y. 1964. A new species of hedgehog from Shansi Province, *Hemiechinus sylvaticus* sp. nov. *Acta Zootaxonomica Sinica*, **1**(1): 31–36. (in Chinese)

Min ZL, Lin W. 1989. The classification of Erinaceidae in Shaanxi Province. *Journal of Northwest University*, **19**(4): 71–79. (in Chinese)

Mori T. 1927. On three new mammals from Manchuria. *Annotationes Zoologicae Japonenses*, **11**(2): 107–109.

Ognev SI. 1951. On the hedgehogs (Erinaceidae) of the Far East. Byulleten Moskovskogo Obshchestva Ispytatelei Prirody, **56**: 8–14. (in Russian)

Pan QH, Wang YX, Yan K. 2007. A Field Guide to the Mammals of China. Beijing: Chinese Forestry Publishing House, 1–420.

Rich TH, Rich PV. 1971. Brachyerix, a Miocene hedgehog from western North America, with a description of the tympanic regions of Paraechinus and Podogymnura. *American Museum Novitates*, **2477**: 1–58.

Satunin K. 1907. Uber neue und wenig bekannte Igel des Zoologischen Museums der Kaiserlichen Akademie der Wissenschaften zu St. Petersburg. *Annuaire du Musee Zoologique de l Academie Imperiale des Sciences de St. Petersbourg*, **11**: 167–190. (in Russian).

Sundevall CJ. 1842. Ofversigt af slagtet Erinaceus. *Kunglica Svenska Vetenskapsa-Akademiens, Handlingar*, **1841**: 215–239.

Thomas O. 1908. The duke of Bedford's zoological exploration in eastern Asia- XI. On mammals from the provinces of Shan-si and Shen-si, northern China. *Proceedings of the Zoological Society of London*, **78**(4): 963–983.

Wang YX. 2003. A Complete Checklist of Mammal Species and Subspecies in China, A Taxonomic and Geographic Reference. Beijing: China Forestry Publishing House, 1–394. (in Chinese)

Karyotypes of field mice of the genus *Apodemus* (Mammalia: Rodentia) from China

Masaharu Motokawa[1,*], Yi Wu[2], Masashi Harada[3], Yuta Shintaku[4,5], Xue-Long Jiang[6], Yu-Chun Li[7,*]

[1] *Kyoto University Museum, Kyoto University, Kyoto* 606-8501*, Japan*
[2] *Key Laboratory of Conservation and Application in Biodiversity of South China, School of Life Sciences, Guangzhou University, Guangzhou Guangdong* 510006*, China*
[3] *Laboratory Animal Center, Graduate School of Medicine, Osaka City University, Osaka* 545-8585*, Japan*
[4] *Wildlife Research Center, Kyoto University, Sakyo, Kyoto* 606-8203*, Japan*
[5] *Japan Monkey Centre, Inuyama, Aichi* 484-0081*, Japan*
[6] *Kunming Institute of Zoology, Chinese Academy of Sciences, Kunming Yunnan* 650223*, China*
[7] *Marine College, Shandong University (Weihai), Weihai Shandong* 264209*, China*

ABSTRACT

Karyotypes of four Chinese species of field mice of the genus *Apodemus* were examined, including *Apodemus chevrieri* (diploid chromosome number, 2*n*=48, fundamental number of autosomal arms, FNa=56), *A. draco* (2*n*=48, FNa=48), *A. ilex* (2*n*=48, FNa=48), and *A. latronum* (2*n*=48, FNa=48). Karyotypes of *A. chevrieri*, *A. draco*, and *A. ilex* are reported here for the first time, providing useful information for their species taxonomy. Determining the karyotypes of all species of *Apodemus* in Asia, both in this and previous studies, provides a solid overview of the chromosome evolution and species differentiation of the genus in East Asia. In addition to allopatric speciation, chromosome rearrangements likely played an important role in the formation of the four *Apodemus* species groups as well as speciation within each group in East Asia. For example, increased centromeric heterochromatin in *A. latronum* may have contributed to the post-mating reproductive isolation from the *A. draco*-*A. ilex*-*A. semotus* clade.

Keywords: Karyotype; Chromosome evolution; Speciation; Taxonomy; Field mice

INTRODUCTION

Field mice of the genus *Apodemus* are common murid species widely distributed in the Palearctic region through to the northern part of the Oriental region. The genus currently includes 20 species (Musser et al., 1996; Musser & Carlenton, 2005), which have been characterized into three species groups based on morphological characters from detailed literature review (Musser et al., 1996): that is, *Apodemus* Group (*A. agrarius*, *A. chevrieri*, *A. speciosus*, *A. peninsulae*, *A. latronum*, *A. draco*, *A. semotus*, *A. gurkha*), *Sylvaemus* Group (*A. sylvaticus*, *A. flavicollis*, *A. uralensis*, *A. mystacinus*, *A. fulvipectus*, *A. heremonensis*, *A. alpicola*, *A. arianus*, *A. hyrcanicus*, *A. ponticus*, *A. rusiges*, *A. wardi*), and *Argenteus* Group (*A. argenteus*). The *Apodemus* Group and *Argenteus* Group consist of species distributed in East Asia, whereas species within the *Sylvaemus* Group are found in western Palearctic region. The *A. agrarius* species from the *Apodemus* Group is widely distributed in the Palearctic region from East Asia to Europe. Currently, however, there is still considerable taxonomic confusion regarding the species boundaries and identification of East Asian *Apodemus* species (Musser et al., 1996), especially those distributed in China.

Several phylogenetic studies using genetic approaches were conducted to reveal the species relationship and validity of the above-mentioned species groups (Filippucci et al., 2002; Liu et al., 2004; Michaux et al., 2002; Serizawa et al., 2000;

Received: 22 January 2018; Accepted: 03 May 2018; Online: 28 May 2018

Foundation items: This study was supported by the National Natural Science Foundation of China (NSFC) Major International (Regional) Joint Research Project Grant (31110103910), National Basic Research Program of China (2013FY111500), JSPS KAKENHI grant JP18H03602, and JSPS Core-to-Core Program B. Asia Africa Science Platforms

[*]Corresponding authors, E-mail: motokawa.masaharu.6m@kyoto-u.ac.jp; li_yuchun@sdu.edu.cn

DOI: 10.24272/j.issn.2095-8137.2018.054

Suzuki et al., 2003, 2008). Suzuki et al. (2008) conducted comprehensive phylogenetic analyses based on mitochondrial and nuclear genes from most species of *Apodemus* and confirmed the distinct lineages of the three species groups, except for *A. gurkha*, which showed an independent lineage from the other species within the *Apodemus* Group.

Concerning the evolutionary history of the genus *Apodemus* in East Asia, Suzuki et al. (2008) determined that the three species groups formed around 6 million years ago (Ma), with the *Apodemus* Group splitting into four ancestral species (*A. agrarius*/*A. chevrieri*, *A. draco* (and *A. ilex*)/*A. semotus*/*A. latronum*, *A. peninsulae*, and *A. speciosus*) around 5 Ma, and then splitting into the currently recognized species around 2 Ma. For these speciation events, Suzuki et al. (2008) assumed that allopatric speciation likely played an important role, followed by range expansion and distribution overlap. The original place for speciation event, however, has not been mentioned and unspecified.

Chromosomal divergence is thought to play a role in reproductive isolation (e.g., King, 1993). Examination of karyotypes of species and populations is important to reconstruct allopatric and sympatric speciation events and clarify the historical changes in species distribution. Species differentiation among congeneric species also participates in cytological reproductive isolation (e.g., King, 1993). While the karyotypes of *Apodemus* species have been relatively well studied (e.g., Matsubara et al., 2004), information on species and populations in China is still limited. Clarification of species karyotypes is important for understanding the diversification of a genus. In this study, we examined the karyotypes of *A. chevrieri*, *A. draco*, *A. ilex*, and *A. latronum* based on specimens collected in China to help fill the gap in current knowledge. Even though the newly reported karyotypes were limited to conventional karyotypes, we expect they will be useful for the evaluation of species taxonomy and will provide an overview of chromosomal evolution and species differentiation. We also examined evolutionary history in consideration of the molecular and chromosomal divergences of *Apodemus* in East Asia.

MATERIALS AND METHODS

A total of 71 specimens from four *Apodemus* species (*A. chevrieri*, *A. draco*, *A. ilex*, and *A. latronum*) in China were examined. Species identification was made by careful examination of cranial characters following Musser et al. (1996), in addition to external characters and measurements. *Apodemus ilex* (mostly distributed in Yunnan, China) is often considered a synonym of *A. draco* (e.g., Musser & Carlenton, 2005); however, molecular phylogeographic data suggest two species (e.g., Liu et al., 2012). In this study, we considered *A. ilex* as a separate species from *A. draco*, even though future study is expected to evaluate their taxonomic status and geographic distribution more accurately. Voucher specimens were deposited in the Key Laboratory of Conservation and Application in Biodiversity of South China, Guangzhou University, Guangzhou (GU), and the Marine College of Shandong University at Weihai (SUS).

Examined specimens and collection localities are as follows: *Apodemus chevrieri* (*n*=11): Mt. Emei, Sichuan, GU MM3566 (male), 3593, 3594, 4478, 4480, 4484 (females), Wolong, Sichuan, SUS S1124, S1264, S1265 (males), S1107, S1236 (females); *Apodemus draco* (*n*=41): Mt. Emei, Sichuan, GU MM3545, 3563, 3564, 3568, 3569, 3570, 3585, 3586, 3596, 3599, 4479, 4483, 4485 (males), 3551, 3565, 3578, 3579, 3587, 3595, 4482 (females); Labahe, Tianquan, Ya'an, Sichuan, GU10073, 10076, 10077, 10094, 10107, 10128 (males), 10074, 10108, 10110 (females); Kangding, Sichuan, GU10137, 10139, 10148 (males), 10135, 10147 (females); Wolong, Sichuan, SUS S1140, S1257, S1266 (males), S1108, S1180, S1245, S1246 (females); *Apodemus ilex* (*n*=9): Ailaoshan, Xinping, Yunnan, SUS S570, S649, S661, S663, S667, S683 (males), S651, S662, S684 (females); *Apodemus latronum* (*n*=10): Kangding, Sichuan, GU10134, 10157 (males), 10136, 10140, 10145, 10151, 10153 (females), Wolong, Sichuan, SUS S1136, S1156 (males), S1134 (female).

Cytological preparations were made from tail and/or lung tissue culture cells using the standard air-drying method described by Harada & Yosida (1978). C-band staining was accomplished as per Sumner (1972) for selected species and specimens. Terminology for chromosomes followed Levan et al. (1964): i.e., metacentric, submetacentric, subtelocentric, and acrocentric. Diploid chromosome number (2*n*) and fundamental number of autosomal arms (FNa) were calculated.

RESULTS

The karyotype of *Apodemus chevrieri* (Figure 1A) consisted of four small meta- or submetacentric pairs (nos. 1–4) and 19 large-to-small acrocentric pairs (nos. 5–23) in autosomes, large acrocentric X chromosome, and small acrocentric Y chromosome. The 2*n* and FNa values were 48 and 54, respectively.

The karyotype of *Apodemus draco* (Figure 1B) consisted of one small metacentric pair (no. 1) and large-to-small acrocentric pairs (nos. 2–23) in autosomes, large acrocentric X chromosome, and small acrocentric Y chromosome. The 2*n* and FNa values were 48 and 48, respectively.

The karyotype of *Apodemus ilex* (Figure 1C) consisted of one small metacentric pair (no. 1) and large-to-small acrocentric pairs (nos. 2–23) in autosomes, large acrocentric X chromosome, and small acrocentric Y chromosome. The 2*n* and FNa values were 48 and 48, respectively.

The karyotype of *Apodemus latronum* (Figure 1D) consisted of one small submetacentric (no. 1) and 22 large-to-small (nos. 2–23) acrocentric pairs in autosomes, large acrocentric X chromosome, and small acrocentric Y chromosome. In several acrocentric pairs, the centromeric region was well developed due to the constitutive heterochromatins, which were well stained following C-band staining (Figure 1E, nos. 2–9). As we could not find clear short arms for those pairs, we considered those pairs to be acrocentric. The 2*n* and FNa values were 48 and 48, respectively.

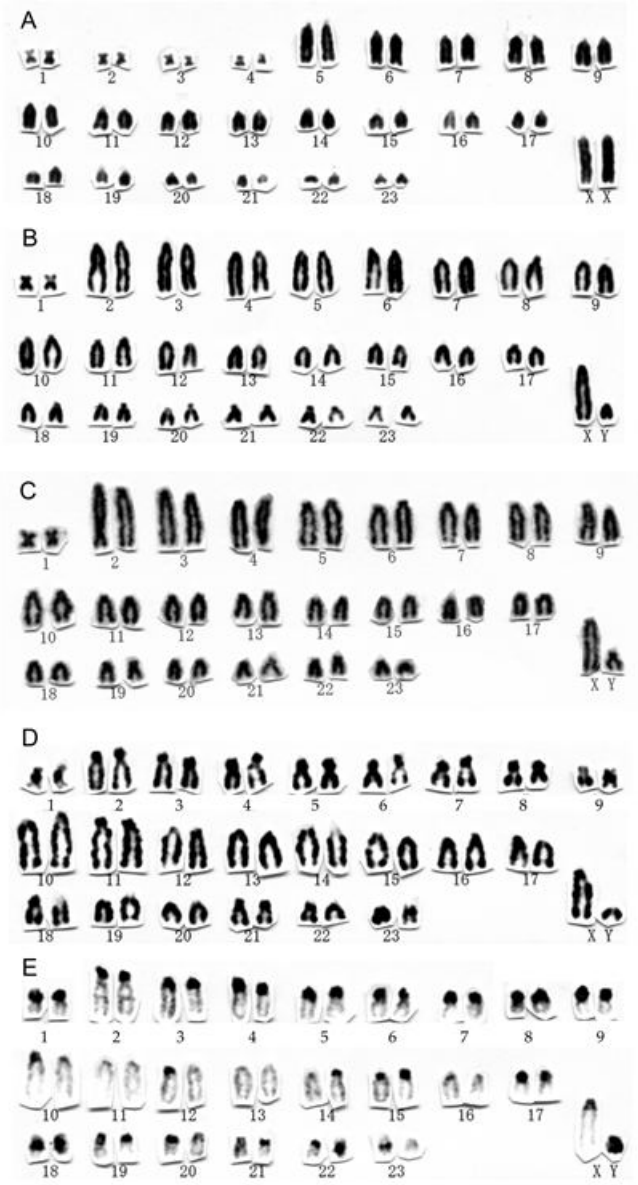

Figure 1 Karyotypes of *Apodemus* species from China

Conventional karyotypes of *A. chevrieri* (A, GU MM3593), *A. draco* (B, M10077), *A. ilex* (C, SUS S649), and *A. latronum* (D, GU10134), as well as the C-band karyotype of *A. latronum* (E, GU10134).

DISCUSSION

We analyzed the karyotypes of four *Apodemus* species from China. Previous karyotypic data from this genus are summarized in Table 1, together with our results from this study.

The karyotype of *A. chevrieri* is reported here for the first time, and was characterized by four small metacentric pairs (2*n*=48, FNa=54). *Apodemus chevrieri* is restricted to southwestern China and based on mitochondrial and nuclear gene phylogenetic studies is thought to be a sister or in-group species of the widely distributed *A. agrarius* (Liu et al., 2004; Suzuki et al., 2003, 2008). Although the karyotype of *A. agrarius* is polymorphic and possesses 3–5 biarmed metacentric autosome pairs (2*n*=48, FNa=52–56, excluding the B chromosome; Boeskorov et al., 1995; Britton-Davidian et al., 1991; Chassovnikarova et al., 2009; Chernukha et al., 1986; Kang & Koh, 1976; Kartavtseva, 1994; Kartavtseva & Pavlenko, 2000; Kefelioğlu et al., 2003; Koh, 1987, 1988, 1989; Král, 1970, 1972; Matsubara et al., 2004; Shbulatova et al., 1991; Soldatović et al., 1969, 1975; Tsuchiya, 1979; Vujošević et al., 1984; Wang et al., 1993; Yiğit et al., 2000), the karyotype with four metacentric pairs (2*n*=48, FNa=54) is regarded as the standard karyotype for *A. agrarius* (see Kartavtseva & Pavlenko, 2000). Therefore, we suggest that there are no clear differences in the conventional karyotypes between *A. chevrieri* and *A. agrarius*; however, further study using differential staining of chromosome arms is expected to clarify any minor differences and rearrangement of chromosome arms between *A. chevrieri* and polymorphic *A. agrarius*, and thus help reevaluate their taxonomic status.

The karyotypes of *A. draco* and *A. ilex* are reported in this study for the first time as correct species identification, with both characterized by one small metacentric pair (2*n*=48, FNa=48), similar to that of *A. semotus* in Taiwan, China (Matsubara et al., 2004; Tsuchiya, 1979). While Chen et al. (1996) reported karyotypes of *A. draco* as 2*n*=48, FNa=46 and *A. peninsulae* as 2*n*=48, FNa=48 from Yunnan Province, China, these two karyotypes were possibly reported based on erroneous identification. We suggest that the former specimens collected from Kunming were *A. peninsulae*, whereas the latter specimens collected from Jianchuan were *A. ilex*. This interpretation of misidentification by Chen et al. (1996) would be congruent with the distribution of *A. draco* (currently *A. ilex*) in Kunming and Jianchuan and *A. peninsulae* in Kunming but not Jianchuan (Zhang, 1997); and that these two species have been considered superficially similar in morphologies and often misidentified before the careful taxonomic revision by Musser et al. (1996).

The karyotype of specimens of "*A. draco*" by Chen et al. (1996), and herewith interpreting to represent *A. peninsulae* showed no differences with the reported *A. peninsulae* karyotype and had only acrocentric chromosomes (2*n*=48, FNa=46; Hayata, 1973; Kartavtseva et al., 2000; Koh, 1986, 1988; Wang et al., 2000). The karyotype of the latter specimens correctly representing *A. ilex* was very similar to the karyotype for *A. ilex* from Yunnan, as well as *A. draco* from Sichuan in this study (2*n*=48, FNa=48) and *A. semotus* from Taiwan, China (2*n*=48, FNa=48; Matsubara et al., 2004; Tsuchiya, 1979) characterized by one small metacentric pair. Although the current study was limited to conventional karyotypes, we report here on the karyotypes of *A. draco* and *A. ilex* for the first time and provide updated information on the karyotype of *A. peninsulae*. These data are important for further study on species taxonomy and identification of the genus *Apodemus* in East Asia.

Table 1 Karyotypes of field mice of the genus *Apodemus* examined in this study and reported in previous studies

Species	Locality	2*n*	FNa	M/SM	ST	A	X	Y	B	Reference
A. chevrieri	Sichuan, China	48	54	4	0	20	A	A	–	This study
A. agrarius	Shandong, China	48	54	4	0	19	A	A	–	Wang et al. (1993)
	Taiwan, China	48	56	5	0	18	A	A	–	Tsuchiya (1979)
	Korea	48	54	4	0	19	A	A	–	Kang & Koh (1976), Koh (1987, 1988, 1989), Matsubara et al. (2004)
	Primorye	48	52	3	0	20	A	A	–	Chernukha et al. (1986)
	Primorye	48	52–54	3–4	0	19–20	A	A	0–1	Kartavtseva & Pavlenko (2000)
	Amur	48	52	3	0	20	A	A	–	Kartavtseva & Pavlenko (2000)
	Khasan	48	54	4	0	19	A	A	–	Boeskorov et al. (1995)
	Khabarovsk	48	52–54	3–4	0	19–20	A	A	0–1	Chernukha et al. (1986), Kartavtseva (1994), Kartavtseva & Pavlenko (2000)
	Siberia	48	52–54	3–4	0	19–20	A	A	–	Boeskorov et al. (1995), Kartavtseva & Pavlenko (2000)
	Altai	48	52	3	0	20	A	A	–	Chernukha et al. (1986)
	Altai	48	54	4	0	19	A	A	–	Kartavtseva & Pavlenko (2000)
	Moskow oblast	48	52	3	0	20	A	A	–	Chernukha et al. (1986)
	Chechen-Ingush	48	52	3	0	20	A	A	–	Chernukha et al. (1986)
	Krasnodar	48	52	3	0	20	A	A	–	Chernukha et al. (1986)
	Ukraine	48	54	4	0	19	A	A	–	Kartavtseva & Pavlenko (2000)
	Moldova	48	52–54	3–4	0	19–20	A	A	–	Kartavtseva & Pavlenko (2000)
	Azerbaijan	48	54	4	0	19	A	A	–	Shbulatova et al. (1991)
	Czechoslovakia	48	54	4	0	19	A	A	–	Král (1970) (1972)
	Poland	48	54	4	0	19	A	A	–	Král (1970)
	Yugoslavia	48	54	4	0	19	A	A	–	Vujošević et al. (1984)
	Yugoslavia	48	52–54	3–4	0	19–20	A	A	–	Soldatović et al. (1969, 1975)
	Bulgaria	48	52–54	3–4	0	19–20	A	A	0–1	Chassovnikarova et al. (2009)
	Greece	48	54	4	0	19	A	A	–	Britton-Davidian et al. (1991)
	Turkey	48	54	4	0	19	A	A	–	Kefelioğlu et al. (2003)
	Turkey	48	56	5	0	18	A	A	–	Yiğit et al. (2000)
A. draco	Sichuan, China	48	48	1	0	22	A	A	–	This study
A. ilex	Yunnan, China	48	48	1	0	22	A	A	–	This study
	Yunnan, China	48	48	1	0	22	A	A	–	Chen et al. (1996) as "*A. peninsulae*"
A. latronum	Sichuan, China	48	48	1	0	22	A	A	–	This study
	Yunnan, China	48	66	8	2	13	A	?	–	Chen et al. (1996)
A. semotus	Taiwan, China	48	48	1	0	22	A	?	–	Matsubara et al. (2004)
A. peninsulae	Yunnan, China	48	46	0	0	23	A	A	–	Chen et al. (1996) as "*A. draco*"
	NE China	48	46	0	0	23	A	A	0–14	Wang et al. (2000)
	Korea	48	46	0	0	23	A	A	6–1	Koh (1986, 1988)
	Russia	48	46	0	0	23	A	A	0–6	Kartavtseva et al. (2000)
	Hokkaido, Japan	48	46	0	0	23	A	A	0–13	Hayata (1973)
A. speciosus	Japan	46–48	54	4–3	1	17–19	A	A	–	Tsuchiya (1974)
	Japan	46–48	54	5–4	0	17–19	A	A	–	Saitoh & Obara (1986)
A. argenteus	Japan	46	50	2	0	20	SM	A	0–1	Yoshida et al. (1975), Obara & Sasaki (1997)
A. gurkha	Nepal	48	50	2	0	21	A	?	–	Matsubara et al. (2004).
	Nepal	48	62–64	4–3	5	14–15	A	A	–	Gemmeke & Niethammer (1982)
Sylvaemus Group										
A. sylvaticus		48	46	0	0	23	A	A	–	Zima & Král (1984), Orlov et al. (1996), Kryštufek & Vohralík (2009)
A. flavicollis		48	46	0	0	23	A	A	1–3	Zima & Král (1984), Orlov et al. (1996), Kryštufek & Vohralík (2009)
A. microps		48	46	0	0	23	A	A	–	Zima & Král (1984), Reutter et al. (2001)
A. alpicola		48	46	0	0	23	A	A	–	Reutter et al. (2001)
A. witherbyi		48	46	0	0	23	A	A	–	Orlov et al. (1996), Kryštufek & Vohralík (2009)
A. uralensis		48	46	0	0	23	A	A	–	Orlov et al. (1996), Kryštufek & Vohralík (2009)
A. ponticus		48	46	0	0	23	A	A	–	Orlov et al. (1996)
A. pallipes		48	46	0	0	23	A	A	–	Gemmeke & Niethammer (1982)
A. epimelas		48	48–50	1–2	0	21–22	A	A	0–1	Belcheva et al. (1988), Zima & Král (1984)
A. mystacinus		48	50	2	0	21	A	A	–	Kryštufek & Vohralík (2009)

Diploid and sex chromosomes were classified into metacentric (M), submetacentric (SM), subtelocentric (ST), and acrocentric (A), and a "?" indicate the Y chromosome was too small to be confirmed. 2*n* and FNa, excluding the B chromosome. –: Not available.

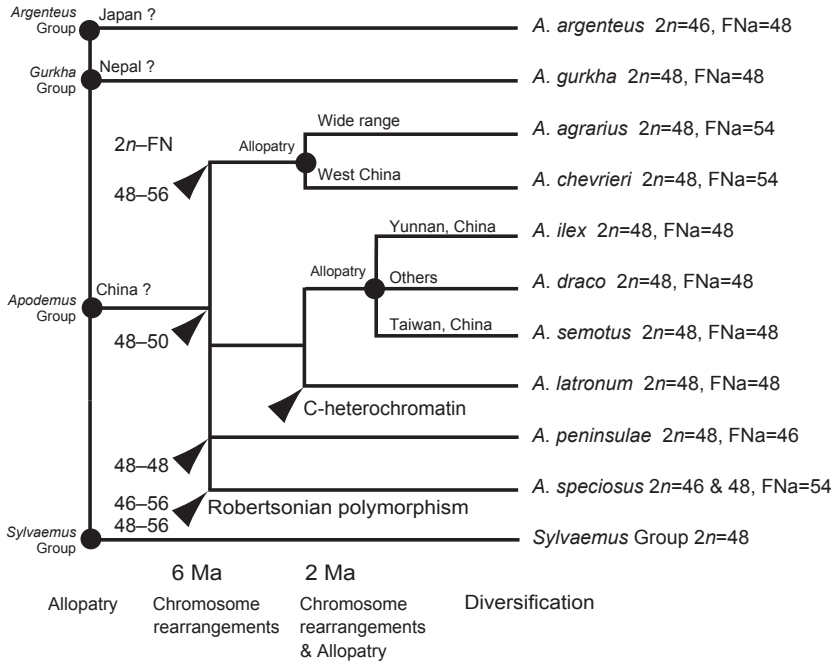

Figure 2 Hypothesized diversification process with allopatric distribution and chromosome changes in the genus *Apodemus* in East Asia

Phylogenetic relationships among species followed the molecular phylogeny of Suzuki et al. (2008). Some chromosome rearrangements referred to Matsubara et al. (2004). Arrowheads and closed circles indicate possible chromosome rearrangements and allopatric speciation, which resulting reproductive isolation. ?: Indicate the hypothetical origination of the clade/lineage.

The karyotype of *A. latronum* was 2*n*=48 and FNa=48, with one small biarmed pair. This chromosome complement was similar to that of *A. draco*, *A. ilex*, and *A. semotus*, but the karyotype differed by having centromeric heterochromatin in many acrocentric pairs. Similar centromeric heterochromatin has been found in previous study on the karyotype of *A. latronum* from Yunnan Province (Chen et al., 1996). Chen et al. (1996) stated that the centromeric heterochromatin formed short arms and thus considered the *A. latronum* karyotype to be 2*n*=48, FNa=66. Although we did not analyze the G-band karyotype of *A. latronum*, based on the C-band karyotype we found no considerable differences between our *A. latronum* karyotype (2*n*=48, FNa=48) and that of Chen et al. (1996) (2*n*=48, FNa=66), despite different FNa values due to the interpretation of centromeric heterochromatin.

We studied the karyotypes of all *Apodemus* species in East Asia and provided a solid overview of chromosome evolution and species differentiation of the genus within East Asia. The chromosome rearrangements in East Asian *Apodemus* were congruent with the species divergence pattern proposed in previous molecular study (Suzuki et al., 2008). Suzuki et al. (2008) recognized four groups as the major DNA phylogenetic clades of the East Asian *Apodemus* subgeneric group: (1) *A. agrarius–A. chevrieri* (=*agrarius* species group), (2) *A. draco–A. ilex–A. semotus–A. latronum* (=*draco* species group), (3) *A. peninsulae*, and (4) *A. speciosus*. Suzuki et al. (2008) stated that these four groups radiated 6 Ma in response to global environmental changes among allopatric populations. Our present study clarified that these four DNA phylogenetic species groups were distinct, with different karyotypes: 2*n*=48, FNa=54 for the *agrarius* group (*A. agrarius*, *A. chevrieri*); 2*n*=48, FNa=48 for the *draco* group (*A. draco*, *A. ilex*, *A. semotus*, *A. latronum*); 2*n*=48, FNa=46 for *A. peninsulae*; and 2*n*=46/48, FNa=54 for *A. speciosus* (Tsuchiya, 1974; Saitoh & Obara, 1986. We suggest that these major chromosome rearrangements among clades played an important role in clade formation through post-mating reproductive isolation, in addition to allopatric distribution.

After the radiation into four groups, further speciation events are thought to have occurred within the *draco* and *agrarius* groups around 2 Ma (Suzuki et al., 2008). In the *draco* group, speciation likely occurred through allopatric speciation due to partitioning of the distribution range in developping geographic barriers, such as among *A. ilex* (Yunnan), *A. draco* (other areas in mainland China), and *A. semotus* (Taiwan, China), with minor chromosome rearrangements unlikely to have contributed to the speciation events of these three allopatric species (Figure 2). On the other hand, the current distribution range between *A. latronum* and *A. draco* and between *A. latronum* and *A. ilex* overlap (e.g., Musser et al., 1996). This suggests that *A. latronum*, which is distributed in the western provinces of Sichuan, Yunnan, Xizang, and

Qinghai, as well as northern Myanmar (Musser & Carlenton, 2005), was not derived through allopatric speciation among the *draco* group. We propose that speciation of *A. latronum* from the *A. draco-A. ilex-A. semotus* clade may have occurred as sympatric speciation, where chromosome rearrangements contributed to form post-mating reproductive isolation at the cytological level. The increased centromeric heterochromatin found in *A. latronum* also influenced post-mating reproductive isolation from the *A. draco-A. ilex-A. semotus* clade, which lacked heterochromatin increase (Figure 2). On the other hand, *A. agrarius* and *A. chevrieri* in the *agrarius* group exhibit slight overlap in their current distribution ranges (Musser et al., 1996); and these two species may have undergone speciation by allopatric distribution, with subsequent expansion and overlap of their distribution ranges, as discussed by Suzuki et al. (2008). The speciation of *A. chevrieri* from *A. agrarius* is, therefore, suggested to have been accompanied by allopatric speciation events, and this evolutionary story may explain the lack of major karyotypic differences between the two species.

In addition, extensive geographical divergences within the species have been reported for morphological and genetic traits in East Asian *Apodemus* species: e.g., *A. chevrieri* (Yue et al., 2012), *A. agrarius* (Sakka et al., 2010), *A. draco* (Fan et al., 2012; Kaneko, 2010, 2012, 2015; Sakka et al., 2010), *A. ilex* (Kaneko, 2010, 2012, 2015; Liu et al., 2012), *A. latronum* (Kaneko, 2010, 2012, 2015; Li & Liu, 2014; Sakka et al., 2010), *A. semotus* (Hsu et al., 2001), *A. peninsulae* (Kaneko, 2010, 2012, 2015; Sakka et al., 2010; Serizawa et al., 2002), *A. speciosus* (Kageyama et al., 2009; Shintaku et al., 2012; Shintaku & Motokawa, 2016; Suzuki et al., 2004; Tomozawa et al., 2014; Tomozawa & Suzuki, 2008), and *A. argenteus* (Suzuki et al., 2004). These complex patterns are thought to have formed through geographic isolation and genetic exchange (e.g., *A. speciosus* between Robertsonian chromosome races; Shintaku & Motokawa, 2016; Suzuki et al., 2004; Tomozawa & Suzuki, 2008) after the formation of each species. More comprehensive analyses using morphology, chromosomes, and DNA markers are expected to clarify the complex evolutionary history of the *Apodemus* genus in East Asia. The present study elucidated the evolutionary pattern of the *Apodemus* genus in East Asia with reference to the major chromosome rearrangements at the among-species level. Future study of major and minor chromosome rearrangements at the within-species level using various chromosome arm staining techniques is expected. The genus *Apodemus* may be considered a good wild animal model to understand the roles of reproductive isolation by allopatric distribution and chromosome rearrangement during speciation events.

COMPETING INTERESTS

The authors declare that they have no competing interests.

AUTHORS' CONTRIBUTIONS

M.M. and Y.C.L. designed the study. M.M., Y.W., M.H., Y.S., X.L.J, and Y.L collected specimens. M.M. made species identification. M.M., M.H., Y.W., and Y.C.L analyzed karyotypes. M.M. and Y.S. made literature surveys. M.M. wrote the manuscript. Y.W., M.H., Y.C.L. revised the manuscript. All authors read and approved the final manuscript.

REFERENCES

Belcheva RG, Topaschka-Ancheva MN, Atanassov N. 1988. Karyological studies of five species of mammals from Bulgarian fauna. *Comptes rendus de l'Academie bulgare des Sciences*, **42**: 125–128.

Boeskorov GG, Kartavtseva IV, Zagorodniuk IV, Belianin AN, Liapunova EA. 1995. Nucleolus organizer regions and B-chromosomes of field mice (Mammalia, Rodentia, *Apodemus*). *Genetika*, **31**(2): 185–192. (in Russian)

Britton-Davidian J, Vahdati M, Benmedhi F, Gros P, Nancé V, Croset H, Guerassimov S, Triantaphyllidis C. 1991. Genetic differentiation in four species of *Apodemus* from southern Europe: *A. sylvaticus, A. flavicollis, A. agrarius* and *A. mystacinus* (Muridae, Rodentia). *Zeitschrift für Säugetierkunde*, **56**: 25–33.

Chassovnikarova T, Atanasov N, Dimitrov H. 2009. Chromosome polymorphism in Bulgarian populations of the striped field mouse (*Apodemus agrarius* Pallas 1771). *Comparative Cytogenetics*, **3**(1): 1–9.

Chen ZP, Liu RQ, Li CY, Wang YX. 1996. Studies on the chromosomes of three species of wood mice. *Zoological Research*, **17**(3): 347–352. (in Chinese)

Chernukha YG, Evdokimova OA, Chechovich AV. 1986. Results of karyologic and immunobiological studies of the striped field mouse (*Apodemus agrarius*) from different areas of its range. *Zoological Journal*, **65**: 471–475. (in Russian)

Fan ZX, Liu SY, Liu Y, Liao LH, Zhang XY, Yue BS. 2012. Phylogeography of the South China field mouse (*Apodemus draco*) on the southeastern Tibetan Plateau reveals high genetic diversity and glacial refugia. *PLoS One*, **7**(5): e38184.

Filippucci MG, Macholán M, Michaux JR. 2002. Genetic variation and evolution in the genus *Apodemus* (Muridae: Rodentia). *Biological Journal of the Linnean Society*, **75**(3): 395–419.

Gemmeke H, Niethammer J. 1982. Zur Characterisierung der Waldmäuse (*Apodemus*) Nepals. *Zeitschrift für Säugetierkunde*, **47**: 33–38.

Harada M, Yosida TH. 1978. Karyological study of four Japanese *Myotis* bats (Chiroptera, Mammalia). *Chromosoma*, **65**(3): 283–291.

Hayata I. 1973. Chromosomal polymorphism caused by supernumerary chromosomes in the field mouse, *Apodemus giliacus. Chromosoma*, **42**(4): 403–414.

Hsu FH, Lin FJ, Lin YS. 2001. Phylogeographic structure of the Formosan wood mouse, *Apodemus semotus* Thomas. *Zoological Studies*, **40**(2): 91–102.

Kageyama M, Motokawa M, Hikida T. 2009. Geographic variation in morphological traits of the large Japanese field mouse, *Apodemus speciosus* (Rodentia, Muridae), from the Izu Island group, Japan. *Zoological Science*, **26**(4): 266–276.

Kaneko Y. 2010. Identification of *Apodemus peninsula*, *draco* and *A. latronum* in China, Korea, and Myanmar by cranial measurements. *Mammal Study*, **35**(1): 31–55.

Kaneko Y. 2012. Horizontal and elevational distributions of *Apodemus peninsulae*, *A. draco* and *A. latronum. Mammal Study*, **37**(3): 183–204.

Kaneko Y. 2015. Latitudinal geographical variation of external and cranial measurements in *Apodemus peninsulae*, *A. draco*, and *A. latronum*. *Mammal Study*, **40**(3): 143–165.

Kang YS, Koh HS. 1976. Karyotype studies on three species of the family Muridae (Mammalia; Rodentia) in Korea. *Korean Journal of Zoology*, **19**(3): 101–112.

Kartavtseva IV. 1994. A description of the B chromosomes in the karyotype of the field mouse *Apodemus agrarius*. *Tsitologiia i Genetika*, **28**(2): 96.

Kartavtseva IV, Pavlenko MV. 2000. Chromosome variation in the striped field mouse *Apodemus agrarius* (Rodentia: Muridae). *Russian Journal of Genetics*, **36**(2): 162–174.

Kartavtseva IV, Roslik GV, Pavlenko MV, Amachaeva EY, Sawaguchi S, Obara Y. 2000. The B-chromosome system of the Korean field mouse *Apodemus peninsulae* in the Russian Far East. *Chromosome Science*, **4**: 21–29.

Kefelioğlu H, Tez C, Gündüz I. 2003. The taxonomy and distribution of *Apodemus agrarius* (Pallas, 1771) (Mammalia: Rodentia) in the European part of Turkey. *Turkish Journal of Zoology*, **27**: 141–146.

King M. 1993. Species Evolution: The Role of Chromosome Change. Cambridge: Cambridge University Press.

Koh HS. 1986. Systematic studies of Korean rodents: II. A chromosome analysis in Korean field mice, *Apodemus peninsulae peninsulae* Thomas (Muridae, Rodentia), from Mungyong, with the comparison of morphometric characters of these Korean field mice to symptric striped field mice, *A. agrarius coreaee* Thomas. *Korean Journal of Systematic Zoology*, **2**: 1–10.

Koh HS. 1987. Systematic studies of Korea rodents: III. Morphometric and chromosomal analyses of striped field mice, *Apodemus agrarius chemuensis* Jones and Johnson, from Jeju-Do. *Korean Journal of Systematic Zoology*, **3**: 24–40.

Koh HS. 1988. Systematic studies of Korean rodents: IV. Morphometric and chromosomal analyses of two species of the genus *Apodemus* (Muridae). *Korean Journal of Systematic Zoology*, **4**: 103–120.

Koh HS. 1989. Systematic studies of Korean rodents. V. Morphometric and chromosomal analyses on island populations of striped field mice (*Apodemus agrarius coreae*) in southwestern coasts of the Korean Peninsula. *Korean Journal of Systematic Zoology*, **5**: 1–12.

Král B. 1970. Chromosome studies in two subgenera of the genus *Apodemus*. *Zoologicke Listy*, **19**(2): 119–134.

Král B. 1972. Chromosome characteristics of Muridae and Microtidae from Czechoslovakia. *Acta Scientiarm Naturalium Academiae Scientiarum Bohemoslovacae Brno*, **6**(12): 1–78.

Kryštufek B, Vohralík V. 2009. Mammals of Turkey and Cyprus. Rodentia II: Cricetinae, Muridae, Spalacidae, Calomyscidae, Capromyidae, Hystricidae, Castoridae. Koper: Zgodovinsko društvo za južno Primorsko.

Levan A, Fredga K, Sandberg AA. 1964. Nomenclature for centromeric position on chromosomes. *Hereditas*, **52**(2): 201–220.

Li S, Liu SY. 2014. Geographic variation of the large-eared field mouse (*Apodemus latronum* Thomas, 1911) (Rodentia: Muridae) with one new subspecies description verified via cranial morphometric variables and pelage characteristics. *Zoological Studies*, **53**: 23.

Liu Q, Chen P, He K, Kilpatrick CW, Liu SY, Yu FH, Jiang XL. 2012. Phylogeographic study of *Apodemus ilex* (Rodentia: Muridae) in Southwest China. *PLoS One*, **7**(2): e31453.

Liu XM, Wei FW, Li M, Jiang XL, Feng ZJ, Hu JC. 2004. Molecular phylogeny and taxonomy of wood mice (genus *Apodemus* Kaup, 1829) based on complete mtDNA cytochrome b sequences, with emphasis on Chinese species. *Molecular Phylogenetics and Evolution*, **33**(1): 1–15.

Matsubara K, Nishida-Umehara C, Tsuchiya K, Nukaya D, Matsuda Y. 2004. Karyotypic evolution of *Apodemus* (Muridae, Rodentia) inferred from comparative FISH analyses. *Chromosome Research*, **12**(4): 383–395.

Michaux JR, Chevret P, Filippucci MG, Macholán M. 2002. Phylogeny of the genus *Apodemus* with a special emphasis on the subgenus *Sylvaemus* using the nuclear IRBP gene and two mitochondrial markers: cytochrome *b* and 12S rRNA. *Molecular Phylogenetics and Evolution*, **23**(2): 123–136.

Musser GG, Brothers EM, Carleton MD, Hutterer R. 1996. Taxonomy and distributional records of Oriental and European *Apodemus*, with a review of the *Apodemus-Sylvaemus* problem. *Bonner Zoologische Beiträge*, **46**(1–4): 143–190.

Musser GG, Carlenton MD. 2005. Superfamily muroidea. *In*: Wilson DE, Reeder DM. Mammal Species of the World: A Taxonomic and Geographic Reference. 3rd ed. Baltimore: The Johns Hopkins University Press, 894–1531.

Obara Y, Sasaki S. 1997. Fluorescent approaches on the origin of B chromosomes of *Apodemus argenteus hokkaidi*. *Chromosome Science*, **1**(1): 1–5.

Orlov VN, Bulatova NS, Nadjafova RS, Kozlovsky AI. 1996. Evolutionary classification of European wood mice of the subgenus *Sylvaemus* based on allozyme and chromosome data. *Bonner Zoologische Beiträge*, **46**: 191–202.

Reutter BA, Nová P, Vogel P, Zima J. 2001. Karyotypic variation between wood mouse species: banded chromosomes of *Apodemus alpicola* and *A. microps*. *Acta Theriologica*, **46**(4): 353–362.

Saitoh M, Obara Y. 1986. Chromosome banding patterns in five intraspecific taxa of the large Japanese field mouse, *Apodemus speciosus*. *Zoological Science*, **3**: 785–792.

Sakka H, Quéré JP, Kartavtseva I, Pavlenko M, Chelomina G, Atopkin D, Bogdanov A, Michaux J. 2010. Comparative phylogeography of four *Apodemus* species (Mammalia: Rodentia) in the Asian Far East: evidence of Quaternary climatic changes in their genetic structure. *Biological Journal of the Linnean Society*, **100**(4): 797–821.

Serizawa K, Suzuki H, Tsuchiya K. 2000. A phylogenetic view on species radiation in *Apodemus* inferred from variation of nuclear and mitochondrial genes. *Biochemical Genetics*, **38**(1–2): 27–40.

Serizawa K, Suzuki H, Iwasa MA, Tsuchiya K, Pavlenko MV, Kartavtseva IV, Chelomina GN, Dokuchaev NE, Han SH. 2002. A spatial aspect on mitochondrial DNA genealogy in *Apodemus peninsulae* from East Asia. *Biochemical Genetics*, **40**(5–6): 149–161.

Shbulatova N, Nadjafova RS, Kozlovsky I. 1991. Cytotaxonomic analysis of species of the genera *Mus*, *Apodemus* and *Rattus* in Azerbaijan. *Journal of Zoological Systematics and Evolutionary Research*, **29**(2): 139–153.

Shintaku Y, Kageyama M, Motokawa M. 2012. Morphological variation in external traits of the large Japanese field mouse, *Apodemus speciosus*. *Mammal Study*, **37**(2): 113–126.

Shintaku Y, Motokawa M. 2016. Geographic variation in skull morphology of

the large Japanese field mice, *Apodemus speciosus* (Rodentia: Muridae) revealed by geometric morphometric analysis. *Zoological Science*, **33**(2): 132–145.

Soldatović B, Dulić B, Savić i Desanka Rimsa I. 1969. Chromosomen zweier arten der Gattung *Apodemus* (*A. agrarius* und *A. mystacinus*-Mammalia, Rodentia) aus Jugoslawien. *Arhiv bioloških nauka Beograd*, **21**: 27–32.

Soldatović B, Savić I, Seth P, Reichenstein H, Tolksdorf M. 1975. Comparative karyological study of the genus *Apodemus* (Kaup 1829). *Acta Veterinaria*, **25**(1): 1–10.

Sumner AT. 1972. A simple technique for demonstrating centromeric heterochromatin. *Experimental Cell Research*, **75**(1): 304–306.

Suzuki H, Sato JJ, Tsuchiya K, Luo J, Zhang YP, Wang YX, Jiang XL. 2003. Molecular phylogeny of wood mice (*Apodemus*, Muridae) in East Asia. *Biological Journal of the Linnean Society*, **80**(3): 469–481.

Suzuki H, Yasuda SP, Sakaizumi M, Wakana S, Motokawa M, Tsuchiya K. 2004. Differential geographic patterns of mitochondrial DNA variation in two sympatric species of Japanese wood mice, *Apodemus speciosus* and *A. argenteus*. *Genes & Genetic Systems*, **79**(3): 165–176.

Suzuki H, Filippucci MG, Chelomina GN, Sato JJ, Serizawa K, Nevo E. 2008. A biogeographic view of *Apodemus* in Asia and Europe inferred from nuclear and mitochondrial gene sequences. *Biochemical Genetics*, **46**(5–6): 329–346.

Tomozawa M, Suzuki H. 2008. A trend of central versus peripheral structuring in mitochondrial and nuclear gene sequences of the Japanese wood mouse, *Apodemus speciosus*. *Zoological Science*, **25**(3): 273–285.

Tomozawa M, Nunome M, Suzuki H, Ono H. 2014. Effect of founding events on coat colour polymorphism of *Apodemus speciosus* (Rodentia: Muridae) on the Izu Islands. *Biological Journal of the Linnean Society*, **113**(2): 522–535.

Tsuchiya K. 1974. Cytological and biochemical studies of *Apodemus speciosus* group in Japan. *Journal of the Mammalogical Society of Japan*, **6**(2): 67–87. (in Japanese)

Tsuchiya K. 1979. Notes on breeding of wood mouse groups for laboratory animal. *Report of Hokkaido Institute of Public Health*, **29**: 102–106. (in Japanese)

Vujošević M, Rimsa D, Zivcović S. 1984. Patterns of G- and C-bands distribution on chromosomes of three *Apodemus* species. *Zeitschrift für Säugetierkunde*, **49**: 234–238.

Wang JX, Zhao XF, Wang XM. 1993. Studies of chromosome of striped field mouse *Apodemus agrarius pallidior* (Rodentia). *Acta Theriologica Sinica*, **13**(4): 283–287. (in Chinese)

Wang JX, Zhao XF, Qi HY, Koh HS, Zhang L, Guan ZX, Wang CH. 2000. Karyotypes and B chromosomes of *Apodemus peninsulae* (Rodentia, Mammalia). *Acta Theriologica Sinica*, **20**(4): 289–296.

Yiğit N, Verimli R, Sözen M, Çolak E, Özkurt Ş. 2000. The karyotype of *Apodemus agrarius* (Pallas, 1771) (Mammalia: Rodentia) in Turkey. *Zoology in the Middle East*, **20**(1): 21–23.

Yoshida MC, Sasaki M, Oshimura M. 1975. Karyotype and heterochromatin pattern of the field mouse, *Apodemus argenteus* Temminck. *Genetica*, **45**(4): 397–403.

Yue H, Fan ZX, Liu SY, Liu Y, Song ZB, Zhang XY. 2012. A mitogenome of the Chevrier's field mouse (*Apodemus chevrieri*) and genetic variations inferred from the cytochrome *b* gene. *DNA and Cell Biology*, **31**(4): 460–469.

Zhang RZ. 1997. Distribution of Mammalian Species in China. Beijing: China Forestry Publishing House. (in Chinese)

Zima J, Král B. 1984. Karyotypes of European mammals II. *Acta Scientarium Naturalium Academiae Scientiarum Bohemoslovacae Brno*, **18**(8): 1–62.

Species identification of crested gibbons (*Nomascus*) in captivity in China using karyotyping- and PCR-based approaches

Wen-Hui Nie[1,*], Jin-Huan Wang[1], Wei-Ting Su[1], Yu Hu[1], Shui-Wang He[1], Xue-Long Jiang[1,*], Kai He[1,2,*]

[1] *Kunming Institute of Zoology, Chinese Academy of Sciences, Kunming Yunnan* 650223*, China*
[2] *Kyoto University Museum, Kyoto University, Kyoto* 606-8417*, Japan*

ABSTRACT

Gibbons and siamangs (Hylobatidae) are well-known for their rapid chromosomal evolution, which has resulted in high speciation rate within the family. On the other hand, distinct karyotypes do not prevent speciation, allowing interbreeding between individuals in captivity, and the unwanted hybrids are ethically problematic as all gibbon species are endangered or critically endangered. Thus, accurate species identification is crucial for captive breeding, particularly in China where studbooks are unavailable. Identification based on external morphology is difficult, especially for hybrids, because species are usually similar in appearance. In this study, we employed G-banding karyotyping and fluorescence *in situ* hybridization (FISH) as well as a PCR-based approach to examine karyotypic characteristics and identify crested gibbons of the genus *Nomascus* from zoos and nature reserves in China. We characterized and identified five karyotypes from 21 individuals of *Nomascus*. Using karyotypes and mitochondrial and nuclear genes, we identified three purebred species and three hybrids, including one F2 hybrid between *N. gabriellae* and *N. siki*. Our results also supported that *N. leucogenys* and *N. siki* shared the same inversion on chromosome 7, which resolves arguments from previous studies. Our results demonstrated that both karyotyping and DNA-based approaches were suitable for identifying purebred species, though neither was ideal for hybrid identification. The advantages and disadvantages of both approaches are discussed. Our results further highlight the importance of animal ethics and welfare, which are critical for endangered species in captivity.

Keywords: F2 hybrid gibbon; Fluorescence *in situ* hybridization; *Nomascus*; Pericentric inversion; Species identification; Animal welfare

INTRODUCTION

The rates of chromosomal evolution are an order of magnitude higher in Mammalia than in most other classes of vertebrates and are strongly correlated with high speciation rates (Bush et al., 1977). High karyotypic diversity and rapid speciation are often observed in taxa characterized by small effective population sizes, which includes the gibbons and siamangs of the small ape family Hylobatidae (Primate). These animals are endemic to southern China, South Asia, and Southeast Asia, and have been assigned into four genera (*Hoolock*, *Hylobates*, *Nomascus*, and *Symphalangus*; Brandon-Jones et al., 2004; Roos & Geissmann, 2001). While siamangs (*Symphalangus*) possess a unique and large gular sac (throat pouch), gibbons share very similar external morphology, and were long acknowledged as a single genus (*Hylobates*). However, *Hoolock* and *Nomascus* were subsequently recognized as full genera based on karyotypic studies, which revealed a unique diploid number (2*n*) of chromosomes among each genus: *Hoolock* (2*n*=38), *Hylobates* (2*n*=44), *Nomascus* (2*n*=52), and *Symphalangus* (2*n*=50) (Chiarelli, 1972; Prouty et al., 1983; Van Tuinen & Ledbetter, 1983). This subdivision, as supported by molecular phylogenetic studies, occurred in the

Received: 21 November 2017; Accepted: 19 March 2018; Online: 03 April 2018

Foundation items: This study was supported by the Wildlife Conservation Program of Yunnan Province, China. K.H. was supported by a JSPS Postdoctoral Fellowship for Overseas Researchers (P16092).

[*]Corresponding authors, E-mail: whnie@mail.kiz.ac.cn; jiangxl@mail.kiz.ac.cn; hekai@mail.kiz.ac.cn

DOI: 10.24272/j.issn.2095-8137.2018.036

Late Miocene approximately 7 Ma (Fan et al., 2017; Springer et al., 2012). Today, 20 species of gibbons and siamangs are recognized, though the number continues to increase due to newly discovered species (Fan et al., 2017).

Speciation in this family is considerably faster than that observed in many other groups of mammals and is considered to be the result of high frequency of chromosomal rearrangement (Misceo et al., 2008), including compound inversion/translocation (Jauch et al., 1992; Koehler et al., 1995a, 1995b; Marks, 1982; Nie et al., 2001; Stanyon & Chiarelli, 1982, 1983; Van Tuinen & Ledbetter, 1983; Yu et al., 1997). Previous comparison between the gibbon (*N. leucogenys*) and human genomes revealed 100 synteny breakpoints, which can facilitate chromosome breakage and rearrangement (Carbone et al., 2006). Gibbons exhibit highly structured society in their populations, which may promote chromosome rearrangement fixation, thereby allowing rapid speciation (Wilson et al., 1975).

The crested gibbon genus *Nomascus* comprises seven recognized species, including *N. concolor* (western black-crested gibbon), *N. gabriellae* (yellow-cheeked gibbon), *N. hainanus* (Hainan gibbon), *N. leucogenys* (northern white-cheeked gibbon), *N. nasutus* (eastern black-crested gibbon), *N. siki* (southern white-cheeked gibbon) (Brandon-Jones et al., 2004; Roos & Geissmann, 2001), and the recently discovered *N. annamensis* (northern buffed-cheeked gibbon) (Thinh et al., 2010). These species are characterized by a variety of morphological, anatomical, karyological, and vocal features (Couturier & Lernould, 1991; Garza & Woodruff, 1994; Schilling, 1984; Thinh et al., 2011).

Although all studied *Nomascus* species have a unique diploid number of 52 (Couturier et al., 1982; Dutrillaux et al., 1975; Van Tuinen & Ledbetter, 1983), they also exhibit considerable interspecific karyotypic variation. Using the R-banding technique, Couturier & Lernould (1991) distinguished the karyotypes for six individuals of *N. leucogenys*, two *N. siki*, three *N. gabriellae*, and several hybrids using a combination of an inversion on chromosome 7 and a translocation between chromosomes 1 and 22. The inversion on chromosome 7 was also confirmed based on the number of hybridization signals provided by human chromosome probes 4 and 22. On unrearranged chromosome 7, one hybridization signal of probe 4 on 7q and one signal of probe 22 on 7p were detected. On rearranged chromosome 7, two signals of each probe were detected, one on each arm of the chromosomes (Koehler et al., 1995b). Heterozygous translocation t (1; 22) has also been identified in hybrids of *N. leucogenys* and *N. gabriellae* (Couturier et al., 1982; Turleau et al., 1983). Using a PCR-based approach, Carbone et al. (2009) detected the inversion on chromosome 7 in *N. leucogenys* but not in *N. siki*. These results disagreed with those of Couturier & Lernould (1991), and thus need to be revisited and clarified using additional samples.

Currently, most gibbon species are endangered or critically endangered. Several species, including *Hylobates lar* and *N. leucogenys*, may have been extirpated from China largely due to poaching. Reintroducing animals from zoos to their original habitat is a goal for conservation but requires accurate identification of purebred animals. Extreme caution must be undertaken in captive breeding as interspecific and intergeneric hybridization can occur between gibbons and siamangs (Hirai et al., 2007; Myers & Shafer, 1979), which do not resulting in reduced fertility among offspring in certain cases (Van Tuinen et al., 1999). Hybrid offspring are difficult to visually identify due to their similar external morphology, with identification using the karyotypic approach considered more reliable. Co-housing of different species has been avoided in many countries and animals are karyotyped for identification, with studbooks maintained as a database for appropriate management. However, this system is not yet well established in China and different species are usually housed together resulting in hybridization and unknown interbreeding history.

In the current study, we examined 21 gibbons using a combination of G-banding karyotyping and fluorescence *in situ* hybridization (FISH). We also sequenced mitochondrial and nuclear fragments across a known inversion breakpoint on chromosome 7 identified in a previous study (Carbone et al., 2009). We examined whether the combination of G-banding and FISH is a reliable approach for species identification. We evaluated the efficiency and accuracy of karyotyping- and PCR-based approaches for the identification of purebred animals and hybrids. We also re-examined whether the pericentric inversion on chromosome 7 is species-specific in *N. leucogenys*.

MATERIALS AND METHODS

Samples

We collected peripheral blood from 20 gibbon individuals raised in Nanning Zoo, Ningbo Zoo, Kunming Zoo, and Huanglianshan National Natural Reserve, and obtained one sample (No.14 in Table 1) of cultured gibbon cells maintained at the Kunming Institute of Zoology, Chinese Academy of Sciences. Fourteen individuals were female and seven were male. All experimental procedures and animal care were performed according to the protocols approved by the Ethics Committee of the Kunming Institute of Zoology, Chinese Academy of Sciences.

Cell culture, metaphase preparation, and G-banding

Chromosome suspensions were obtained from lymphocyte cultures. Cell culture and metaphase preparations were performed following conventional procedures (Hungerford, 1965). Briefly, whole blood was cultivated in the presence of phytohaemagglutinin in RPMI 1640 medium supplemented with 10% fetal bovine serum. After 68–70 h of growth, colchicine was added to the cell cultures to a final concentration of 0.4–0.8 μg/mL. The cell cultures were incubated for another 2–4 h before harvest. We treated the cells with hypotonic solution (0.075 mol/L KCl) for 20 min, with thrice fixation in 3:1 methanol/glacial acetic acid. Slides were prepared by applying 10 μL of metaphase suspension onto dry and clean slides, which were then allowed to air dry. G-banding was performed following Seabright (1971). All karyotypes were analyzed after G-banding.

FISH, image capture, and processing

We used a biotin-labeled probe of the human 22 chromosome. Fluorescence *in situ* hybridization, detection, image capture, and processing were carried out following Yang et al. (2000) and Nie et al. (2002). We detected fluorescence signals using a layer of Cy3-avidin (1:1 000 dilution; Amersham Pharmacia Biotech, USA). After detection, slides were mounted in Vectashield mounting medium with DAPI (4′6-diamidino-2-phenylindole, Vector Laboratories, USA). Digital images were acquired using a CytoVision system (Applied Imaging Co., USA) with a CCD camera mounted on a Zeiss microscope (Germany). We associated the hybridization signals with specific chromosome regions based on DAPI-banding patterns.

Table 1 Samples used in this study and a summary of karyotypic characteristics including the FISH signals on the chromosome 7, the lengths of chromosomes 1 and 22, the results of PCR using primer sets BP and HSA, as well as the identification results based on each approach

Nick Name	House	FISH (signal on chr. 7) (pairs)	Chr. 1	Chr. 22	Karyotype	BP	HSA	Cyt *b* genes	Final identification
Su-Su	Nanning Zoo	2	Long (Normal)	Short (Normal)	*N. leucogenys*	N/A	N/A	N/A	N/A
Bei-Li	Nanning Zoo	2	Long (Normal)	Short (Normal)	*N. leucogenys*	+	–	*N. leucogenys*	*N. leucogenys*
Gou-Dan	Nanning Zoo	2	Long (Normal)	Short (Normal)	*N. leucogenys*	+	–	*N. leucogenys*	*N. leucogenys*
San-Mei	Nanning Zoo	2	Long (Normal)	Short (Normal)	*N. leucogenys*	N/A	N/A	N/A	N/A
No14	Missing	2	Long (Normal)	Short (Normal)	*N. leucogenys*	+	–	*N.* cf. *leucogenys*	*N.* cf. *leucogenys*
No name	Kunming Zoo	2	Long (Normal)	Short (Normal)	*N. leucogenys*	N/A	N/A	N/A	N/A
NB1	Ningbo Zoo	2	Long (Normal)	Short (Normal)	*N. leucogenys*	N/A	N/A	N/A	N/A
NB2	Ningbo Zoo	2	Long (Normal)	Short (Normal)	*N. leucogenys*	N/A	N/A	N/A	N/A
HLS3	Huanglianshan Nature Reserve	2	Long (Normal)	Short (Normal)	*N. leucogenys*	N/A	N/A	N/A	N/A
HLS4	Huanglianshan Nature Reserve	2	Long (Normal)	Short (Normal)	*N. leucogenys*	N/A	N/A	N/A	N/A
Fang-Fang	Nanning Zoo	2	Short	Long	*N. siki*	N/A	N/A	N/A	N/A
E'gui	Nanning Zoo	2	Short	Long	*N. siki*	+	–	*N. siki*	*N. siki*
Qingguangyan	Nanning Zoo	2	Short	Long	*N. siki*	N/A	N/A	N/A	N/A
Laoer	Nanning Zoo	2	Short	Long	*N. siki*	N/A	N/A	N/A	N/A
Da-Shan	Nanning Zoo	2	Short	Long	***N. siki***	+	–	***N. gabriellae***	*N. siki* ♂ × (*N. siki* ♂ ×*N. gabriellae* ♀) ♀
316	Nanning Zoo	1	Short	Long	*N. gabriellae*	–	+	*N. gabriellae*	*N. gabriellae*
Bai-Shou	Nanning Zoo	1	Short	Long	*N. gabriellae*	–	+	*N. gabriellae*	*N. gabriellae*
Jing-Jing	Nanning Zoo	1	Short	Long	*N. gabriellae*	–	+	*N. gabriellae*	*N. gabriellae*
Mei-Mei	Nanning Zoo	2	1 short, 1 long	1 short, 1 Long	*N. leucogenys*×*N. siki*	+	–	*N. leucogenys*	*N. leucogenys*× *N. siki*
Xiao-Xiao	Nanning Zoo	1 and a half	Short	Long	*N. gabriellae*×*N. siki*	+	+	*N. leucogenys*	*N. gabriellae*× *N. siki*
A-Huang	Nanning Zoo	1 and a half	Short	Long	*N. gabriellae*×*N. siki*	N/A	N/A	N/A	N/A

The karyotype and mitochondrial of Da-Shan suggest different specific affinities. +: The positive result of PCR using primer set BP or HAS. –: The negative result of PCR using primer set BP or HAS. N/A: Not available.

Amplification, sequencing, and species identification

After karyotyping, we extracted total DNA from the cultured cells using a commercial DNA extraction kit (Blood & Cell Culture DNA Mini Kit, Qiagen, Germany). The DNA extracted from 10 samples was considered acceptable for subsequent analyses as other samples were not well preserved after karyotyping. We amplified and sequenced cyt *b* genes using the primer pair L14724_hk3 (5′-GGACTTATGACATGAAAAATCATCGTTG-3′) and H15915_hk3 (5′-GATTCCCCATTTCTGGTTTACAAGAC-3′). We also conducted PCR using the primers provided in Carbone et al. (2009) (263C9_BP_L with 263C9_BP_R (BP hereafter) and 263C9_BP_L with 263C9_HSA22_R (HSA hereafter)), targeting a fragment across a breakpoint on chromosome 7. According to Carbone et al. (2009), HSA primers should amplify a fragment across a breakpoint in species without an inversion (e.g., *Hylobates* spp., *N. gabriellae*, and *N. siki*), and BP primers should result in positive amplification only for *N. leucogenys*. The mitochondrial and nuclear amplicons were sequenced using a ABI 3730 sequencer (Applied Biosystems, USA).

We identified species based on the karyotyping and sequencing results using the following strategy: (1) we identified the species based on its karyotype; (2) we verified the karyotyping results using PCR with primer sets BP and HSA; (3) we BLAST each cyt *b* gene against the GenBank nucleotide database; (4) we estimated a gene tree to verify the BLAST results using our cyt *b* genes accompanied by a set of sequences representing the recognized *Nomascus* species downloaded from GenBank; and (5) we repeated the karyotyping and amplification/sequencing in triplicate in cases where the mitochondrial, nuclear sequencing, and karyotyping results conflicted (e.g., sample Da-Shan, see Results and Discussion). A final purebred or hybrid and species identification was determined.

We constructed the maximum likelihood gene tree using RAxML v8.2.10 and the CIPRES Science Gateway (Stamatakis, 2014). In addition to the obtained cyt *b* sequences, 17 cyt *b* sequences representing seven recognized species were downloaded from GenBank (Supplementary Table S1) and aligned with our sequences using MAFFT v7.3 (Katoh & Standley, 2014). We partitioned the alignments by codon positions (three partitions). We used GTR+G as the evolutionary model for each partition as RAxML does not accept models other than GTR or GTR+G. We ran each analysis using the rapid bootstrapping algorithm and let RAxML halt bootstrapping automatically.

RESULTS

Identified karyotypic species

The diploid number (2*n*) of all analyzed gibbons was 52. G-banding revealed different lengths of chromosomes 1 and 22, and FISH revealed two, three, or four fluorescence signals on chromosome 7 (Figure 1). Considering the G-banded karyotyping and FISH results, we recognized five karyotypes representing three karyotypic species and two hybrids, with the latter two distinguished by nonhomologous pairing.

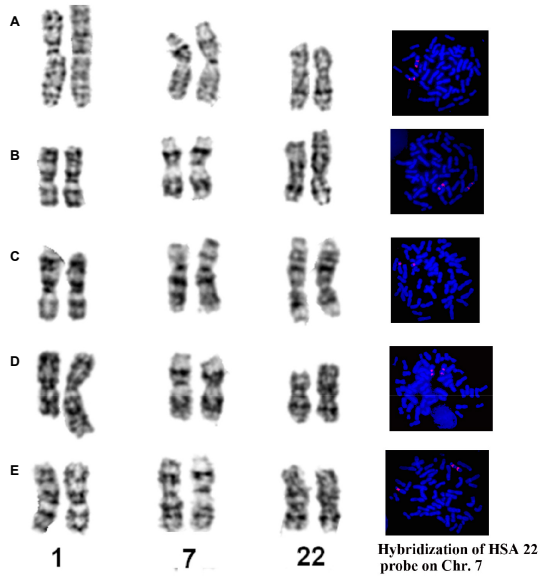

Figure 1 Comparison of G-banded chromosomes 1, 7, and 22 and FISH results with human 22 chromosome-specific probe in different Nomascus species and their hybrids

A: *Nomascus leucogenys*; B: *Nomascus siki*; C: *Nomascus gabriellae*; D: hybrid of *N. leucogenys*×*N. siki*; E: hybrid of *N. gabriellae*×*N. siki*.

Nomascus leucogenys (Figure 2)

The G-banded karyotypes of 10 individuals (7♀, 3♂) were similar to the G-banded (Van Tuinen & Ledbetter, 1983) and R-banded karyotypes for *N. leucogenys* (Couturier & Lernould, 1991). Chromosomes 1 and 22 were normal. Two pairs of FISH signals were found on chromosome 7, supporting a pericentric inversion event (Figure 1A).

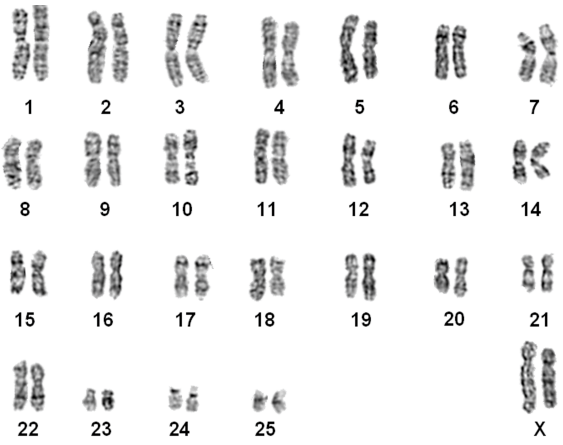

Figure 2 G-banded karyotype of a northern white-cheeked gibbon (*N. leucogenys*)

Nomascus siki (Figure 3)

The karyotypes of five samples (3♀, 2♂) were identical to those of *N. siki* reported by Couturier & Lernould (1991).

Compared with *N. leucogenys*, a balanced translocation between chromosome pairs 1 and 22 was detected, resulting in one pair of shortened chromosome 1 and one pair of derived chromosome 22 (t (1; 22)). Similar to that observed in *N. leucogenys*, FISH demonstrated a pericentric inversion event on chromosome 7 (Figure 1B). The sample "Da-Shan" had a typical siki-karyotype.

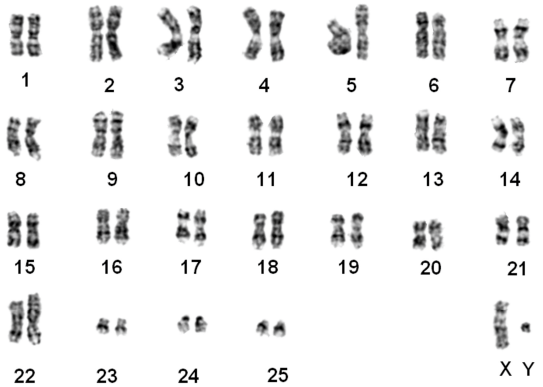

Figure 3 G-banded karyotype of a southern white-cheeked gibbon (*N. siki*)

***Nomascus gabriellae* (Figure 4)**

The G-banded karyotypes of three animals (1♀, 2♂) were the same as that of *N. gabriellae* (Couturier & Lernould, 1991). This karyotype was similar to *N. siki* in the presence of t (1; 22). Only one pair of FISH signals were observed on chromosome 7, thus differing from *N. siki* and *N. leucogenys* (Figure 1C).

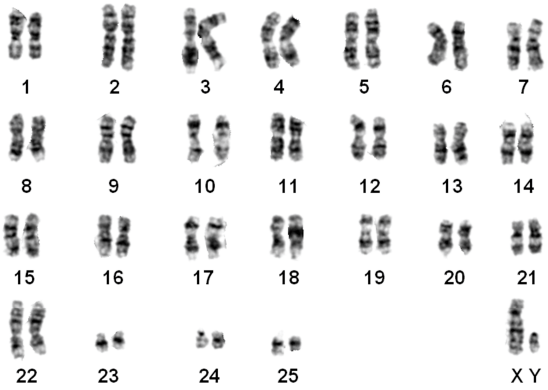

Figure 4 G-banded karyotype of a yellow-cheeked gibbon (*N. gabriellae*)

***Nomascus leucogenys*×*Nomascus* siki hybrid (Figure 5)**

The G-banded karyotype of one specimen was unique, characterized by a heterozygous translocation. One chromosome 1 and 22 were normal, similar to that of *N. leucogenys*, and the other chromosome 1 and 22 were similar to that of *N. siki*, indicating one translocation t (1; 22). Two pairs of FISH signals were observed on chromosome 7, indicating a pericentric inversion event (Figure 1D). This specimen was identified as a hybrid of *N. leucogenys*×*N. siki*.

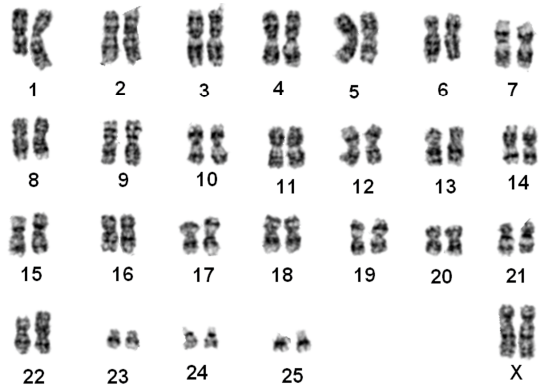

Figure 5 G-banded karyotype of a *N. leucogenys*×*N. siki* hybrid

***Nomascus gabriellae*×*Nomascus siki* hybrid (Figure 6)**

The distinct G-banded karyotype of two individuals was similar to that of *N. siki* and *N. gabriellae* in the presence of t (1; 22). FISH detected three fluorescence signals on chromosome 7, indicating heterozygous pericentric inversion (Figure 1E). These two individuals were identified as hybrids of *N. gabriellae*×*N. siki*.

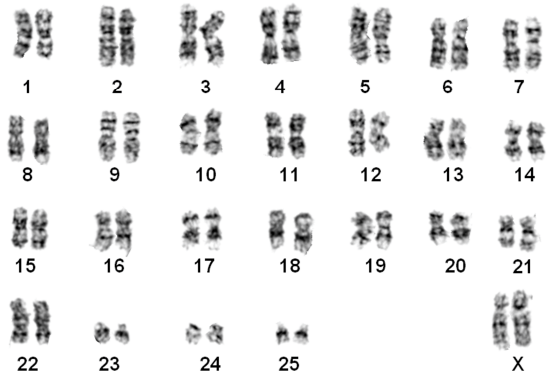

Figure 6 G-banded karyotype of a *N. leucogenys*×*N. siki* hybrid

Mitochondrial and nuclear sequences

We determined the complete cyt *b* sequences for 10 individuals representing the three purebred species (*n*=7) and two hybrids (*n*=3) identified in the karyotypic analyses. All new sequences are available in GenBank under accession Nos. MH188408–MH188428 (Supplementary Table S1). Five out of the seven purebred animals were supported by BLAST and phylogenetic analyses using the cyt *b* gene and the other two were not (Figure 7). One sample (Da-Shan) was identified as *N. siki* based on its karyotype, but its mitochondrial gene was typical of *N. gabriellae*, which also supported by our phylogenetic analyses (bootstrap value (BS)=98). Sample

14 was identified as *N. leucogenys* based on its karyotype but could not be identified unambiguously as it was equally similar to *N. leucogenys* and *N. siki*. It was closely related to (BS=84) and formed a sister lineage of these two species on the phylogenetic tree (BS=52). The cyt *b* genes of the two hybrids identified in the karyotypic analyses (Xiao-Xiao and Mei-Mei) corresponded to one of their parental species (BS≥88). On our cyt *b* genetic tree (Figure 7), sample 14 was a close relative to (BS=84) and formed a sister lineage with *N. siki*+*N. leucogenys* (BS=52).

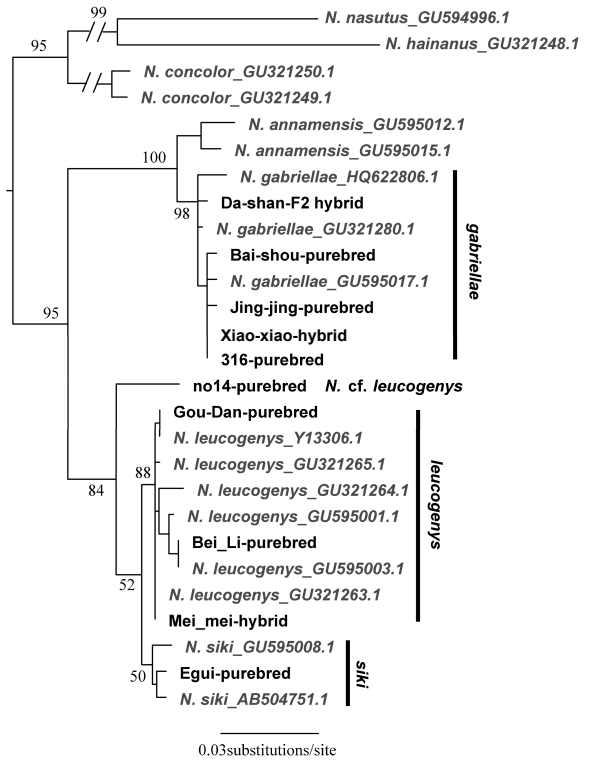

Figure 7 Maximum-likelihood gene tree estimated using the cyt *b* genes of *Nomascus* species

Branch lengths correspond to substitution rates. Numbers on branches are bootstrap values. Sequences downloaded from GenBank are in gray and GenBank accession Nos. are shown.

The PCR results using the HSA and BP primer sets were concordant with the karyotypic results. The PCR results using the BP primers (confirming the inversion) were positive for purebred *N. leucogenys*, *N. siki*, and the *N. leucogenys*×*N. siki* hybrid (Mei-Mei) and were negative when using the HSA primers for these samples (Table 1). The PCR results using the BP primers were negative for purebred *N. gabriellae* but positive when using the HSA primers. For the hybrid identified as *N. gabriellae*×*N. siki* (Xiao-Xiao), PCR and sequencing were successful using both BP and HSA primers. For Da-Shan, the PCR results were positive using BP primers and negative using HSA primers, which were congruent with its karyotype (*siki* type) but disagreed with its mitochondrial gene results.

Because the karyotype and PCR results were congruent, we assigned seven samples as purebred species and identified another two as hybrids. One sample (14) was identified as *N.* cf. *leucogenys* as it did not cluster with the other *N. leucogenys* sequences downloaded from GenBank. We considered Da-Shan as an F2 hybrid of *N. gabriellae* and *N. siki* due to the inconsistent patterns revealed by karyotyping and PCR using the HSA and BP primers (*siki*), and the mitochondrial phylogeny (*gabriellae*) (Table 1).

DISCUSSION

We used karyotypic- and PCR-based approaches to examine the affinities of *Nomascus* species characterized by high karyotypic diversity. We determined the specific karyotypes of each species as well as the existence of an inversion on chromosome 7 in *N. siki* and *N. leucogenys*. We also revealed the definitive existence of hybrids in zoos in China, which calls attention to the animal ethics and welfare issues related to endangered species breeding in captivity. Using the *Nomascus* species as our focal taxa, we evaluated the accuracy and efficiency of both approaches in identifying purebred and hybrid species.

Our results supported that *N. gabriellae*, *N. leucogenys*, and *N. siki* are distinguishable based on translocation t (1; 22) and inversion on chromosome 7 (Figures 1–5), even though *N. leucogenys* and *N. siki* diverged from each other only recently. Couturier & Lernould (1991) revealed that *N. hainanus* does not have an inversion on chromosome 7 or translocation t (1; 22), and therefore has a distinct karyotype. It would be interesting to examine the G-banded karyotypes and FISH results of *N. concolor* as well as *N. annamensis*, which is sister to *N. gabriellae* and recognized only recently (Thinh et al., 2010). Due to interspecific karyotypic variation, hybrids can be easily distinguished based on heterozygous R-, G-banded karyotypes and FISH results (Couturier & Lernould, 1991; this study). In wild populations, hybridization of *Hylobates* species such as *H. lar*×*H. pileatus*, *H. lar*×*H. agilis*, and *H. muelleri*×*H. agilis*/*H. albibarbis* has been observed (Brockelman & Gittins, 1984). Hybridization between *Nomascus* species in the wild has not been reported, which is likely due to their allopatric distribution. However, we observed heterozygous karyotypes in captive *Nomascus* animals, congruent with previous study (Couturier & Lernould, 1991). Our results support the possibility of nonhomologous pairing during meiophase (Figures 5,6), which is an interesting characteristic in Hylobatidae. Because gibbons have very strong social structures and usually live in small family groups, such nonhomologous pairing may be easily fixed during evolutionary histories and further promote diversification and speciation, resulting in high species diversity within the family.

Our FISH and DNA analyses supported the existence of an inversion on chromosome 7 in both *N. leucogenys* and *N. siki* (Figures 1–3), consistent with the findings of Couturier & Lernould (1991), though not supported by Carbone et al. (2009). The negative results obtained in the latter study may

be due to the hair sample used to represent *N. siki*, which is known for low DNA quantity as well as the existence of PCR inhibitors.

The phylogenetic position of sample 14 was an interesting finding. Its karyotype was identical to the other *N. leucogenys* samples (Table 1), which was not supported by the mitochondrial gene tree (Figure 7). We repeated amplification and sequencing three times for this sample. The sequences were identical, indicating no cross-sample contamination, and no premature codon was observed, indicating it was not a pseudogene. There are two hypothetical scenarios that may explain these results. One is incomplete lineage sorting between *N. leucogenys* and *N. siki*, resulting in non-monophyletic relationships. This situation has never been observed because the effective population sizes of gibbon species are usually small. Alternatively, this sample might represent a distinct and unknown taxon, which is a close relative but not identical to *N. leucogenys* or *N. siki*. The sample was obtained from the Kunming Institute of Zoology, Chinese Academy of Sciences, in 1993 and the information on the animal was not recorded in detail. Unfortunately, neither hypothesis could be supported or rejected in the current study.

Similar to previous studies, our study supported that hybridization has occurred in captivity. However, fertility may be less impacted as identification of Da-Shan showed it to be a likely F2 hybrid of *N. gabriellae* and *N. siki*, despite there being no available studbook. This is the first record of a cross-back F2 hybrid in *Nomascus* as most other countries have well-established systems in place to prevent interbreeding of gibbons in captivity, with many animals also previously karyotyped. Continuous interbreeding and production of fertile offspring may spread across zoos in China because there are only limited numbers of gibbons in zoos, and correct species identification of their offspring will become far more difficult after several generations and recombination. Our findings call for the introduction of a system to prevent gibbon interbreeding in captivity and for better welfare and awareness of these animals.

The R-banding technique can distinguish different karyotypes of *Nomascus* species (Couturier & Lernould, 1991), but is both difficult and time-consuming. Herein, we demonstrated that G-banding in combination with FISH is a reliable approach for identifying karyotypic characteristics. This approach was also appropriate for species identification, though it was limited in identifying cross-back hybrid F2 individuals and did not recognize Da-Shan as a hybrid (Table 1). As per Carbone et al. (2009), we agree that PCR and sequencing can be applicable for examining chromosome inversion and species identification. This approach does not require high quality cultured cells or karyotyping techniques and is applicable for DNA samples with low quality and/or low yield, which certainly include, but are not limited to saliva, urine, hair, and feces. The known limitation is that accurate identification of hybrids relies on a finely established system with known karyotypes, breakpoints, and primers. In our case, it easily distinguished *N. leucogenys*/*N. siki* from *N. gabriellae*, but could not easily distinguish *N. leucogenys*/*N. siki* from the hybrid of *N. leucogenys*×*N. siki*.

COMPETING INTERESTS

The authors declare that they have no competing interests.

AUTHORS' CONTRIBUTIONS

W.H.N., K.H. and X.L.J. conceived of the experiments. J.H.W., W.T.S. and Y.H. cultured the cells, prepared the chromosomal suspensions and performed G-banding and chromosome-painting experiments. S.W.H. completed all molecular experiments. W.H.N., K.H. and X.L.J. analyzed the data, wrote and revised the paper. All of the authors read and approved the final manuscript.

ACKNOWLEDGEMENTS

We are grateful to the Directors of Nanning Zoo, Ningbo Zoo, Kunming Zoo, and Huanglianshan National Nature Reserve for allowing us to sample blood from the gibbons for this study.

REFERENCES

Brandon-Jones D, Eudey AA, Geissmann T, Groves CP, Melnick DJ, Morales JC, Shekelle M, Stewart CB. 2004. Asian primate classification. *International Journal of Primatology,* **25**(1): 97–164.

Brockelman WY, Gittins SP. 1984. Natural hybridization in the *Hylobates lar* species group: implications for speciation in gibbons. *In*: Preuschoft H, Chivers DJ, Brockelman WY, Creel N. The Lesser Apes: Evolutionary and Behavioural Biology. Edinburgh: Edinburgh University Press, 498–532.

Bush GL, Case SM, Wilson AC, Patton JL. 1977. Rapid speciation and chromosomal evolution in mammals. *Proceedings of the National Academy of Sciences of the United States of America,* **74**(9): 3942–3946.

Carbone L, Vessere GM, Ten Hallers BFH, Zhu BL, Osoegawa K, Mootnick A, Kofler A, Wienberg J, Rogers J, Humphray S, Scott C, Harris RA, Milosavljevic A, De Jong PJ. 2006. A high-resolution map of synteny disruptions in gibbon and human genomes. *PLoS Genetics,* **2**(12): e223.

Carbone L, Mootnick AR, Nadler T, Moisson P, Ryder O, Roos C, De Jong PJ. 2009. A chromosomal inversion unique to the northern white-cheeked gibbon. *PLoS One,* **4**(3): e4999.

Chiarelli B. 1972. The karyotypes of the gibbons. *In*: Rumbaugh DM. Gibbon and Siamang. Basel: Karger, 90–102.

Couturier J, Dutrillaux B, Turleau C, De Grouchy J. 1982. Comparaisons chromosomiques chez quatre especes ou sous-especes de gibbons. *Annales de Genetique,* **25**(1): 5–10.

Couturier J, Lernould JM. 1991. Karyotypic study of four gibbon forms provisionally considered as subspecies of *Hylobates* (*Nomascus*) *concolor* (Primates, Hylobatidae). *Folia Primatologica,* **56**(2): 95–104.

Dutrillaux B, Rethoré MO, Aurias A, Goustard M. 1975. Analysis of the karyotype of two species of gibbons (*Hylobates lar* and *H. concolor*) by various banding techniques. *Cytogenetic and Genome Research,* **15**(2): 81–91.

Fan PF, He K, Chen X, Ortiz A, Zhang B, Zhao C, Li YQ, Zhang HB, Kimock C, Wang WZ, Groves C, Turvey ST, Roos C, Helgen KM, Jiang XL. 2017. Description of a new species of Hoolock gibbon (Primates: Hylobatidae)

based on integrative taxonomy. *American Journal of Primatology,* **79**(5): e22631.

Garza JC, Woodruff DS. 1994. Crested gibbon (*Hylobates* (*Nomascus*)) identification using noninvasively obtained DNA. *Zoo Biology,* **13**(4): 383–387.

Hirai H, Hirai Y, Domae H, Kirihara Y. 2007. A most distant intergeneric hybrid offspring (Larcon) of lesser apes, *Nomascus leucogenys* and *Hylobates lar*. *Human Genetics,* **122**(5): 477–483.

Hungerford DA. 1965. Leukocytes cultured from small inocula of whole blood and the preparation of metaphase chromosomes by treatment with hypotonic KCl. *Stain Technology,* **40**(6): 333–338.

Jauch A, Wienberg J, Stanyon R, Arnold N, Tofanelli S, Ishida T, Cremer T. 1992. Reconstruction of genomic rearrangements in great apes and gibbons by chromosome painting. *Proceedings of the National Academy of Sciences of the United States of America,* **89**(18): 8611–8615.

Katoh K, Standley DM. 2014. MAFFT: iterative refinement and additional methods. *In*: Russell DJ. Multiple Sequence Alignment Methods. Totowa, NJ: Humana Press, **1079**: 131–146.

Koehler U, Arnold N, Wienberg J, Tofanelli S, Stanyon R. 1995a. Genomic reorganization and disrupted chromosomal synteny in the siamang (*Hylobates syndactylus*) revealed by fluorescence *in situ* hybridization. *American Journal of Physical Anthropology,* **97**(1): 37–47.

Koehler U, Bigoni F, Wienberg J, Stanyon R. 1995b. Genomic reorganization in the concolor gibbon (*Hylobates concolor*) revealed by chromosome painting. *Genomics,* **30**(2): 287–292.

Marks J. 1982. Evolutionary tempo and phylogenetic inference based on primate karyotypes. *Cytogenetics and Genome Research,* **34**(3): 261–264.

Misceo D, Capozzi O, Roberto R, Dell'Oglio MP, Rocchi M, Stanyon R, Archidiacono N. 2008. Tracking the complex flow of chromosome rearrangements from the Hominoidea Ancestor to extant *Hylobates* and *Nomascus* Gibbons by high-resolution synteny mapping. *Genome Research,* **18**(9): 1530–1537.

Myers RH, Shafer DA. 1979. Hybrid ape offspring of a mating of gibbon and siamang. *Science,* **205**(4403): 308–310.

Nie WH, Rens W, Wang JH, Yang FT. 2001. Conserved chromosome segments in *Hylobates hoolock* revealed by human and *H. leucogenys* paint probes. *Cytogenetics and Genome Research,* **92**(3–4): 248–253.

Nie WH, Wang JH, O'Brien PCM, Fu BY, Ying T, Ferguson-Smith MA, Yang FT. 2002. The genome phylogeny of domestic cat, red panda and five mustelid species revealed by comparative chromosome painting and G-banding. *Chromosome Research,* **10**(3): 209–222.

Prouty LA, Buchanan PD, Pollitzer WS, Mootnick AR. 1983. A presumptive new hylobatid subgenus with 38 chromosomes. *Cytogenetics and Genome Research,* **35**(2): 141–142.

Roos C, Geissmann T. 2001. Molecular phylogeny of the major hylobatid divisions. *Molecular Phylogenetics and Evolution,* **19**(3): 486–494.

Schilling D. 1984. Song bouts and duetting in the concolor gibbon. *In*: Preuschoft H, Chivers DJ, Brockelman WY, Creel N. The Lesser Apes: Evolutionary and Behavioural Biology. Edinburgh: Edinburgh University Press, 390–403.

Seabright M. 1971. A rapid banding technique for human chromosomes. *The Lancet,* **298**(7731): 971–972.

Springer MS, Meredith RW, Gatesy J, Emerling CA, Park J, Rabosky DL, Stadler T, Steiner C, Ryder OA, Janečka JE, Fisher CA, Murphy WJ. 2012. Macroevolutionary dynamics and historical biogeography of primate diversification inferred from a species supermatrix. *PLoS One,* **7**(11): e49521.

Stamatakis A. 2014. RAxML version 8: a tool for phylogenetic analysis and post-analysis of large phylogenies. *Bioinformatics,* **30**(9): 1312–1313.

Stanyon R, Chiarelli B. 1982. Phylogeny of the Hominoidea: the chromosome evidence. *Journal of Human Evolution,* **11**(6): 493–504.

Stanyon R, Chiarelli B. 1983. Mode and tempo in primate chromosome evolution: implications for hylobatid phylogeny. *Journal of Human Evolution,* **12**(3): 305–315.

Thinh VN, Mootnick AR, Thanh VN, Nadler T, Roos C. 2010. A new species of crested gibbon, from the central Annamite mountain range. *Vietnamese Journal of Primatology,* **4**(1): 1–12.

Thinh VN, Hallam C, Roos C, Hammerschmidt K. 2011. Concordance between vocal and genetic diversity in crested gibbons. *BMC Evolutionary Biology,* **11**: 36.

Turleau C, Créau-Goldberg N, Cochet C, De Grouchy J. 1983. Gene mapping of the gibbon. Its position in primate evolution. *Human Genetics,* **64**(1): 65–72.

Van Tuinen P, Ledbetter DH. 1983. Cytogenetic comparison and phylogeny of three Species of hylobatidae. *American Journal of Physical Anthropology,* **61**(4): 453–466.

Van Tuinen P, Mootnick AR, Kingswood SC, Hale DW, Kumamoto AT. 1999. Complex, compound inversion/translocation polymorphism in an ape: presumptive intermediate stage in the karyotypic evolution of the agile gibbon *Hylobates agilis*. *American Journal of Physical Anthropology,* **110**(2): 129–142.

Wilson AC, Bush GL, Case SM, King MC. 1975. Social structuring of mammalian populations and rate of chromosomal evolution. *Proceedings of the National Academy of Sciences of the United States of America,* **72**(12): 5061–5065.

Yang FT, Graphodatsky AS, O'Brien PCM, Colabella A, Solanky N, Squire M, Sargan DR, Ferguson-Smith MA. 2000. Reciprocal chromosome painting illuminates the history of genome evolution of the domestic cat, dog and human. *Chromosome Research,* **8**(5): 393–404.

Yu DH, Yang FT, Liu RQ. 1997. A comparative chromosome map between human and *Hylobates hoolock* built by chromosome painting. *Acta Genetica Sinica,* **24**(5): 417–423. (in Chinese)

Impacts of late Quaternary environmental change on the long-tailed ground squirrel (*Urocitellus undulatus*) in Mongolia

Bryan S. McLean[1,*], Batsaikhan Nyamsuren[2], Andrey Tchabovsky[3], Joseph A. Cook[4]

[1] *University of Florida, Florida Museum of Natural History, Gainesville, FL* 32611*, USA*
[2] *Department of Biology, School of Arts and Sciences, National University of Mongolia, Ulaan Baatar* 11000*, Mongolia*
[3] *Laboratory of Population Ecology, A.N. Severtsov Institute of Ecology and Evolution, Moscow* 119071*, Russia*
[4] *University of New Mexico, Department of Biology and Museum of Southwestern Biology, Albuquerque, NM* 87131*, USA*

ABSTRACT

Impacts of Quaternary environmental changes on mammal faunas of central Asia remain poorly understood due to a lack of comprehensive phylogeographic sampling for most species. To help address this knowledge gap, we conducted the most extensive molecular analysis to date of the long-tailed ground squirrel (*Urocitellus undulatus* Pallas 1778) in Mongolia, a country that comprises the southern core of this species' range. Drawing on material from recent collaborative field expeditions, we genotyped 128 individuals at two mitochondrial genes (cytochrome *b* and cytochrome oxidase I; 1 797 bp total). Phylogenetic inference supports the existence of two deeply divergent infraspecific lineages (corresponding to subspecies *U. u. undulatus* and *U. u. eversmanni*), a result in agreement with previous molecular investigations but discordant with patterns of range-wide craniometric and external phenotypic variation. In the widespread western *eversmanni* lineage, we recovered geographically-associated clades from the: (a) Khangai, (b) Mongolian Altai, and (c) Govi Altai mountain ranges. Phylogeographic structure in *U. u. eversmanni* is consistent with an isolation-by- distance model; however, genetic distances are significantly lower than among subspecies, and intra-clade relationships are largely unresolved. The latter patterns, as well as the relatively higher nucleotide polymorphism of populations from the Great Lakes Depression of northwestern Mongolia, suggest a history of range shifts into these lowland areas in response to Pleistocene glaciation and environmental change, followed by upslope movements and mitochondrial lineage sorting with Holocene aridification. Our study illuminates possible historical mechanisms responsible for *U. undulatus* genetic structure and contributes to a framework for ongoing exploration of mammalian response to past and present climate change in central Asia.

Keywords: Central Asia; Gobi Desert; Great Lakes Depression; Mongolia; Phylogeography

INTRODUCTION

Urocitellus undulatus Pallas 1778 is a charismatic, medium-bodied ground-dwelling sciurid distributed across central Asia, including portions of Siberia, Mongolia, northwestern China, and easternmost Kazakhstan and Kyrgyzstan (Helgen et al., 2009; Kryštufek & Vohralík, 2013; Ognev, 1947; Wilson & Reeder, 2005). Although the genus

Received: 06 September 2017; Accepted: 02 January 2018; Online: 08 March 2018

Foundation items: Expeditions were funded primarily by grants from the National Science Foundation (USA; DBI-9411976 supplement (1999), DEB-0717214 (2009-2012), DEB-1258010 (2015-2016)). B.S.M. was partially supported by a Peter Buck Predoctoral Fellowship during the 2015 Mongolian expedition. Data generation and analysis herein was supported by the National Science Foundation (DEB-1258010) and the American Society of Mammalogists (ASM Fellowship to B.S.M.)

[*]Corresponding author, E-mail: bryansmclean@gmail.com

DOI: 10.24272/j.issn.2095-8137.2018.042

Urocitellus (comprised of 12 species formerly subsumed within *Spermophilus*; Helgen et al., 2009) is distributed across much of the Holarctic region, *U. undulatus* is the only exclusively Palearctic species in this clade (Wilson & Reeder, 2005; McLean et al., 2016b). To date, various single- and multilocus investigations (Tsvirka et al., 2008; Ermakov et al., 2015; McLean et al., 2016b; Simonov et al., 2017) have revealed that *U. undulatus* is comprised of two deeply divergent lineages recognizable as well-defined subspecies (Kryštufek & Vohralík, 2013) or semi-species (Pavlinov & Lissovsky, 2012). These are an eastern lineage (*undulatus*) in western and central Siberia, northern Mongolia, and the Amur region of southeastern Siberia, and a western lineage (*eversmanni*) in western Mongolia, northern China, and Kazakhstan. However, our understanding of the full diversity and evolutionary and biogeographic history of this species across its vast range remains incomplete.

Although *U. undulatus* has been the subject of persistent morphological and molecular focus over the past three decades (Ermakov et al., 2015; Linetskaya & Linetskii, 1989; McLean et al., 2016b; Simonov et al., 2017; Tsvirka et al., 2008; Vorontsov et al., 1980), more expansive genetic datasets are necessary to test existing taxonomic hypotheses and illuminate the historical demography and biogeography of this species. Unfortunately, however, a lack of spatially comprehensive sampling and associated genetic data exists for this and many other central Asian vertebrate taxa. This data gap precludes identification of the broader abiotic and biotic processes acting to shape phylogeographic patterns and vertebrate community structure across this expansive region. For taxa with relatively high morphological conservatism (such as *Urocitellus*), such datasets are particularly crucial to refine our understanding of the true genomic and biogeographic histories of lineages.

The most significant lack of phylogeographic sampling from *U. undulatus* is in Mongolia, a country that nevertheless comprises the southern core of this species range. Several pressing evolutionary and biogeographical questions hinge on improved genetic sampling of Mongolian populations. First, although each of the subspecific lineages of *U. undulatus* (*undulatus* and *eversmanni*) is documented within the country, what are their exact geographic distributions? Second, do any populations in Mongolia display patterns of mixed mtDNA ancestry and, if so, where are these populations located? Third, how have known late Quaternary environmental changes shaped phylogeographic structure within the widespread western lineage (*eversmanni*)? Specifically, this lineage occupies an environmentally and climatically heterogeneous range in Mongolia, including multiple mountain systems (Khangai, Mongolian Altai, Govi Altai) that were subject to late Pleistocene glaciation, downward expansion of permafrost, and other environmental changes.

In this paper, we present the most comprehensive molecular phylogeographic analysis of *U. undulatus* in Mongolia to date. Drawing on material collected during expeditions of the Museum of Southwestern Biology (New Mexico, USA) from 1999–2016, we genotyped samples from across the entire Mongolian range of *U. undulatus* at two mitochondrial genes (cytochrome *b* (cyt *b*) and cytochrome oxidase I (*COI*), 1 797 bp total). We document population genetic variation and structure, and use those data to explore the potential effects of known late Pleistocene environmental changes on genetic patterns. Our work provides new information on the evolutionary and biogeographic history of *U. undulatus* in western Mongolia and lays a foundation for further analyses in this and similarly distributed central Asian mammals.

MATERIALS AND METHODS

Samples and sequencing

Specimens used in this study are housed at the University of New Mexico Museum of Southwestern Biology (MSB). Mongolian samples were collected during joint MSB-National University of Mongolia expeditions in 1999 (Tinnin et al., 2002), 2009–2012 (with University of Kansas and University of Nebraska), and 2015–2016 (with Northern Michigan University). Cumulative efforts of these expeditions include >6 500 cataloged mammal specimens from across major Mongolian vegetative and faunal provinces, many of which are associated with ecto- and endoparasite specimens archived at MSB Division of Parasites or University of Nebraska Manter Lab of Parasitology. All field methods followed guidelines of institutional animal care and use committees as well as the American Society of Mammalogists Guide for Use of Wild Mammals in Research (Sikes et al., 2011), and were focused on collection of “holistic” mammal specimens (e.g., Dunnum & Cook, 2012; McLean et al., 2016a; Yates et al., 1996). Cumulatively, these materials represent an unparalleled resource for establishing Mongolian faunal baselines in an era of ongoing global climate and environmental change.

We selected 128 specimens of *U. undulatus* for sequencing and analysis (Figure 1; Supplementary Table S1; GenBank accession Nos. MG883400–MG883654). The dataset included 119 individuals from 11 different Mongolian aimags (political land designations analogous to provinces or states) as well as putative representatives of both subspecies (as delineated by Kryštufek & Vohralík, 2013). The dataset also included nine individuals of *U. u. undulatus* from Sakha Republic in northern Siberia. We selected sequences of the Columbian ground squirrel (*U. columbianus*) from GenBank as the outgroup for phylogenetic analysis. Frozen tissue samples of all *U. undulatus* individuals (liver, muscle, or dried muscle) were subjected to lysis in a solution of 600 μL tissue lysis buffer and 12–15 μL reconstituted proteinase K (Omega E.Z.N.A. kit; Omega Bio-tek, Inc., USA) for up to 24 hours. Genomic DNA was isolated using a standard salt/ethanol extraction procedure. To reduce the potential for PCR inhibition, all dried muscle samples were processed prior to lysis by removing debris, cutting into sub-centimeter sized pieces, and washing in 100% ethanol for 15 min at room temperature, vortexing several times; these were then washed in STE buffer under refrigeration for 12–16 h. Final extractions were quantified flourometrically using a Qubit Broad Range assay kit (Life Technologies Corp., USA).

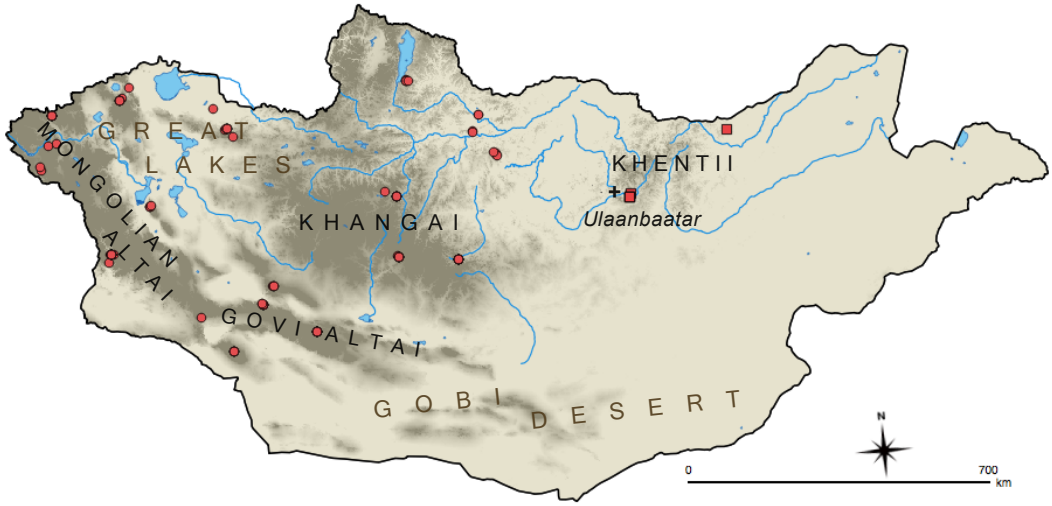

Figure 1 Map of Mongolia showing major landscape features and sampling localities of *U. undulatus*

Higher elevations are shown in darker colors and major mountain ranges and landscape features are indicated with text. Collection localities of samples used in this study indicated by red circles (*U. u. eversmanni*) and squares (*U. u. undulatus*).

We used the primer pair MVZ05/MVZ14 (5′-CGAAGC TTGATATGAAAAACCATCGTTG/CTTGATATGAAAAACCATCG TTG-3′; Smith & Patton, 1993) to amplify all 1 140 bp of the mitochondrial cyt *b* gene. We used the primer pair HCO2198/ LCO1490 (5′-TAAACTTCAGGGTGACCAAAAAATCA/GGTC AACAAATCATAAAGATATTGG-3′; Folmer et al., 1994) to amplify 657 bp of the mitochondrial *COI* gene. Amplification of both mtDNA regions took place in 25 μL reactions, with annealing temperatures of 52 ℃ and 48 ℃, respectively. Purified PCR products were sequenced using Big Dye Terminator 3.1 technology (Applied Biosystems, USA) on an ABI 3130 automated DNA sequencer in the Molecular Biology Facility in the Department of Biology at University of New Mexico. Sequences were manually edited in Sequencher v5.3 (Gene Codes Corp., Michigan, USA) and aligned with MUSCLE v3.7 (Edgar, 2004) using default settings on the CIPRES science gateway (www.phylo.org; Miller et al., 2010).

We used the R packages pegas (Paradis et al., 2017b) and popGenome (Pfeifer et al., 2017) to calculate standard population genetic statistics, and to test for signals of population expansion based on the Tajima's *D* statistic. Partial deletion of positions with missing data was performed when calculating pairwise nucleotide-based metrics (nucleotide diversity and pairwise number of nucleotide differences). We inferred phylogeny for all samples in a Bayesian framework. First, we used PartitionFinder v2.1 (Lanfear et al., 2017) to simultaneously infer the best-fit partitioning scheme and models of sequence evolution for the concatenated mtDNA matrix, as evaluated using the AICc metric. We conducted Bayesian phylogenetic inference in MrBayes v3.2.3 (Ronquist & Huelsenbeck, 2003) on CIPRES, using the optimal partitioning scheme inferred above. Two independent MCMC analyses composed of 4 Metropolis-coupled chains each (the default) were used to estimate posterior distributions of tree topologies, running both analyses for 10 000 000 generations, sampling every 1 000 generations, and discarding the first 25% of samples as burn-in. Convergence of all parameters was assessed in Tracer v1.6.0 (Rambaut et al., 2014) by visualizing trace plots and ensuring effective sample sizes >200.

To characterize population structure in *U. undulatus*, we performed an analysis of molecular variance (AMOVA) of all samples in the R package poppr (Kamvar et al., 2014). For each gene, we included subspecies (*undulatus*, *eversmanni*) and aimag of origin (12 total in our dataset) as factors. We also tested significance of the observed variance patterns with 4 999 randomizations. Because political boundaries may only weakly capture landscape-scale genetic structure, we next tested consistency of our data with an isolation-by-distance (IBD) model, focusing only on *U. u. eversmanni*. For that test, we used functions in the R packages ape (Paradis et al., 2017a) and raster (Hijmans et al., 2017) to compute pairwise genetic (*P*-values) and geographic (in meters) distances, respectively. We calculated correlations between these matrices using the mantel function in vegan (Oksanen et al., 2017) and assessed statistical significance using 4 999 permutations of the geographic distance matrix. Finally, we visualized spatial patterns of mtDNA diversity by computing a minimum-spanning haplotype network (Bandelt et al., 1999) in PopART (http://popart.otago.ac.nz), using just the significantly more variable cyt *b* gene.

RESULTS

The best-fit partitioning scheme for the concatenated mtDNA matrix included a different partition for each codon position within the cyt *b* and *COI* genes (although codon position 2 for both genes shared the same partition; Table 1). The Tamura-Nei (TrN) substitution model or

one of its extensions (TrN with equal base frequencies, gamma-distributed heterogeneity, and/or invariant sites) was preferred for all partitions (Table 1). Phylogenetic inference in MrBayes recovered two major clades (*U. u. undulatus* and *U. u. eversmanni* sensu Kryštufek & Vohralík, 2013) with strong support (PP=1; Figure 2). The average uncorrected genetic distance (mean±*SD*) between these clades is 5.84%±0.19 for cyt *b*, but a more modest 2.67%±0.20 for *COI*. Notably, the maximum inter-clade distance for *COI* (3.16%) is concordant with Ermakov et al.'s (2015) estimate of 3.5% using this same marker but different individuals. For reference, average uncorrected distances between all samples of *U. undulatus* and the two *U. columbianus* outgroups are 8.21%±0.14 and 4.99%±0.16 for cyt *b* and *COI*, respectively. However, we note that *U. undulatus* and *U. columbianus* may not share a most recent common ancestor (McLean et al., 2016b).

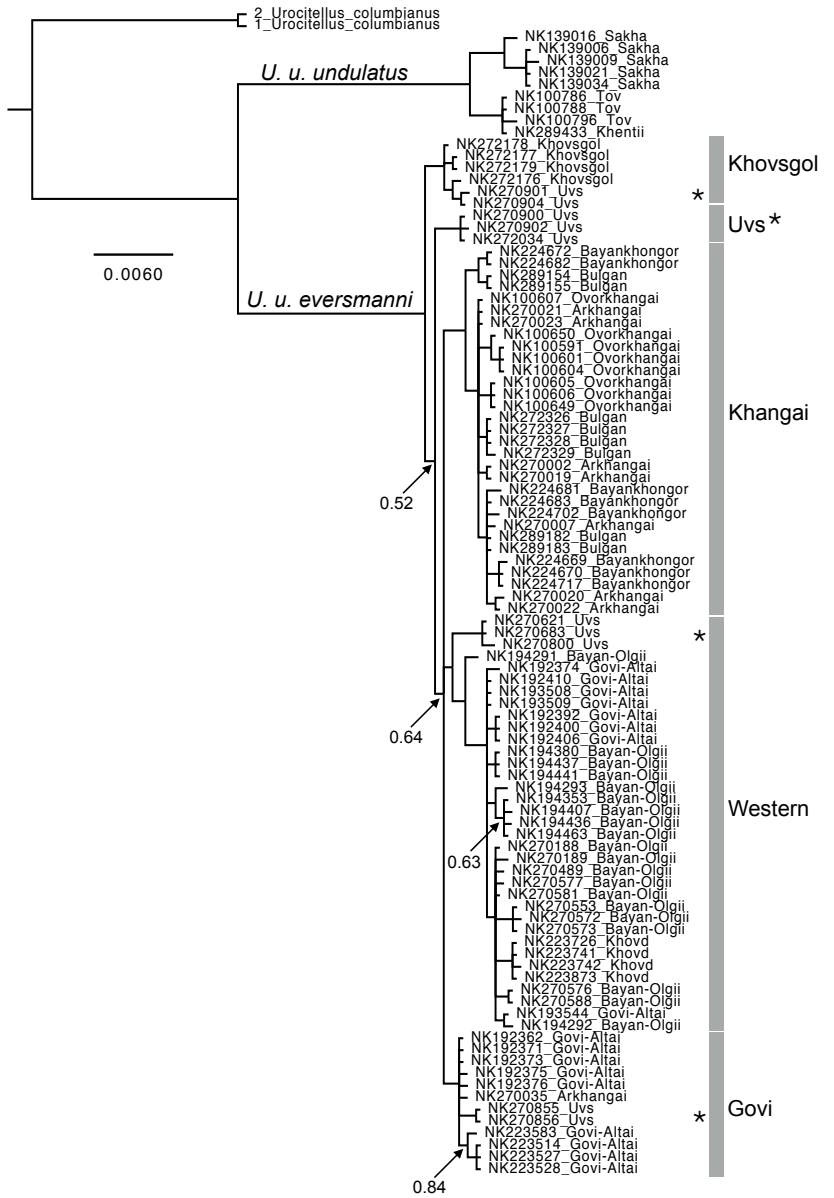

Figure 2 Majority-rule consensus phylogram of *Urocitellus undulatus* based on Bayesian inference in MrBayes

Subspecies and major clades (within *U. u. eversmanni* only) are indicated by text. The tree is rooted on the split from the Nearctic *U. columbianus*. Branches with posterior probabilities less than 0.9 (i.e., between 0.5 and 0.9) are indicated by arrows. Identical cyt *b* haplotypes are represented by a maximum of 3 individuals in the tree; additional duplicate haplotypes were trimmed for clarity (*n*=32). Asterisks denote individuals from Uvs Aimag.

Table 1 Best-fit models of evolution according to the AICc metric for partitions of the concatenated mtDNA matrix

	Model	No. sites
cyt *b* position 1	TrNEF + G	380
cyt *b* position 2 + *COI* position 2	Trn + I	599
cyt *b* position 3	TrN + G	380
COI position 1	TrN	219
COI position 3	TrN	219

Both the genotyping results (Table 2) and phylogenetic inference confirmed hypotheses that the *U. u. eversmanni* lineage is widespread across western Mongolia, occurring in far northern (Khövsgöl), southern (Govi Altai), and westernmost (Bayan-Ölgii) aimags. Conversely, the nominal eastern lineage (*U. u. undulatus*) occupies a more restricted range in the country; individuals taken from as far east as Khövsgöl Aimag, Bulgan Aimag and the southeastern Khangai Mountains maintain evolutionary affinity with the western *U. u. eversmanni* lineage (Figure 2). We found no evidence for mtDNA admixture (i.e., presence of haplotypes from multiple subspecies) in any population surveyed, including those proximate to the apparent phylogeographic break between *undulatus* and *eversmanni*, suggesting a persistent lack of gene flow between these two subspecific lineages.

Within the widespread *U. u. eversmanni* lineage, three geographically-associated subclades are strongly supported in the MrBayes topology, from (1) the Khangai Mountains and surrounding regions ("Khangai" clade); (2) the Mongolian and Govi Altai and surrounding highland regions ("Western" clade); and (3) additional ranges of the Govi Altai ("Govi" clade). Additional, more narrowly distributed genetic clusters were also recovered and include populations from Khövsgöl and Uvs Aimags (Figure 2), although we note that some clades exhibit incomplete lineage sorting. For example, individuals from Uvs Aimag are associated with four distinct genetic clusters or subclades in the Bayesian phylogeny (asterisks in Figure 2). Finer-scale associations with landscape features such as rivers were not evident in our dataset.

Despite the incomplete geographic sorting of mtDNA haplotypes and general lack of fine-scale population patterning, there is detectable phylogeographic structure within Mongolian *U. u. eversmanni*. AMOVAs support a role for broad provincial classifications in mtDNA variation, with 21.7% and 33.9% of molecular variance in cyt *b* and *COI*, respectively, attributable to aimag of origin after accounting for subspecific variation (Table 3). Both values are greater than expected by chance (Table 3). A statistically significant correlation was also found between matrices describing raw genetic distances and raw geographic distances within *U. u. eversmanni* in cyt *b* (r=0.58, P<0.01) and *COI* (r^2=0.38, P<0.01), thereby supporting an isolation-by-distance hypothesis in this subspecies.

Table 2 Population genetic summary statistics for *Urocitellus undulatus eversmanni*, partitioned by gene

n	*H*	*Hd*	*S*	*k*	π
cyt *b* (1 140bp)					
110	47	0.91	67	9.60	8.71×10^{-3}
COI (657bp)					
111	22	0.88	23	2.16	3.29×10^{-3}

n: Number of samples, *H*: Number of haplotypes, *Hd*: Haplotype diversity, *S*: Number of polymorphic sites, *k*: Average number of nucleotide differences, π: Nucleotide diversity.

Table 3 Results of analysis of molecular variance (AMOVA) for both genes and all samples of *Urocitellus undulatus*

	Degrees of freedom	Sum of squared deviations	Variance	Variance relative to expected	*P*
cyt *b*					
Between subspecies	1	2.84	0.05 (8.9)	Greater	0.01
Among aimags	10	15.66	0.12 (21.7)	Greater	0.01
Within aimags	115	42.88	0.37 (69.3)	Less	0.01
Total	126	61.38	0.54 (100)		
COI					
Between subspecies	1	4.25	0.08 (14.9)	Greater	0.01
Among aimags	10	21.33	0.18 (33.9)	Greater	<0.01
Within aimags	116	31.65	0.27 (51.2)	Less	<0.01
Total	127	57.23	0.53 (100)		

Nevertheless, we emphasize that divergences among *U. undulatus* subclades are very low. This can be visualized in the minimum-spanning haplotype network (Figure 3), and is borne out in uncorrected pairwise genetic distances computed within the clade of (mean±*SD*) 0.63%±0.39 for cyt *b* and 0.33%±0.22 for *COI*. Those distances are roughly an order of magnitude lower than between *U. u. eversmanni* and *U. u. undulatus* (Ermakov et al., 2015; this study). They are also lower than those found within *U. u. eversmanni* populations from the adjacent Altai region of southern Russia (Simonov et al., 2017), although the latter study used the noncoding and more variable mtDNA control region. In addition, although there was more variation within than among aimags, AMOVAs suggest that there is a significantly

lower amount of molecular variance within aimags than expected by chance, highlighting the shallow differentiation that exists in broad geographic regions. Finally, we recovered negative values of Tajima's *D* for both genes in *U. u. eversmanni* (cyt *b*, *D*=–2.09; *COI*, *D*=–1.47) and across all samples of *U. undulatus* (cyt *b*, *D*=–1.52; *COI*, *D*=–0.82), although the result was only significant at the *P*<0.01 level for *U. u. eversmanni* cyt *b* (*P*>0.10 for all others).

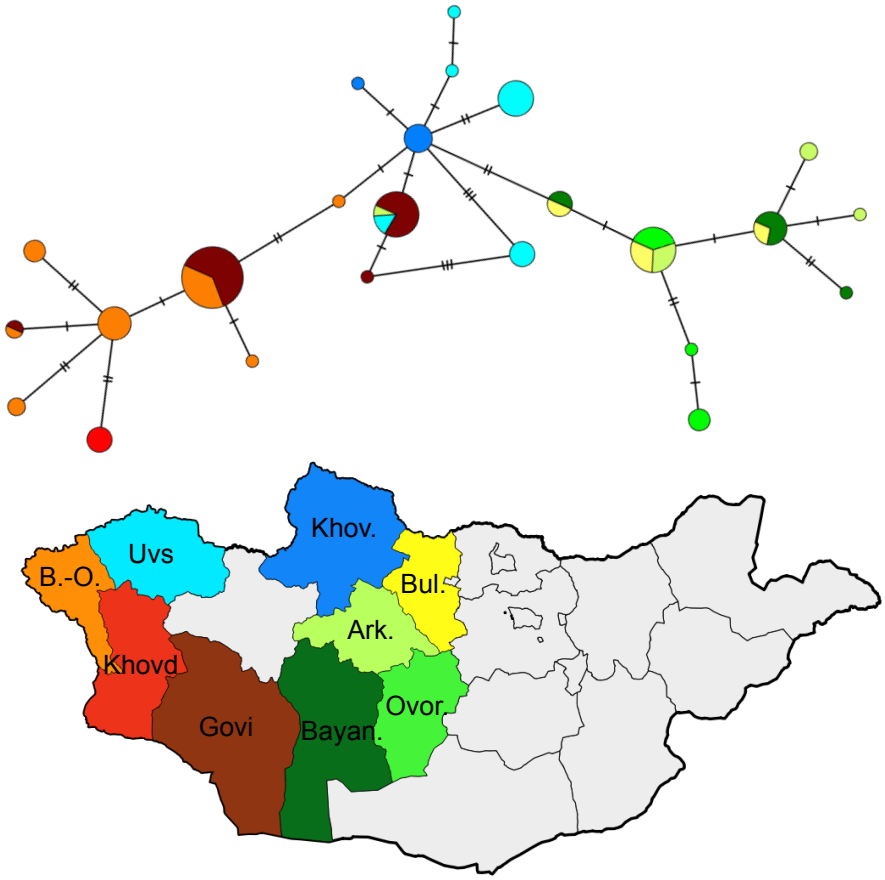

Figure 3 Minimum-spanning haplotype network of all *Urocitellus undulatus eversmanni* samples used in this study

Individuals in haplotype network (top) are colored by aimag of origin, with colors corresponding to the map (below). Notches indicate single nucleotide substitutions. Note the map does not include the distribution of *U. u. undulatus* (B.-O.=Bayan-Olgii, Govi=Govi-Altai, Khov.=Khovsgol, Bul.=Bulgan, Ark.=Arkhangai, Ovor.=Ovorkhangai, Bayan.=Bayankhongor).

DISCUSSION

Relatively little is known about range-wide patterns of genetic structure and endemicity in many central Asian mammal species. This information gap precludes tests of existing taxonomic hypotheses and limits deeper knowledge of how past environmental changes across this vast region have influenced mammalian diversification. This is particularly true for ecomorphologically conservative taxa, such as *U. undulatus*, where molecules and morphology might be expected to give cryptic or conflicting historical signals. Indeed, the few phylogeographic investigations of non-volant vertebrate taxa (e.g., *Phrynocephalus* lizards, Wang & Fu, 2004; *Rhombomys* gerbils, Ning et al., 2007; *Bufo* toads, Zhang et al., 2008; *Meriones* gerbils and *Allactaga*, *Dipus* jerboas, Liao et al., 2016) in central Asia to date hint at significant impacts of late Pleistocene environmental change on population genetic diversity and geographic structure in this region. Our analysis of *U. undulatus* allows us to establish preliminary hypotheses of mammalian spatiotemporal response to late Quaternary change within Mongolia that can be further tested in this and other sympatric species.

On a range-wide scale, our results support the existing systematic hypothesis (Kryštufek & Vohralík, 2013; Pavlinov & Lissovsky, 2012) that *U. undulatus* is comprised of two deeply divergent lineages (*undulatus* and *eversmanni*). The strong phylogeographic break between these lineages, which stretches from southern Lake Baikal (Russia) through eastern

Selenge and Töv Aimags (Mongolia), contrasts, however, with previously published patterns of cranial shape variation. Specifically, morphological studies (Kryštufek & Vohralík, 2013; Linetskaya & Linetskii, 1989; Vorontsov et al., 1980) found populations from Yakutia and the Amur region of Russia to be highly divergent in cranial shape, while populations from the remainder of the range extending across southern Siberia and northern Mongolia exhibited a broad longitudinal cline in cranial shape. Because body size varies significantly in *U. undulatus*, and cranial morphology is highly allometric in *Urocitellus* ground squirrels (e.g., Robinson & Hoffmann, 1975), it seems likely that cranial shape data (especially those based on linear measurements) largely reflect body size differences, which may or may not be useful for elucidating evolutionary structure in this species. More robust tests of species limits and phylogeographic hypotheses in *U. undulatus*, as well as of our assertion of a lack of gene flow between *undulatus* and *eversmanni*, await data from additional and independent regions of the nuclear genome.

Considering the *eversmanni* lineage which makes up the bulk of our sampling, our results provide new insights into effects of late Quaternary climate change on historical biogeography of this taxon across Mongolia. The record of late Pleistocene and Holocene environmental change in this region includes extensive plateau and mountain valley glaciation, specifically in the Khangai, Mongolian Altai, and Govi Altai ranges; extensive downward expansion of permafrost; and intermittent formation and draining of lakes at both higher and lower elevations (Böhner & Lehmkuhl, 2005; Grunert et al., 2000; Lehmkuhl, 1998; Lehmkuhl & Lang, 2001). Montane glaciation and the expansion of permafrost should have driven downslope range shifts in *U. undulatus*, as this species prefers mesic steppe habitats and requires deeper permafrost levels for construction of hibernacula. These range shifts, in turn, should have promoted increased mixing of populations across lowlands of western Mongolia between 30–12 kya.

Consistent with that scenario, we found shallow divergence between major mtDNA clusters within *U. u. eversmanni*. However, because many of these mitochondrial lineages are restricted to mid- and high-elevation steppe habitats (e.g., in the Govi Altai) and unlikely to experience high levels of gene flow, low divergences are likely to be signatures of past (i.e., latest Quaternary) population mixing across lowlands of western Mongolia. The shallow but significant geographic structure that does exist among geographically and ecologically disparate populations of *U. u. eversmanni* could, in turn, have been generated by partial lineage sorting and haplotypic divergence following expansion into more favorable areas and cessation of population connectivity.

Zhang et al. (2008) found a similar pattern of reduced haplotype and nucleotide diversity in green toads (*Bufo viridis*) inhabiting eastern Central Asia. Their data support a history of refugial isolation in montane regions of northwest China and eastern Kazakhstan followed by rapid postglacial expansion into surrounding basins. Liao et al. (2016) described a similar pattern in the jerboa *Allactaga sibirica* in China. Conversely, our data, including low population structure and negative values for Tajima's *D* in *U. u. eversmanni*, suggest recent upslope range expansions from lowland refugia. Therefore, from an elevational perspective, these studies support opposite historical scenarios that likely reflect differences in the need of amphibians to track water availability versus that of steppe mammals. Gür (2013) and Liao et al. (2016) describe a third pattern in Anatolian ground squirrels (*Spermophilus xanthoprymnus*) in Turkey and gerbils and jerboas (*Meriones meridianus* and *Dipus sagitta*) in northern China, suggesting that these species expanded their areal, but not elevational, distributions during the late Pleistocene in conjunction with expansion of cold steppe habitats and deserts.

If our hypothesis of lowland Pleistocene range shifts is correct, the most extensive corridors for gene flow among ancient populations of *U. u. eversmanni* may have been in the "Great Lakes Depression" and "Valley of the Govi Lakes". Those lowland regions, located between major Mongolian mountain ranges, are mostly contiguous with a broad longitudinal band of mesic steppe that transverses Mongolia and forms a corridor for more arid-adapted taxa such as Mongolian gazelle (*Procapra gutturosa*) and Tolai hare (*Lepus tolai*; Batsaikhan et al., 2014). However, Pleistocene environments in this region were likely more mesic than today and may have included a mixture of steppe and forest elements (Grunert et al., 2000; Böhner & Lehmkuhl, 2005). Downward expansion of mesic floral and faunal elements into the Great Lakes Depression during the late Pleistocene would have provided suitable habitat for an increasingly mesic-adapted suite of vertebrate species such as *U. undulatus*.

As a post hoc investigation of this scenario, and to more thoroughly parse AMOVA results, we calculated population genetic statistics (haplotype and nucleotide diversity) for all aimags with at least 15 sampled individuals (Uvs, Bayan-Ölgii, and Govi Altai). While Uvs Aimag contains lower haplotype diversity (0.71) than either Bayan-Ölgii or Govi Altai aimags (0.91 and 0.80, respectively), it has higher nucleotide diversity (6.69×10^{-3} vs. 2.37×10^{-3} and 4.92×10^{-3}, respectively). This increased nucleotide polymorphism could have resulted from confinement of multiple *U. u. eversmanni* lineages within a Pleistocene refugium spread across the Great Lakes Depression and surrounding basins, followed by rapid range expansion into favorable montane habitats that became increasingly disjunct with Holocene climate changes, yielding the phylogeographic and demographic signals we detected. Simonov et al. (2017) demonstrated elevated mtDNA diversity in *U. u. eversmanni* from the southern Altai Mountains in Russia, and suggested that those populations may also have been isolated in lowland glacial refugia. Our data strongly support their hypothesis that one of these refugia was in the Great Lakes Depression. However, we cannot completely rule out refugia elsewhere in northern Mongolia, such as in Khövsgöl Aimag, a region proximate to the Great Lakes Depression, but from which we were only able to sample six individuals from a relatively small area.

Currently, Pleistocene paleoenvironments of western

Mongolia are somewhat poorly constrained, preventing more precise and detailed links between small mammal historical biogeography and past environmental change. Grunert et al. (2000) proposed a lowstand (i.e., lowered lake levels due to local or regional environmental change) for both Uvs Nuur and Bayan Nuur during the Last Glacial Maximum (LGM), which would have led to exposure of even more extensive areas in the Great Lakes Depression than are available today. While these lake lowstands are somewhat counterintuitive given the relatively mesic conditions inferred for other mid-latitude regions during the LGM, a similar pattern of glacial lowstands has been described from lakes in nearby northwestern China (Fang, 1991). Conversely, the southern Altai Mountains in Russia experienced formation of large glacial lakes during the late Pleistocene (e.g., Rudoy, 2002). Understanding the extent to which these idiosyncratic landscape-level responses interacted with regional-scale environmental variability to impact the distribution and demography of *U. undulatus* will require linking all currently available sequence datasets with new genetic data in a range-wide phylogeographic framework.

CONCLUSION

We analyzed the phylogeography of the long tailed ground squirrel (*Urocitellus undulatus*) across the southern core of its large central Asian range. Phylogenetic and population genetic inferences based on mtDNA strongly support the presence of two major lineages in Mongolia (*U. u. undulatus* and *U. u. eversmanni*). Within the more widespread *U. u. eversmanni*, we identified statistically significant but extremely shallow phylogeographic structure, with modern genetic clusters associated with Mongolian mountain systems (Khangai Mountains, Mongolian and Govi Altai). Together, our analyses support a late Pleistocene history of extensive population admixture in *U. u. eversmanni*, possibly across the Great Lakes Depression and contiguous lowlands of north-west Mongolia, followed by geologically recent diversification in postglacial isolation. In addition to providing new geographic context for *U. undulatus* systematics and phylogeography, our study establishes hypotheses of distributional and demographic response to past environmental change in mesic-adapted central Asian mammal species which may be tested using robust, genomic-scale datasets.

COMPETING INTERESTS

The authors declare that they have no competing interests.

AUTHORS' CONTRIBUTIONS

B.S.M. designed the study, extracted genomic DNA, sequenced mitochondrial genes of interest, and performed all statistical analyses. B.S.M., B.N., A.T., and J.A.C. wrote and revised the manuscript. All authors read and approved the final manuscript.

ACKNOWLEDGEMENTS

We thank the many researchers, students, and assistants involved in our logistically challenging Mongolian fieldwork over the past two decades, without whose efforts this study would not have been possible.

REFERENCES

Bandelt HJ, Forster P, Röhl A. 1999. Median-joining networks for inferring intraspecific phylogenies. *Molecular Biology and Evolution*, **16**(1): 37–48.

Batsaikhan N, Samiya R, Shar S, Lkhagvasuren D, King SRB. 2014. A Field Guide to the Mammals of Mongolia. 2nd ed. London: Zoological Society of London.

Böhner J, Lehmkuhl F. 2005. Environmental change modelling for Central and High Asia: pleistocene, present and future scenarios. *Boreas*, **34**(2): 220–231.

Dunnum JL, Cook JA. 2012. Gerrit smith miller: his influence on the enduring legacy of natural history collections. *Mammalia*, **76**(4): 365–373.

Edgar RC. 2004. MUSCLE: multiple sequence alignment with high accuracy and high throughput. *Nucleic Acids Research*, **32**(5): 1792–1797.

Ermakov OA, Simonov E, Surin VL, Titov SV, Brandler OV, Ivanova NV, Borisenko AV. 2015. Implications of hybridization, NUMTs, and overlooked diversity for DNA barcoding of Eurasian ground squirrels. *PLoS One*, **10**(1): e0117201.

Fang, J. 1991. Lake evolution during the past 30,000 years in China, and its implications for environmental change. *Quaternary Research*, **36**: 37–60.

Folmer O, Black M, Hoeh W, Lutz R, Vrijenhoek R. 1994. DNA primers for amplification of mitochondrial cytochrome c oxidase subunit I from diverse metazoan invertebrates. *Molecular Marine Biology and Biotechnology*, **3**(5): 294–299.

Grunert J, Lehmkuhl F, Walther M. 2000. Paleoclimatic evolution of the Uvs Nuur basin and adjacent areas (Western Mongolia). *Quaternary International*, **65–66**: 171–192.

Gür H. 2013. The effects of the Late Quaternary glacial–interglacial cycles on Anatolian ground squirrels: range expansion during the glacial periods? *Biological Journal of the Linnean Society*, **109**(1): 19–32.

Helgen KM, Cole FR, Helgen LE, Wilson DE. 2009. Generic revision in the Holarctic ground squirrel genus Spermophilus. *Journal of Mammalogy*, **90**(2): 270–305.

Hijmans RJ, van Etten J, Cheng J, Mattiuzzi M, Sumner M, Greenberg JA, Lamigueiro OP, Bevan A, Racine EB, Shortridge A, Ghosh A. 2017(2017-11-13). Raster: geographic data analysis and modeling Version 2.6-7. https://cran.r-project.org/web/packages/raster/.

Kamvar, ZN, Tabima JF, Grünwald NJ. 2014. *Poppr*: an R package for genetic analysis of populations with clonal, partially clonal, and/or sexual reproduction. *PeerJ*, **2**: e281.

Kryštufek B, Vohralík V. 2013. Taxonomic revision of the Palaearctic rodents (Rodentia). Part 2. Sciuridae: *Urocitellus*, *Marmota* and *Sciurotamias*. *Lynx*, **44**: 27–138.

Lanfear R, Frandsen PB, Wright AM, Senfeld T, Calcott B. 2017. PartitionFinder 2: new methods for selecting partitioned models of evolution for molecular and morphological phylogenetic analyses. *Molecular Biology and Evolution*, **34**(3): 772–773.

Lehmkuhl F. 1998. Quaternary glaciations in central and western Mongolia. *Quaternary Proceedings*, **6**: 153–167.

Lehmkuhl F, Lang A. 2001. Geomorphological investigations and

luminescence dating in the southern part of the Khangay and the Valley of the Gobi Lakes (Central Mongolia). *Journal of Quaternary Science*, **16**(1): 69–87.

Liao J, Jing D, Luo G, Wang Y, Zhao L, and Liu N. 2016. Comparative phylogeography of *Meriones meridianus*, *Dipus sagitta*, and *Allactaga sibirica*: Potential indicators of the impact of the Qinghai-Tibetan Plateau uplift. *Mammalian Biology,* **81**:31–39.

Linetskaya ON, Linetskii AI. 1989. Species differences in the craniometric variation among ground squirrels of the Eastern Palearctic (subgenus Urocitellus). *In*: Sovremennye Podkhody K Izucheniyu Izmenchivosti (Modern Approaches to the Study of Variability). Vladivostok: Dal'nevostochnoe Otdelenie, Akademiya Nauk SSSR, 99–105.

McLean BS, Bell KC, Dunnum JL, Abrahamson B, Colella JP, Deardorff ER, Weber JA, Jones AK, Salazar-Miralles F, Cook JA. 2016a. Natural history collections-based research: progress, promise, and best practices. *Journal of Mammalogy*, **97**(1): 287–297.

McLean BS, Jackson DJ, Cook JA. 2016b. Rapid divergence and gene flow at high latitudes shape the history of Holarctic ground squirrels (*Urocitellus*). *Molecular Phylogenetics and Evolution*, **102**: 174–188.

Miller MA, Pfeiffer W, Schwartz T. 2010. Creating the CIPRES Science Gateway for inference of large phylogenetic trees. *In*: Proceedings of the 2010 Gateway Computing Environments Workshop (GCE). New Orleans, LA, USA: IEEE, 1–8.

Ning SL, Zhou LZ, Zhang BW, Zhao TB, Zou GY. 2007. Phylogeographic patterns of the great gerbil *Rhombomys opimus* in China based on mitochondrial cytochrome b gene sequence variations. *Acta Zoologica Sinica*, **53**(4): 630–640. (in Chinese)

Ognev SI. 1947. Zveri SSSR I Prilezhashchikh Stran. Gryzuny (Prodolzhenie). (Zveri Vostochnoi Evropy I Severnoi Azii) (Mammals of the USSR and Adjacent Countries: Rodents (continued). (Mammals of Eastern Europe and Northern Azii)). 5th ed. Moscow: Akademiya Nauk SSSR.

Oksanen J, Blanchet FG, Friendly, M, Kindt R, Legendre P, McGlinn D, Minchin PR, O'Hara RB, Simpson GL, Solymos P, Henry M, Stevens H, Szoecs E, Wagner H. 2017(2017-12-01). Vegan: community ecology package Version 2.4-5. https://cran.r-project.org/web/packages/vegan/

Paradis E, Bolker B, Claude J, Cuong HS, Desper R, Durand B, Dutheil J, Gascuel O, Heibl C, Lawson D, Lefort V, Legendre P, Lemon J, Noel Y, Nylander J, Opgen-Rhein R, Popescu AA, Schliep K, Strimmer K, de Vienne D. 2017a. Package "ape. " Version 4.0. http://ape-package.ird.fr/.

Paradis E, Jombart T, Schliep K, Potts A, Winter D. 2017b(2017-05-03). Pegas: population and evolutionary genetics analysis system Version 0.10. http://ape-package.ird.fr/pegas.html

Pavlinov IY, Lissovsky AA. 2012. The Mammals of Russia: A Taxonomic and Geographic Reference. Moscow: KMK Scientific Press.

Pfeifer B, Wittelsbuerger U, Li H, Handsaker B. 2017(2017-07-04). PopGenome: an efficient Swiss army knife for population genomic analyses Version 2.2.4. https://cran.r-project.org/web/packages/PopGenome/.

Rambaut A, Suchard MA, Xie W, Drummond AJ. 2014. Tracer. Version 1.6.0. http://beast.community/tracer.

Robinson JW, Hoffmann RS. 1975. Geographical and interspecific cranial variation in big-eared ground squirrels (*Spermophilus*): a multivariate study. *Systematic Zoology*, **24**(1): 79–88.

Ronquist F, Huelsenbeck JP. 2003. MrBayes 3: Bayesian phylogenetic inference under mixed models. *Bioinformatics*, **19**(12): 1572–1574.

Rudoy AN. 2002. Glacier-dammed lakes and geological work of glacial superfloods in the late Pleistocene, southern Siberia, Altai mountains. *Quaternary International*, **87**(1): 119–140.

Sikes RS, Gannon WL, the Animal Care and Use Committee of the American Society of Mammalogists. 2011. Guidelines of the American Society of Mammalogists for the use of wild mammals in research. *Journal of Mammalogy*, **92**(1): 235–253.

Simonov EP, Dvilis AE, Lopatina NV, Litvinov YN, Moskvitina NS, Ermakov OA. 2017. The influence of late Pleistocene mountain glaciations on the genetic differentiation of long-tailed ground squirrel (*Urocitellus undulatus*). *Russian Journal of Genetics*, **53**(5): 614–622.

Smith MF, Patton JL. 1993. The diversification of South American murid rodents: evidence from mitochondrial DNA sequence data for the akodontine tribe. *Biological Journal of the Linnean Society*, **50**(3): 149–177.

Tinnin DS, Dunnum JL, Salazar-Bravo J, Batsaikhan N, Burt MS, Gardner SL, Yates TL. 2002. Contributions to the Mammalogy of Mongolia, with a checklist of species for the country. Albuquerque, NM: The Museum of Southwestern Biology.

Tsvirka MV, Spiridonova LN, Korablev VP. 2008. Molecular genetic relationships among East Palaerctic ground squirrels of the genus *Spermophilus* (Sciuridae, Rodentia). *Russian Journal of Genetics*, **44**(8): 966–974.

Vorontsov NN, Frisman LV, Lyapunova EA, Mezhova ON, Serdyuk VA, Fomicheva II. 1980. The effect of isolation on the morphological and genetical divergence of populations. *Genetica*, **52**(1): 339–359.

Wang YZ, Fu JZ. 2004. Cladogenesis and vicariance patterns in the toad-headed lizard *Phrynocephalus versicolor* species complex. *Copeia*, **2004**(2): 199–206.

Wilson DE, Reeder DM. 2005. Mammal Species of the World. 3rd ed. Baltimore, Maryland: Johns Hopkins University Press.

Yates TL, Jones C, Cook JA. 1996. Preservation of voucher specimens. *In*: Wilson DE, Cole FR, Nichols JD, Rudran R, Foster MS. Measuring and Monitoring Biological Diversity: Standard Methods for Mammals. Washington, DC: Smithsonian Institution Press, 265–274.

Zhang YJ, Stöck M, Zhang P, Wang XL, Zhou H, Qu LH. 2008. Phylogeography of a widespread terrestrial vertebrate in a barely-studied Palearctic region: green toads (*Bufo viridis* subgroup) indicate glacial refugia in Eastern Central Asia. *Genetica*, **134**(3): 353–365.

Zoological Research Editorial Board

ZOOLOGICAL RESEARCH
动物学研究
Bimonthly, Since 1980

Project for Enhancing International Impact of China STM Journals

中国精品科技期刊 中国科技核心期刊 中国百强报刊

Edited by Editorial Office of Zoological Research

(Kunming Institute of Zoology, Chinese Academy of Sciences, 32 Jiaochang Donglu, Kunming, Yunnan, Post Code: 650223 Tel: +86 871 65199026 E-mail: zoores@mail.kiz.ac.cn)

Sponsored by Kunming Institute of Zoology, Chinese Academy of Sciences; China Zoological Society©

Supervised by Chinese Academy of Sciences

Published by Science Press (16 Donghuangchenggen Beijie, Beijing 100717, China)

Printed by Kunming Xiaosong Plate Making & Printing Co, Ltd

Domestic distribution by Yunnan Post and all local post offices in China

International distribution by China International Book Trading Corporation (Guoji Shudian) P.O.BOX 399, Beijing 100044, China

Advertising Business License 广告经营许可证：滇工商广字66号

Domestic Postal Issue No.: 64-20

Price: 15.0 USD/80.0 CNY

ISSN 2095-8137